THE REGULATION AND SIGNIFICANCE OF INTRAPULMONARY ARTERIOVENOUS ANASTOMOSES IN HEALTHY HUMANS

by

STEVEN S. LAURIE

A DISSERTATION

Presented to the Department of Human Physiology
and the Graduate School of the University of Oregon
in partial fulfillment of the requirements
for the degree of
Doctor of Philosophy

September 2012

DISSERTATION APPROVAL PAGE

Student: Steven S. Laurie

Title: The Regulation and Significance of Intrapulmonary Arteriovenous Anastomoses in Healthy Humans

This dissertation has been accepted and approved in partial fulfillment of the requirements for the Doctor of Philosophy degree in the Department of Human Physiology by:

Dr. Andrew T. Lovering	Chairperson
Dr. John R. Halliwill	Member
Dr. Christopher T. Minson	Member
Dr. Eric A. Johnson	Outside Member
Dr. Erik R. Swenson	Non-UO Member

and

Kimberly Andrews Espy	Vice President for Research & Innovation/Dean of the Graduate School

Original approval signatures are on file with the University of Oregon Graduate School.

Degree awarded September 2012

DISSERTATION ABSTRACT

Steven S. Laurie

Doctor of Philosophy

Department of Human Physiology

September 2012

Title: The Regulation and Significance of Intrapulmonary Arteriovenous Anastomoses in Healthy Humans

Intrapulmonary arteriovenous anastomoses (IPAVA) have been known to exist as part of the normal pulmonary vasculature for over 50 years but have been underappreciated by physiologists and clinicians. Using a technique called saline contrast echocardiography we and others have demonstrated that during exercise or when breathing low oxygen gas mixtures IPAVA open, but breathing 100% oxygen during exercise prevents them from opening. However, the mechanism(s) for this dynamic regulation and the role IPAVA play in affecting pulmonary gas exchange efficiency remain unknown.

In Chapter IV the infusion of epinephrine and dopamine into resting subjects opened IPAVA. While it is possible this opening was due to the direct vasoactive action of these catecholamines, the opening may simply be due to increases in cardiac output and pulmonary artery systolic pressure secondary to the cardiac effects of these drugs.

In Chapter V I used Technetium-99m labeled macroaggregated albumin (^{99m}Tc-MAA) to quantify blood flow through IPAVA in exercising healthy humans. Initial attempts to correct for attenuation of the emitted signal were unsuccessful due to the time necessary for data acquisition and the resulting accumulation of free-^{99m}Tc. However, I

used a blood sample to calculate freely circulating ^{99m}Tc which could be subtracted from the shunt fraction. Using this procedure I demonstrated for the first time using filtered solid particles that breathing 100% oxygen reduces blood flow through IPAVA during exercise.

Finally, in Chapter VI I tackled the elephant in the room surrounding IPAVA in healthy humans: do these vessels play a role in pulmonary gas exchange efficiency? Our data suggest that the efficiency of pulmonary gas exchange is dependent on the driving pressure gradient for oxygen and the distance to blood flowing through the core of IPAVA. As such, with increases in exercise intensity the diffusion distance and transit time of blood at the core of IPAVA prevent complete gas exchange, thus blood flow through IPAVA acts as a shunt.

This dissertation includes previously unpublished co-authored material.

CURRICULUM VITAE

NAME OF AUTHOR: Steven S. Laurie

GRADUATE AND UNDERGRADUATE SCHOOLS ATTENDED:

University of Oregon, Eugene
University of California, Davis

DEGREES AWARDED:

Doctor of Philosophy, Human Physiology, 2012, University of Oregon
Master of Science, Human Physiology, 2009, University of Oregon
Bachelor of Science, Exercise Biology, 2004, University of California

AREAS OF SPECIAL INTEREST:

Intrapulmonary Arteriovenous Anastomoses
Pulmonary Vascular Physiology
Pulmonary Gas Exchange
Exercise Physiology

PROFESSIONAL EXPERIENCE:

Graduate Teaching Fellow, Department of Human Physiology, University of Oregon, September 2007-June 2011

GRANTS, AWARDS, AND HONORS:

Caroline tum Suden/Francis A. Hellebrandt Professional Opportunity Award, American Physiological Society, May 2012

Eugene Evonuk Memorial Graduate Fellowship In Environmental or Stress Physiology, Department of Human Physiology, University of Oregon, June 2011

Clarence and Lucille Dunbar Scholarship, College of Arts and Sciences, University of Oregon, May 2011

Marthe E. Smith Memorial Science Scholarship, College of Arts and Sciences, University of Oregon, April 2010

Clarence and Lucille Dunbar Scholarship, College of Arts and Sciences, University of Oregon, April 2009

PUBLICATIONS:

Laurie SS, Elliott JE, Goodman RD, & Lovering AT. Catecholamine-induced opening of intrapulmonary arteriovenous anastomoses in healthy humans at rest. *J Appl Physiol.* (**In revision**) 2012.

Elliott JE, Choi Y, Laurie SS, Yang X, Gladstone IM & AT Lovering. To the Editor: Reply to "Sonic echocardiography: what does it mean when there are no bubbles in the left ventricle?" *J Appl Physiol* 110: 296-297, 2011.

Elliott JE, Choi Y, Laurie SS, Yang X, Gladstone IM, and AT Lovering. Effect of initial gas bubble composition on detection of inducible intrapulmonary arteriovenous shunt during exercise in normoxia, hypoxia or hyperoxia. *J Appl Physiol* 110: 35-45, 2011.

Lovering AT, Elliott JE, Beasley KM, and SS Laurie. Pulmonary pathways and mechanisms regulating transpulmonary shunting into the general circulation: an update. *Injury, Int. J. Care Injured,* 41(S2): S16-S23, 2010.

Laurie SS, Yang X, Elliott JE, Beasley KM, and AT Lovering. Hypoxia-induced intrapulmonary arteriovenous shunting at rest in healthy humans. *J Appl Physiol* 109: 1072-1079, 2010.

ACKNOWLEDGMENTS

This dissertation represents a midway point of a journey I began with my direct advisor, Andy Lovering, in a lab that we built from literally the ground up. His guidance, insight, mentorship, and friendship have supported me along the way and developed in me an excitement and confidence for the journey that lies ahead. I will be forever grateful for all he has done for me and feel proud and honored to have shared the journey with him. In addition, John Halliwill and Chris Minson have been indispensable mentors in my development as a student and as a scientist and I know they will both continue to be mentors and friends of mine throughout the years to come. The final two members of my dissertation committee, Eric Johnson and Erik Swenson, have been incredibly helpful and provided a critical perspective as I fully developed the scope of this dissertation, for which I am truly grateful.

I also want to thank Dr. Igor Gladstone for his tremendous support and enthusiasm and for teaching me how to find my way through the politics of biomedical research with the help of a little chocolate. Dr. Jerry Hawn, who has instilled in me the essence of calm and patience, has been a wonderful and essential member of my team as well. And, a special thank you to my fellow grad students, especially Jon Elliott, Kara Beasley, Chi-An Wang, and Jenni Minor, who have all been wonderful friends throughout the past five years.

The work I have undertaken over the past 5 years has truly been a team effort. Dr. Mathews Fish enthusiastically welcomed our research team into the Oregon Heart & Vascular Institute and his team, especially Tom, Dixie, Toni, and Scott, always met us

with smiles on their faces and went out of their way to think of unique and creative ways to solve whatever problems I could come up with.

My girlfriend Stephanie has provided an enormous amount of love and support throughout the writing of this dissertation. Having someone in the trenches with me writing her own dissertation has been absolutely invaluable and essential to my success. I hope I have provided the same level of support for you as you have for me.

Finally, I have to convey a very special thank you to my parents Kathy and Bill and my brother Tim, who have all provided unconditional love and support for everything I have chosen to tackle throughout my life. Thank you from the bottom of my heart.

TABLE OF CONTENTS

Chapter Page

I. INTRODUCTION 1
Historical Perspective 2
Background and Significance 4
Statement of Problem 7
Purpose and Hypotheses 8
Aim #1 8
Aim #2 9
Aim #3 9

II. REVIEW OF THE LITERATURE 11
Introduction 11
Pulmonary Vasculature Development 11
Pulmonary Blood Flow Regulation 13
Exercise 14
Gravity 14
Hypoxia 16
Hyperoxia 19
Anatomical Evidence for Pulmonary Arteriovenous Anastomoses 19
Intrapulmonary Arteriovenous Anastomoses Detected Using Saline Contrast Echocardiography 21
Pulmonary Gas Exchange Efficiency 22
Potential Factor – $\dot{V}/\dot{Q}$ Mismatch 22
Potential Factor – Diffusion Limitation 23
Potential Factor – Shunt 24
Experimental Evidence Supporting These Factors 25
Non-capillary Gas Exchange 26
100% Oxygen Technique 27

III. METHODS 29
Informed Consent 29
Patent Foramen Ovale Screening 29
Pulmonary Artery Systolic Pressure 32
Lung Function 34
Forced Vital Capacity 34
Slow Vital Capacity 35
Whole-body Plethysmography 36
Diffusion Capacity for Carbon Monoxide 37
Subject Instrumentation 37
Intravenous Catheter 37
Radial Artery Catheter 38
Esophageal Temperature Probe 39
Oxygen Saturation and Heart Rate 40
Echocardiography Measurements 40
Saline Contrast Echocardiography 40

Chapter Page

Pulmonary Artery Systolic Pressure 42
Cardiac Output 42
Exercise Testing 43
Metabolic Rate 43
VO_2peak Testing 43
Exercise Protocols 44
Measurement of Blood Gases 45
Tonometry 45
Arterial Blood Draw and Analysis 46
Delivery of Inspired Gas Mixtures 47
Drug Infusions 48
Nuclear Medicine Imaging and Analysis 49
MAA Filtering and Technetium-99m Labeling 50
SPECT/CT Imaging 51
Post-processing Data Reconstruction and Analysis 53
Planar Imaging 54

IV. CATECHOLAMINE-INDUCED OPENING OF INTRAPULMONARY ARTERIOVENOUS ANASTOMOSES IN HEALTHY HUMANS AT REST 56
Introduction 56
Methods 58
Echocardigraphic Screening and Lung Function Testing 58
Resting Epinephrine and Dopamine Infusions 59
Hypoxia and Beta-blockade 60
Statistics 61
Results 61
Subject Characterization and Lung Function 61
Bubble Scores 61
Cardiac Output and PASP 62
Discussion 66
Saline Contrast Echocardiography 67
Epinephrine and Dopamine Effects on Pulmonary Vasculature 68
Hypoxia and Beta-Blockade 68
Cardiac and PASP Effects Due to Epinephrine and Dopamine 69
Effect of Breathing 100% Oxygen During EPI and DA Infusions on Blood Flow Through IPAVA 71
Similarities Between IPAVA and Supernumerary Arteries 72
Summary 74

V. BREATHING 100% OXYGEN DURING EXERCISE REDUCES BLOOD FLOW THROUGH INDUCIBLE INTRAPULMONARY ARTERIOVENOUS ANASTOMOSES IN HEALTHY HUMANS 76
Introduction 76
Methods 78

Chapter Page

Echocardigraphic Screening, Lung Function, and VO_2peak Testing 78
MAA Filtering and Technetium-99m Labeling 78
Study Conditions 80
Imaging 81
Post-processing Data Reconstruction and Analysis 82
Correction for Free-^{99m}Tc in the Blood 83
Statistics 84
Results 84
Discussion 90
Filtering of MAA 90
Quantification of Free-^{99m}Tc 90
Consistencies Between TTSCE and MAA Data 92
Summary 92

VI. THE CONTRIBUTION OF INDUCIBLE INTRAPULMONARY ARTERIOVENOUS ANASTOMOSES TO PULMONARY GAS EXCHANGE EFFICIENCY DURING EXERCISE IN HEALTHY HUMANS 94
Introduction 94
Methods 96
Echocardigraphic Screening, Lung Function, and VO_2peak Testing 96
Subject Instrumentation 96
Exercise Protocols 97
Pulmonary Gas Exchange Efficiency 97
Saline Contrast Echocardiography for Detection of IPAVA 98
Pulmonary Artery Systolic Pressure 99
Statistics 99
Results 99
Discussion 104
Could Blood Flowing Through IPAVA Act Like a Shunt? 106
Non Capillary Gas Exchange 113
100% Oxygen Technique 116
Classifying Pulmonary Gas Exchange Inefficiency into Three Discrete Categories 117
Summary 118

VII. CONCLUSIONS 121
Main Findings 121
Comparisons Between Exercise-induced and Hypoxia-induced Opening of IPAVA. 123
Implications & Future Directions 125

Chapter Page

REFERENCES CITED 128

LIST OF FIGURES

Figure Page

4.1. Bubble Scores 63

4.2. Representative Echocardiograms 64

4.3. Bubble Scores Before and After Propranolol Infusion 65

4.4. Cardiac Output and PASP 65

4.5. Cardiac Output vs. PASP 66

4.6. Schematic of 'Preterminal Arteriole' 73

5.1. SPECT/CT Reconstructions 86

5.2. Bubble Scores 88

5.3. Shunt Fractions 88

5.4. Free-^{99m}Tc 89

5.5. Timing Effect on Shunt Fraction 89

6.1. Protocol 1 Bubble Scores 103

6.2. Protocol 2 Bubble Scores 104

6.3. $AaDO_2$ 104

LIST OF TABLES

Table Page

4.1. Anthropometrics, Pulmonary Function, and DL_{CO} Data 62

5.1. Anthropometrics, Pulmonary Function, Diffusion Capacity for CO, and Peak Exercise Capacity Data 85

5.2. *Ex vivo* binding efficiency of ^{99m}Tc-MAA 85

6.1. Anthropometrics, Pulmonary Function, Diffusion Capacity for CO, and Peak Exercise Capacity Data 100

6.2. Metabolic, blood gas, and hemodynamic data at rest and during exercise [Protocol 1] 101

6.3. Metabolic, blood gas, and hemodynamic data at rest and during exercise [Protocol 2] 102

CHAPTER I

INTRODUCTION

With every heart beat blood is pumped from the right ventricle into the pulmonary circulation before it returns to the left side of the heart, while blood in the left ventricle is pumped into the systemic circulation before it returns to the right side of the heart. This design puts these two circulations in series with each other and allows the pulmonary circulation to achieve two critically important tasks. First, the exchange of gases between pulmonary blood and alveolar gas allows oxygen to diffuse into the blood and carbon dioxide to diffuse out before this blood is pumped into the systemic circulation. Second, the pulmonary microvasculature acts as a sieve to filter the blood and prevent potential emboli from entering the systemic circulation where they could become lodged in systemic organs such as the heart or brain.

Large diameter intrapulmonary arteriovenous anastomoses (IPAVA), however, provide an additional pathway for blood flow, and this bypasses the alveolar-capillary interface, which is classically considered to be the gas exchange unit. If blood flows through this alternative pathway it may potentially impair pulmonary gas exchange efficiency as well as bypass the filtering ability of the pulmonary microcirculation. Recently, controversy has arisen surrounding the existence, regulation, and significance of large diameter IPAVA. Accordingly, the overall purpose of this dissertation is to determine the role of and significance for IPAVA in healthy humans. The first objective in this dissertation was to identify a potential mechanism regulating the opening of IPAVA in healthy humans. The second objective was to use an anatomical approach to quantify changes in blood flow through IPAVA during normoxic versus hyperoxic

exercise, and the third objective was to determine if the blood flowing through open IPAVA during exercise impairs pulmonary gas exchange efficiency.

HISTORICAL PERSPECTIVE

The historical paths of respiratory physiology have been at best tumultuous, and at worst a propagation of immense inaccuracy. I would like to begin this dissertation with a few stories as recounted by Dr. John West (192) that are part of the inaccurate history of respiratory physiology and relate these lessons to our current understanding of pulmonary vascular regulation.

The first story involves the development of our understanding of the pulmonary circulation. Claudius Galen (129-199AD) was one of the first scientists to apply clinical observations to explain and understand physiological processes. He described that the liver produced blood, which would only flow through the pulmonary artery to nourish the lung, while the remainder would cross invisible interventricular 'pores' to reach the left side of the heart. *'Pneuma'* would be brought from the lung to the left side of the heart through the pulmonary vein and combine with the blood that had traversed through the 'pores' and subsequently flow to the remainder of the body. Galen's ideas were enthusiastically embraced and proliferated unchallenged for centuries, due in part to Arabic scholars such as Avicenna (circa 980-1037) who created a virtual medical encyclopedia of the time. Galen's 'pores' continued unchallenged until the Arab scholar Ibn Al Nafis (1210-1288) wrote his treatise *Commentary on the Anatomy of the Canon of Avicenna* and more than suggested that all of the blood traveled through the lung where it could be permeated with air (193).

Unaware of Ibn Al Nafis' writings, Michael Servetus (1509-1553) also challenged Galen's interventricular 'pores' and described how the blood changed colors as it flowed through the pulmonary circulation, though the explanation for this was still two centuries away. While this point in history could have represented a true step forward in overcoming the crucial inaccuracy put forth by Galen, Servetus and his book were deemed heretical by the Catholic Church and were burned at the stake in 1553. It wasn't until 1616 that William Harvey (1578-1657) first presented his ideas that blood circulated continuously throughout the lung and the body and in 1628 described both the lesser (pulmonary) and greater (systemic) circulations. Despite puzzling anatomists for centuries who could find no such pores, Galen's scheme had been allowed to flourish for over 1400 years and represented the propagation of a gross inaccuracy in our understanding of blood flow through the lung.

The next story occurred during the late nineteenth and early twentieth century as our understanding of oxygen was developing. Not surprising, a few inaccuracies developed and scientific controversy ensued. In 1870, Christian Bohr and his colleagues suggested that oxygen was actively secreted in the lung and this idea soon gained support from the eminent respiratory physiologist John Scott Haldane. Haldane claimed to prove this hypothesis by finding the average arterial PO_2 to be 200 mmHg, much higher than that of air. However, August Krogh, a pupil of Bohr's, continued to refine techniques to measure arterial PO_2 and always showed it to be less than alveolar PO_2, and thus less than that of air as well. Meanwhile, Krogh's wife Marie was investigating the diffusing capacity of the lung for carbon monoxide and demonstrated that oxygen could sufficiently enter the pulmonary blood through diffusion alone and that active secretion

was not necessary. Therefore, only in the past 100 years has it been fully accepted that oxygen gains entry through the lung solely via passive diffusion and not active secretion.

Taking into consideration the lessons from these historical accounts, it is not surprising that potential inaccuracies in our understanding of cardiopulmonary physiology and pulmonary gas exchange have again persevered despite anatomically based evidence suggesting alternative explanations than those more conveniently accepted throughout the literature. The impetus for this dissertation lies at the confluence of ideas stemming from the first two stories, where pulmonary blood flow meets pulmonary ventilation and pulmonary gas exchange occurs. Ironically, Galen's idea was perpetuated for centuries by ignoring the fact that there was no anatomical evidence to support 'interventricular pores'. Today however, anatomical evidence supports the existence and importance of IPAVA, yet these data have been largely ignored.

BACKGROUND AND SIGNIFICANCE

One of the most fundamental roles of the lung is to efficiently exchange oxygen and carbon dioxide between the alveolar air and the blood flowing through pulmonary capillaries. The efficiency of pulmonary gas exchange is both defined and quantified by the difference between the alveolar and arterial partial pressure of oxygen ($AaDO_2$) and can worsen due to three accepted causes: diffusion limitation, ventilation-perfusion (V/Q) mismatch, and/or right-to-left shunt. While it is well known that the efficiency of pulmonary gas exchange is not perfect at rest and worsens during incremental exercise (30), identifying which of the three possible causes is contributing to this inefficiency remains an unresolved and controversial area of research (71, 95).

When taking into account the diffusion capacity of the blood-gas barrier, pulmonary capillary blood volume, shape of the oxyhemoglobin dissociation curve, and chemical interactions between O_2 and CO_2, complete partial pressure equilibration between the alveolar air and pulmonary capillary blood occurs in about 0.25 sec at rest at sea level (154, 181). A diffusion limitation could occur if the transit time of red blood cells flowing through pulmonary capillaries was reduced below 0.25 sec preventing the complete equilibration of gases between the alveoli and pulmonary capillary blood. During exercise, cardiac output increases up to five fold so the transit time could decrease significantly. Fortunately the transit time is determined by the ratio of capillary blood volume to cardiac output. With the tripling of capillary blood volume that occurs due, in part, to exercise-induced increases in left atrial pressure (135), there is sufficient time for the complete equilibration of gases even with a five fold increase in cardiac output (rest: 70ml / 83ml/sec=0.84 sec; max exercise: 210ml / 415 ml/sec=0.51sec) (181). Thus, diffusion limitation is an unlikely explanation for the reduction in pulmonary gas exchange efficiency that occurs during incremental exercise at sea level.

The other two causes that could reduce pulmonary gas exchange efficiency at rest or during exercise are the inefficient matching of alveolar ventilation ($\dot{V}$) with pulmonary blood flow ($\dot{Q}$) and shunt. The multiple inert gas elimination technique (MIGET) was developed with the intention to quantify the contributions from $\dot{V}/\dot{Q}$ mismatch and shunt based on the retention and excretion of six inert gases of varying solubility (184, 185) and represents one of the only techniques used to quantify the contributing factors to pulmonary gas exchange inefficiency. If the pulmonary gas exchange inefficiency measured during exercise is not predicted by MIGET to be a result of $\dot{V}/\dot{Q}$ mismatch

and/or shunt, then it is *assumed* that a diffusion limitation must be occurring to explain the measured inefficiency, despite the unlikeliness of this happening in individuals breathing room air. MIGET, however, cannot differentiate between that portion of pulmonary gas exchange inefficiency suggested to be due to diffusion limitation, and that known to be caused by the anatomical post-pulmonary shunt of the Thebesian venous drainage and the bronchial venous drainage.

Using this gas exchange-dependent technique, the role of $\dot{V}/\dot{Q}$ mismatch during exercise at sea level has been inconsistent, with data demonstrating either no significant increase in $\dot{V}/\dot{Q}$ mismatch during exercise (136), a non-significant increase (41, 173), or a significant increase only at higher levels of exercise, VO_2>2.5 L/min (58) or VO_2>3.0 L/min (186). Despite these inconsistencies, the $AaDO_2$ widened during increases in exercise intensity in every study and significant contributions from a right-to-left shunt (intrapulmonary or intracardiac) were not detected using this technique. These investigators have also used the 100% oxygen technique to support their assertion that there is no detectable intrapulmonary shunt during exercise (58, 178, 182). Thus, despite the variable findings obtained with gas exchange dependent techniques and the unlikely probability that diffusion limitation would occur during exercise in normoxia, $\dot{V}/\dot{Q}$ mismatch and diffusion limitation have classically been identified as the only contributing factors to pulmonary gas exchange inefficiency that occurs during exercise. This represents the current dogma for factors affecting pulmonary gas exchange efficiency at rest and during exercise in healthy humans.

Rather than using gas exchange-dependent techniques, such as the MIGET and 100% oxygen technique, we and others have used anatomic based techniques such as

detecting intravenously injected microspheres in the pulmonary venous effluent, detecting intravenously injected radio-labeled macroaggregates outside of the lung using gamma camera imaging, and detecting intravenously injected microbubbles in the left ventricle using saline contrast echocardiography to consistently demonstrate that large diameter intrapulmonary arteriovenous anastomoses (IPAVA) exist in the lung under a variety of conditions (99, 129, 151, 172). Large diameter IPAVA in healthy human lungs could allow blood to bypass the classically-considered alveolar-capillary gas-exchanging unit and theoretically act like a shunt. These pathways are suggested to be closed at rest, but open in healthy human lungs during exercise (32, 159) consistent with conditions when pulmonary gas exchange efficiency worsens and consistent with microsphere data in dogs (156). However, when subjects breathe 100% oxygen during exercise, these large diameter IPAVA are suggested to be closed (97). Thus, if IPAVA were contributing to pulmonary gas exchange inefficiency during exercise in normoxia, using the 100% oxygen technique to detect contributions due to shunt would close IPAVA and at least partially explain why intrapulmonary shunt is not detected using this gas-exchange dependent technique (178).

STATEMENT OF PROBLEM

Despite decades of research that either unknowingly or unwillingly failed to recognize the existence and potential importance of IPAVA, our understanding of their regulation and significance in the human pulmonary circulation remains rudimentary at best. Exercise and/or hypoxic gas mixtures open large diameter IPAVA, however the mechanism(s) underlying the opening of these pathways are not known. Once open, their role in pulmonary gas exchange efficiency remains controversial. The classical

understanding of the contributing factors to pulmonary gas exchange inefficiency is rooted in gas exchange-dependent techniques (MIGET and 100% oxygen) that demonstrate variable and/or inconsistent results. Specifically, these results are not consistent with the extensive anatomic-based studies that preceded these gas-exchange dependent techniques for over 100 years, which directly demonstrated the existence of large diameter IPAVA. The diffusion gradient needed to reach the blood flowing through the center of a large diameter IPAVA could theoretically prevent at least some of the blood flowing through IPAVA from participating in pulmonary gas exchange and it could therefore act like a shunt. However, a negative contribution to pulmonary gas exchange efficiency by IPAVA has not been directly demonstrated.

PURPOSE AND HYPOTHESES

The purpose of this dissertation is to identify potential mechanisms regulating the patency of intrapulmonary arteriovenous anastomoses and determine their physiologic significance, if any, in healthy humans.

Aim #1

The mechanism(s) regulating the opening and closing of IPAVA are currently unknown. However, a common link between their opening during exercise or when breathing hypoxic gas mixtures at rest, and their closure when breathing hyperoxic gas mixtures during exercise may be activation of the sympathetic nervous system. Binding of epinephrine to β-receptors in the pulmonary vasculature can lead to vasodilation (101), however binding to α-receptors may cause vasoconstriction and increased resistance (123). The balance between these competing influences appears to favor binding to α-receptors during normal tone, but binding to β-receptors during increased tone and may

play a role in determining blood flow through IPAVA. The plasma concentration of Dopamine also increases during exercise and binds to dopaminergic, β- and α-receptors and therefore has the potential to affect IPAVA patency as well. Therefore, **Aim #1** tested the hypothesis that the intravenous infusion of epinephrine or dopamine opens IPAVA in subjects at rest breathing (A) room air and (B) 100% oxygen as detected by saline contrast echocardiography.

Aim #2

Using saline contrast echocardiography in exercising subjects breathing 100% oxygen demonstrates a reduction or elimination of microbubbles in the left heart. However, no studies have attempted to directly quantify a reduction in blood flow through IPAVA during exercise in subjects breathing 100% oxygen. Therefore, **Aim #3** used planar Gamma-camera imaging of ^{99m}Technetium labeled macroaggregated albumin (^{99m}Tc-MAA) to test the hypothesis that breathing 100% oxygen during exercise reduces blood flow through IPAVA. To do this, subjects were injected with filtered ^{99m}Tc-MAA during three separate conditions and then immediately underwent planar scanning using a dual-headed Gamma camera to simultaneously acquire anterior and posterior images. The three conditions included: (1) at rest and (2) during cycle-ergometer exercise breathing room air and (3) during cycle-ergometer exercise breathing 100% oxygen.

Aim #3

In order for blood flowing through IPAVA to act like a shunt and contribute to the widening of the $AaDO_2$, that blood must not fully participate in pulmonary gas exchange. **Aim #3** tested the hypothesis that blood flowing through IPAVA negatively contributes to pulmonary gas exchange efficiency by acting like a shunt. To do this we measured the

$AaDO_2$ in subjects at rest and during cycle-ergometer exercise while breathing 40% oxygen when contributions from diffusion limitation and V/Q inequality are eliminated, leaving only shunt (IPAVA and post-pulmonary) as a possible factor affecting pulmonary gas exchange efficiency.

The hypotheses of these three Aims will be tested in Chapters IV-VI, respectively of this dissertation. Chapter IV is in review with the *Journal of Applied Physiology* and Jonathan E. Elliott, Randall D. Goodman, and Andrew T. Lovering are co-authors. I performed the experimental work and the methods were developed equally between all authors. The writing is entirely mine. J.E. Elliott and A.T. Lovering provided editorial assistance. In Chapter V, the manuscript is in preparation for publication in *Journal of Applied Physiology* with Randall D. Goodman, Dixie Aaring, Thomas Voelkel, Scott Stewart, Toni Bamford, Igor M. Gladstone, Mathews I. Fish, and Andrew T. Lovering as coauthors. I performed the experimental work along with the help of all coauthors. The writing is entirely mine and co-authors provided editorial assistance. In Chapter VI, the manuscript is in preparation with Jonathan E. Elliott, Kara M. Beasley, Randall D. Goodman, Igor M. Gladstone, Jerold M. Hawn, and Andrew T. Lovering as coauthors. Drs. I.M. Gladstone and J.M. Hawn placed the radial artery catheters in all subjects. All other co-authors assisted in data collection. A.T. Lovering helped develop the protocols and provided editorial assistance. R.D. Goodman performed all echocardiography and Doppler ultrasound measurements for all experiments.

CHAPTER II

REVIEW OF THE LITERATURE

INTRODUCTION

This review of pertinent literature was designed to present a comprehensive understanding of pulmonary vascular control and begins with pulmonary vascular development and the regulation of blood flow during various physiological perturbations such as exercise or breathing hyperoxic or hypoxic gas mixtures. Next, the historical anatomical precedent for the existence of IPAVA is presented before describing recent work using saline contrast echocardiography which frame our current, yet limited understanding of the regulation of IPAVA. This foundation led to the development of the studies discussed in Chapters IV and V of this dissertation, which investigate the possible mechanisms regulating the opening of IPAVA as well as quantification of blood flow through these unique vessels. Finally, this chapter shifts from pulmonary vascular control to pulmonary gas exchange efficiency where I describe the inconsistencies surrounding the accepted factors affecting pulmonary gas exchange efficiency. Together, these data underscore the need to establish whether or not IPAVA play a significant role in affecting pulmonary gas exchange efficiency.

PULMONARY VASCULATURE DEVELOPMENT

Blood flow returns from the systemic circulation to the right side of the heart where it is pumped into the pulmonary circulation before it returns to the left side of the heart to be pumped into the systemic circulation. This design places the lung in series with the systemic circulation and creates a unique feature by which the pulmonary circulation receives the entirety of the cardiac output. Accordingly, pulmonary vascular

control and blood flow regulation are important for maintaining the efficient matching between alveolar ventilation and pulmonary blood flow, while maintaining a pressure about 1/5 that of the systemic circulation.

The pulmonary vascular tree develops in coordination with a branching airway tree to closely match lung airways with pulmonary vasculature and thus provide maximal surface area for gas exchange to occur (155). Branches of pulmonary arteries continue to narrow, ultimately distributing into a fine capillary network that envelops alveoli like a sheet, allowing red blood cells to pass virtually single file through capillaries. Even when the transpulmonary vascular pressure is greatest in Zone III conditions, the mean capillary diameter is only 6.5μm, with the greatest never exceeding 13μm (45). This fine network of pulmonary capillaries creates an extremely large surface area for the diffusion of gases to occur between capillary blood and alveolar air, while also acting as a physical sieve to prevent the passage of thrombi into the systemic circulation, a second critically important task of the pulmonary microcirculation.

The branching from the pulmonary artery into arterial branches has been described by two main types of vessels: (a) conventional arteries, which run along the airways and branch into terminal arterioles which feed the capillary bed; and (b) supernumerary arteries, which branch from conventional arteries at ninety degree angles, do not have accompanying airways, and take a shorter and more direct route to the capillary bed (34, 148, 155). While the matched branching of conventional arteries with successive airway generations intuits to provide the best possible chance for the exchange of gases, it is unclear what benefit supernumerary arteries provides to the overall pulmonary vasculature design. Additionally, supernumerary arteries may account for up

to 40% of the total pulmonary arteries, appear poorly perfused under resting conditions, and contain a sphincter (34) or baffle valve (148) that could allow for selective regulation of blood flow through supernumerary arteries and thus actively influence the regulation of pulmonary blood flow and/or pressure (21). The entrance to supernumerary arteries has been measured to be as large as 800-1,000μm in diameter, narrowing to 50-200μm in diameter at their distal end. Thus, these vessels have the potential to greatly influence total pulmonary vascular resistance if blood flowing through these vessels bypasses the fine capillary network and anastomoses to the pulmonary venous circulation. Unfortunately, after the initial description of these vessels in 1965, a total of only five studies have been undertaken to specifically investigate the mechanisms responsible for the regulation of blood flow through these vessels (21, 147, 148, 174, 175), a few studies have investigated the role these vessels may play in the development of arterial lesions in pulmonary hypertension (13, 42, 201), and only one has included these vessels in models of pulmonary arterial and venous trees in an attempt to uncover the functional significance of supernumerary arteries (22). Outside of these few studies, very little is known about supernumerary arteries and therefore studying these vessels represents a vast area for future research into pulmonary vasculature control.

PULMONARY BLOOD FLOW REGULATION

In Chapters IV-VI of this dissertation I detail my studies of human subjects at rest and during exercise while breathing various gas mixtures containing normal, increased, and decreased concentrations of oxygen. Additionally, some of my previous work investigating IPAVA regulation had subjects breathe hypoxic gas mixtures at rest (89). Thus, it is important to highlight the pulmonary hemodynamic responses to these types of

physiologic perturbations in order to place IPAVA responses in context of known pulmonary vascular responses.

Exercise

During exercise cardiac output can increase up to six-fold and, in order to prevent excessive rises in pulmonary artery pressure, blood flow resistance through the pulmonary vasculature must decrease. This is traditionally thought to be achieved, in part, through an increase in left atrial pressure which helps to recruit and distend the pulmonary vasculature and results in adequate red blood cell transit time and diffusing area through pulmonary capillaries for the complete diffusion of oxygen into the blood while maintaining a low driving pressure at the delicate alveolar-capillary interface (135, 181). IPAVA are also recruited during exercise, as first demonstrated in exercising humans using saline contrast echocardiography (32), and subsequently using large diameter microspheres in exercising dogs (156). In Chapter VI, I present data from exercising subjects who demonstrate greater bubble scores with increasing exercise intensity, suggesting a graded response by IPAVA as pulmonary pressures and flows increase. However, it is not known if the increase in left atrial pressure is also the direct cause of IPAVA recruitment, or if there is some other mechanism regulating blood flow through these unique vessels. Still, the physiologic benefit of blood flow through IPAVA has not been determined.

Gravity

It seems logical that another acute perturbation that could effect pulmonary blood flow distribution would be the effects due to gravity, such as when in the supine versus standing position. Over 50 years ago it was first suggested that gravity might be the

primary determinant of the distribution of blood flow throughout the lung and multiple studies demonstrated support for such a concept (81, 195, 196). However, in what appears to be a theme in respiratory physiology, debate surrounding the role of gravity in determining pulmonary perfusion continues (46, 76). Evidence is mounting that there is a greater genetic basis to the anatomical heterogeneity of blood flow distribution and that gravity plays more of a minor role in blood flow distribution (11, 47-49, 51, 57, 68, 113). Additional evidence in support of a minimal role for gravity in determining blood flow distribution comes from studies in which the gravitational force was altered and blood flow distribution was measured. Glenny and colleagues flew with piglets in the NASA KC-135 aircraft which flies in a series of parabolas to create alternating weightlessness and gravity 1.8 times greater than normal (50). After injecting 15.5 μm diameter microspheres during conditions of weightlessness (0G), normal gravity (1G), and hypergravity (1.8G), the lungs were removed, dried, cut into 2-cm^3 cubes, and blood flow to each cube was determined. This study revealed that the slope of the perfusion gradient of blood flow down the lung was the same in 0G, 1G, and 1.8G conditions, suggesting that the vertical pressure gradient due to gravity does not explain the blood flow distribution pattern from the apices to the base of the lung. Additionally, I believe one of the most striking studies to demonstrate how pulmonary blood flow distribution can be influenced to a greater degree by factors other than gravity measured pulmonary blood flow distribution in human subjects spun in a human centrifuge to create hypergravity three times normal gravity (3G) and demonstrated blood flow distribution moving from the dependent to the nondependent region of the lung as gravitational forces increased in the opposite direction (120)!

While we have not (yet) studied blood flow through IPAVA in human subjects in a human centrifuge or while riding in a plane flying in a parabolic pattern, we do have some data to suggest that in resting subjects, moving from the supine to upright position can alter blood flow through IPAVA. Over the past 5 years we have screened ~200 subjects in the left lateral decubitus position for presence of a patent foramen ovale (PFO) using saline contrast echocardiography. We have found that in a normal, healthy, asymptomatic population, ~33% of subjects demonstrate 1-3 bubbles appearing in the left heart not due to a PFO, suggesting patent IPAVA. We invited 15 of these subjects back to the lab for further testing up to 13 months after their initial screening and all demonstrated the same indication of a patent IPAVA at rest while in the left lateral decubitus position. After these subjects stood upright another bubble injection was performed and 14/15 subjects no longer demonstrated open IPAVA. These data may suggest that the location of large diameter IPAVA are in the apices of the lung and that moving from supine to upright posture reduces blood flow to the apices, and thus reduces blood flow through IPAVA. This hypothesis gains support from early anatomical work by Tobin and Zariquiey in which large diameter arteriovenous anastomoses were visualized in the apices of the lung (172), and more recently by Stickland, *et al* who also demonstrated a postural effect in subjects studied using saline contrast echocardiography (159).

Hypoxia

In addition to the exercise-induced increases in pulmonary artery blood flow and pressure, vasoactive agents in alveolar air or mixed venous blood can influence pulmonary vascular tone and redistribute blood flow. In 1946 von Euler and Liljestrand

were the first to demonstrate that ventilating cats with low oxygen increased pulmonary artery pressure and suggested that oxygen was having a direct effect on pulmonary vascular smooth muscle to cause vasoconstriction (179). The following year Motley, *et al.* (112) demonstrated hypoxic pulmonary vasoconstriction in man breathing 10% oxygen and since then there has been an extensive amount of work conducted to identify the mechanisms that underlie hypoxic pulmonary vasoconstriction (HPV). The initiation of HPV was debated in the *Journal of Applied Physiology* Point:Counterpoint series (189, 191) and directly confronted the notion that hypoxia results in a greater production of reactive oxygen species (ROS) by the mitochondrion, which acts as the primary sensor of hypoxia. It is, however, accepted that hypoxia inhibits the $K_{V1.5}$ channels (5, 190) which leads to an increase in intracellular Ca^{2+} through both L-type Ca^{2+} channels (39) as well as store-operated Ca^{2+} channels (187), and ultimately leads to constriction of pulmonary vascular smooth muscle cells in distal pulmonary arteries to cause vasoconstriction (1). This represents a response that is opposite that of the systemic circulation, in which systemic arterioles dilate in response to reduced oxygen tension in order to increase blood flow and preserve oxygen delivery. The depolarization of pulmonary artery smooth muscle cells is not endothelium-dependent; however, the endothelium may release an unidentified agent that can modulate the response to hypoxia (2). Thus, the oxygen sensor for HPV is believed to reside within the pulmonary artery smooth muscle cell itself.

Smooth muscle cells in smaller pulmonary arteries demonstrate the greatest contraction response, while larger arteries do not respond to hypoxia in the same fashion (103, 104). Because it is the smooth muscle cell itself that is detecting and responding to low PO_2, the majority of the stimulus for these myocytes is due to hypoxic alveolar gas,

however hypoxemic mixed venous blood returning to the lungs from the systemic circulation also contributes to the total vasoconstrictor response (105, 106). This response to hypoxia begins within seconds, but full hypoxic pulmonary vasoconstriction develops over two hours or more (31), suggesting there to be a rapid phase and slow phase to HPV (168). Interestingly, $K_{V1.5}$ mRNA and protein are expressed to a greater degree in small (<40 μm) compared to large (100-200 μm) distal pulmonary arteries (6), and longitudinal differences between proximal conductance arteries and more distal resistance arteries in Ca^{2+} channel density (39) suggest a location-dependent effect of HPV based on potassium depolarization and/or calcium channel density.

An extremely thorough, extensive, and up to date review on HPV was recently published (166) that integrates much of the recent cellular and molecular work that has been accomplished in the past few decades. While it highlights the effects of hypoxia on pulmonary vascular smooth muscle and helps clarify some of the controversy that exists regarding the mechanisms required for HPV to occur, the exact mechanism initiating HPV remains incompletely understood.

While this vasonconstricting response to hypoxia appears unique to the pulmonary vasculature, IPAVA in humans, dogs, and rats operate similarly to systemic vessels and open in response to hypoxia (10, 89, 115). We speculated that IPAVA could be remnant fetal vessels similar to the ductus arteriosus which is patent during fetal development when the PO_2 is much lower than in the adult (149) and constricts in response to high levels of oxygen (37, 176). One major difference between the ductus arteriosus and IPAVA, however, is that after closure it becomes the ductus ligamentum and does not retain the ability to dilate in hypoxic conditions.

A final note of interest regarding hypoxia and the recruitment of IPAVA is that while increases in left atrial pressure are believed to recruit and distend pulmonary capillaries with the onset of exercise, left atrial pressure does not appear to increase in response to hypoxia (54). Thus, this potential recruitment mechanism for IPAVA in hypoxia appears unlikely.

Hyperoxia

In addition to low oxygen, high oxygen tension also causes a redistribution of pulmonary blood flow. Using a sheep model, Melsom, *et al.* (110) injected 15μm microspheres into sheep ventilated with either hypoxia (FIO_2=0.12) or hyperoxia (FIO_2=0.40) for 10 min and demonstrated a low correlation between local flow in normoxia and exposure to hypoxia that was similar to the correlation between normoxia and hyperoxia. Similarly, an increase in $\dot{V}/\dot{Q}$ heterogeneity was seen in pigs ventilated with both hypoxic (FIO_2=0.09) and hyperoxic (FIO_2=0.50) gas mixtures as well (64). Because hypoxic pulmonary vasoconstriction is not contributing to blood flow heterogeneity in human subjects breathing room air (4), the above data would suggest that hyperoxia is altering the distribution of pulmonary blood flow through a mechanism other than simply reducing hypoxic pulmonary vasoconstriction. The mechanism(s) causing the hyperoxic redistribution of pulmonary blood flow are unknown.

ANATOMICAL EVIDENCE FOR PULMONARY ARTERIOVENOUS ANASTOMOSES

In 1939 a review of anatomical literature by Clara (24) listed numerous systemic vascular beds that contain arteriovenous anastomoses including the skin, nose, ear, ovary, kidney, stomach, small intestine, and brain. Further evidence for arteriovenous

anastomoses in the systemic circulation exists in dogs (93), the human ear (127), and dog, sheep and goat tongue (126, 128). Thus, in addition to the conventional and supernumerary arteries in the pulmonary circulation which both deliver blood flow to the capillary bed, intrapulmonary arteriovenous anastomoses may also be a component of the normal pulmonary vasculature that would allow some of the blood to bypass the capillary-alveolar interface. Prinzmetal and colleagues first demonstrated large diameter arteriovenous anastomoses existed in the heart when glass spheres of 10-400μm injected into the left coronary artery were recovered from the coronary sinus, ranging from 70-170μm (130). This same group also injected glass microspheres into rabbit liver, dog spleen, and rabbit, dog, and cat lungs which were then retrieved from the venous effluent, signifying that the microspheres passed through large diameter arteriovenous anastomoses (129). Also using the glass microsphere technique, IPAVA were identified in dogs (115) and post-mortem human lungs (170, 172). In fact, anatomic descriptions based on plastic casts made by Tobin indicate the presence of arteriovenous shunts to be in the apex of the lung, in the form of a loop, lacking muscle or elastic tissue in their walls, and large enough to allow passage of 200μm glass spheres (170). By 1953 it was, "generally accepted that arterio-venous anastomoses exist in the lungs" (151). Unfortunately, while their existence appeared "generally accepted," their significance remained unknown. Possibly for this reason, or due to attempts to explain pulmonary gas exchange efficiency, which failed to demonstrate a role for intrapulmonary shunting, the existence of these apparently ubiquitous vessels was ignored, disregarded, and forgotten for the next few decades. Recently, additional microsphere evidence in dogs, isolated human and baboon lungs, and rats has brought these potentially important vessels back

into the discussion of pulmonary vasculature (10, 99, 156), while nuclear medicine imaging of ^{99m}Tc-labeled macroaggregates of albumin (^{99m}Tc-MAA) in healthy humans breathing room air have *quantified* an increase in blood flow through exercise-induced IPAVA (96, 197). Not surprisingly, controversy about the existence of and role for these vessels has emerged (71, 95).

INTRAPULMONARY ARTERIOVENOUS ANASTOMOSES DETECTED USING SALINE CONTRAST ECHOCARDIOGRAPHY

Another anatomic-based technique called transthoracic saline contrast echocardiography (TTSCE) has been used to study IPAVA in healthy humans (32, 35, 89, 94, 97, 157). TTSCE uses ultrasound to visualize the heart while air bubbles in saline are injected into an arm vein. These bubbles travel in the venous blood returning to the right side of the heart and appear as a "cloud of echoes". As this blood with bubbles in it then travels through the pulmonary circulation, the small diameter capillaries act as a sieve to filter out the microbubbles and prevent them from returning to the left side of the heart. However, when large diameter IPAVA open, they provide a pathway for the bubbles to bypass the pulmonary capillaries and these bubbles subsequently return to the left heart and thus the patency of IPAVA can be non-invasively determined using this anatomic-based technique.

Using this technique we and others have demonstrated that IPAVA are closed at rest, but open in healthy humans during exercise (32, 159) or in resting subjects breathing low levels of oxygen (hypoxia) (89). However, when subjects breathe 100% oxygen during exercise, bubbles do not appear in the left heart, suggesting that large diameter IPAVA are closed (97). However, while these studies demonstrated the existence and

provided potential insight into the regulation of arteriovenous anastomoses in the pulmonary circulation, their physiologic roles as part of the normal pulmonary circulation are not yet proven.

PULMONARY GAS EXCHANGE EFFICIENCY

If blood flow through these large diameter arteriovenous anastomoses does not fully participate in pulmonary gas exchange, then IPAVA could act like a shunt and contribute negatively to pulmonary gas exchange efficiency. However, as I will describe below, a technique developed to investigate the role of shunt in pulmonary gas exchange efficiency ruled out such a possibility and consequently, much of the anatomical data collected over multiple decades has been essentially disregarded or forgotten.

We have speculated that large diameter IPAVA divert blood flow away from the alveoli and pulmonary capillaries and thus reduce pulmonary gas exchange efficiency, but no study has directly determined if the opening of IPAVA negatively affects pulmonary gas exchange efficiency as defined by the $AaDO_2$. Therefore, in order to identify why the $AaDO_2$ is not perfect at rest and increases during exercise (7, 29, 30), the potential factors contributing to pulmonary gas exchange inefficiency will be considered below, followed by any support for these factors found in the literature.

Potential Factor – $\dot{V}/\dot{Q}$ Mismatch

The matching of alveolar ventilation ($\dot{V}$) and pulmonary blood flow ($\dot{Q}$) is fundamentally necessary for the maintenance of pulmonary gas exchange efficiency and prevention of arterial hypoxemia. Thus, the significant alveolarization and microvascular growth and development that occur postnatally involve a coordination of growth via a cross talk of paracrine signals, such as the release of vascular endothelial growth factor

from alveolar epithelial cells to stimulate the associated microvascular development (19, 155). Further regional matching of ventilation and perfusion may be occurring via hypoxic pulmonary vasoconstriction, which occurs through direct effects of oxygen on the vascular wall of both the pulmonary arterioles and venules, with contributions from both the alveolar PO_2, as well as the mixed venous PO_2 (12, 14, 15, 38). The goal of this matching is to help divert blood flow away from poorly ventilated areas and towards areas with a higher driving pressure of oxygen to result in complete equilibration between alveolar PO_2 and end capillary PO_2 (118). However, in humans resting at sea level this does not appear to play a role in determining perfusion heterogeneity (4). Therefore, at rest when both ventilation and perfusion are well below their maximum capacities and local matching due to hypoxic pulmonary vasoconstriction contributes minimally, a normal resting $AaDO_2$ of 6 Torr could be entirely accounted for by a fixed postpulmonary shunt from the Thebesian and bronchial circulations (see below) of 1.5% of the cardiac output (assuming PAO_2=103 Torr, $P\bar{v}O_2$=40 Torr, and normal body temperature and partial pressure to saturation relationships (83)) without negative contributions from $\dot{V}/\dot{Q}$ mismatch.

Potential Factor – Diffusion Limitation

At rest, the transit time of red blood cells within the pulmonary capillary is sufficiently long for the complete diffusion of oxygen as indicated above in the *Introduction*. With the onset of exercise, the increase in left atrial pressure that occurs in concert with the increase in cardiac output recruits and distends pulmonary capillaries to increase capillary blood volume and minimize the reduction in transit time of red blood cells flowing past the alveolar-capillary interface (135). Because the complete

equilibration of oxygen between the alveoli and pulmonary capillary blood occurs in ~0.25 sec, a diffusion limitation due to insufficient transit time stemming from increased cardiac output seems highly unlikely, even at maximal exercise in subjects breathing room air (181).

Potential Factor – Shunt

Any right-to-left shunt will allow venous blood to directly mix with blood that has already participated in gas exchange, thus lowering the PO_2 in that mixed blood. Sources of anatomic right-to-left shunt include intracardiac, such as a patent foramen ovale (PFO), postpulmonary, such as the drainage from the Thebesian and bronchial circulations, and intrapulmonary, such as pulmonary arteriovenous malformations. The most comprehensive autopsy study detected a probe-patent PFO incidence of 27.3% in the general population (56), while echocardiography bubble studies indicate similar incidence of 25-30% (150, 200). Thus, ~1/3 of the population could have an anatomic right-to-left shunt between the right and left atrium which could negatively affect pulmonary gas exchange efficiency. At rest, there is a small, but significant increase in the $AaDO_2$ in PFO positive subjects, however no difference during exercise, possibly due to increases in left atrial pressure preventing blood from flowing into the left atrium (98). This suggests that the presence of a PFO does not explain why the $AaDO_2$ widens during exercise. All individuals, however, do have an anatomic right-to-left shunt stemming from the venous drainage of the Thebesian and bronchial circulations, which return some of their venous blood directly to the left side of the heart (8, 90, 171). Attempts to directly quantify this blood flow utilizing the 100% oxygen technique are difficult to accurately measure due to errors associated with measuring the high PO_2, but range from 0.18-2.2%

of the cardiac output (58, 173, 182). Finally, a significant body of anatomical based evidence demonstrates the existence of large diameter IPAVA (32, 89, 99, 115, 129, 131, 156, 157, 172) and if blood flowing through these anastomoses did not participate in gas exchange with an alveolus, it would result in a shunt and cause a reduction in pulmonary gas exchange efficiency.

Experimental Evidence Supporting These Factors

The classical understanding of the partitioning of possible contributing factors ($\dot{V}/\dot{Q}$ mismatch, diffusion limitation, and shunt) to pulmonary gas exchange inefficiency is based on data collected at rest and during cycle ergometry exercise using the multiple inert gas elimination technique (MIGET) (184, 185) and the 100% oxygen technique. These data suggest $\dot{V}/\dot{Q}$ mismatch accounts for the pulmonary gas exchange inefficiency at low and moderate exercise intensities, with an additional contribution from diffusion limitation only at higher levels of exercise intensity (>250-300W). Furthermore, these studies have measured a variable degree of postpulmonary shunt (~0.18-2.2% of cardiac output) and a non-significant or undetectable contribution from intrapulmonary shunt, neither of which are suggested to contribute to the $AaDO_2$ (58, 173, 182).

The MIGET determines contributions from $\dot{V}/\dot{Q}$ mismatch and shunt to pulmonary gas exchange inefficiency by quantifying the distribution of retention and excretion of six inert gases of varying solubility (184, 185). Theoretically, these gases should be retained and excreted in a predictable pattern that depends on the $\dot{V}/\dot{Q}$ heterogeneity of the lung, including regions of shunt.

In Chapter VI of this dissertation I describe in great detail the high variability in results that MIGET has detected between multiple studies and will only highlight some of these results in this section.

Briefly, if the measured $AaDO_2$ exceeds that predicted from $\dot{V}/\dot{Q}$ and shunt by the MIGET, the assumption is put forth that the remainder of the $AaDO_2$ is caused by a combination of postpulmonary (bronchial and Thebesian) shunt and diffusion limitation because the MIGET cannot detect these contributions which will, without a doubt, cause the $AaDO_2$ to widen. While $\dot{V}/\dot{Q}$ mismatch has been suggested to increase with exercise intensity at sea level, this often does not reach significance, especially at lower workloads, while some subjects demonstrate no increase in $\dot{V}/\dot{Q}$ mismatch during exercise, yet the $AaDO_2$ consistently widens (122, 136, 144, 182). Consequently, the explanation for the widening of a significant portion of the $AaDO_2$ falls on the assumption of a diffusion limitation despite neither a direct measurement of such impairment, nor any other support that such diffusion limitation to oxygen could theoretically or even likely occur (154, 181), while intrapulmonary and postpulmonary shunt are considered negligible contributing factors.

Non-capillary Gas Exchange

It is not entirely clear why the MIGET technique demonstrates such variable results regarding $\dot{V}/\dot{Q}$ mismatch or why an assumed diffusion limitation is accepted when a large body of evidence suggests an alternative explanation that IPAVA could be diverting blood flow away from the pulmonary gas exchange unit and acting as a shunt. A potentially critical flaw in the overall analysis of the excretion and retention pattern of the MIGET gases fails to account for interactions occurring between the airways and

arterioles which would influence the overall excretion and retention profile of inert gases (44, 153). This possibility of conducting airway gas exchange identifies only one problem in the attempts to quantify pulmonary gas exchange using a gas exchange-dependent technique that must rely on assumptions about the locations of inert gas exchange, which may be at best over-simplified and at worst incorrect.

100% Oxygen Technique

Another assumption used to support the lack of intrapulmonary shunt detection by the MIGET was by Vogiatzis, *et al* who attempted to quantify intrapulmonary shunt in subjects exercising while breathing 100% oxygen and apply that shunt fraction to normoxic exercise. The assumption was that breathing 100% oxygen was not causing any alteration to the pulmonary vasculature that could affect the quantification of shunt (143, 178). However, as stated above in *Aim #1*, hyperoxia appears to dynamically close IPAVA (97) as well as cause a redistribution in pulmonary blood flow (110). In this situation, any potential contributions from IPAVA to the $AaDO_2$ would not be detected and the 100% oxygen technique would only detect post-pulmonary and intracardiac shunt contributions.

In summary, the MIGET has been used to quantify the contributions from $\dot{V}/\dot{Q}$ mismatch and shunt to pulmonary gas exchange inefficiency and assumes that any gas exchange inefficiency not explained by these two factors can only be due to a diffusion limitation. Anatomical data demonstrate that large diameter intrapulmonary arteriovenous anastomoses exist in the pulmonary circulation that could theoretically act like a shunt, but the MIGET and the 100% oxygen technique do not detect shunt as a contributing

factor during exercise. Thus, the role of IPAVA acting as shunts remains a controversial, not yet proven hypothesis.

For these reasons, we believe, the potential role for IPAVA in affecting pulmonary gas exchange efficiency have been prematurely disregarded and discounted. However it is exactly because of the inconsistency in results by MIGET, along with the clear anatomic evidence that IPAVA have the potential to play a role in pulmonary gas exchange efficiency that the core understanding of factors affecting pulmonary gas exchange efficiency *must* be reconsidered and modified to reflect the totality of the pulmonary vasculature. The innovative approach used in this dissertation to quantify the contributing factors to pulmonary gas exchange inefficiency is entirely novel and directly challenges the prevailing understanding of factors contributing to pulmonary gas exchange inefficiency.

CHAPTER III

METHODS

INFORMED CONSENT

All protocols completed as part of this dissertation were approved by the University of Oregon Office for Protection of Human subjects. The nuclear medicine study in Chapter V was conducted in part at the Oregon Heart & Vascular Institute and received additional approval by the PeaceHealth Institutional Review Board and the State of Oregon Radiation Safety Board. I verbally discussed all procedures, risks, and benefits with every subject and each subject provided written informed consent prior to participation.

PATENT FORAMEN OVALE SCREENING

The foramen ovale is an opening in the fetal circulation that allows blood to flow from the right atrium to the left atrium of the heart. After birth, the resistance to blood flow through the pulmonary circulation drops, reducing pressure on the right side of the heart to less than that on the left side of the heart. Consequently, a flap of tissue covers the foramen ovale and seals it to prevent blood from flowing into the left atrium. However, in ~1/3 of the population, this flap of tissue does not completely seal, resulting in a patent foramen ovale (PFO) and the potential for blood to continue to flow from right to left atrium (56). Saline contrast echocardiography is a technique developed to determine if an individual has a PFO. This technique involves placing an ultrasound probe against the chest near the apex of the heart and directing the ultrasound beam up through the apex towards the base of the heart. This placement allows all four chambers of the heart to be visualized and the tissue is displayed as white, while the blood appears

black and does not reflect the ultrasound. This view is called the apical four-chamber view. The ability to accurately image the apical four-chamber view (as well as measure the peak velocity of the tricuspid regurgitation, detailed below) of a beating heart under the variety of conditions presented in this dissertation (i.e. drug infusions or exercise) is technically difficult and was accomplished by a licensed registered diagnostic cardiac sonographer with 25 years experience, including 5 years conducting research with our group.

To detect the presence of a PFO, saline and air are agitated back and forth between two 10ml syringes. This agitation creates microbubbles which are rapidly and forcefully injected into a peripheral arm vein. These saline microbubbles travel in the venous blood and enter the right side of the heart. Saline microbubbles are echogenic and reflect ultrasound. Thus, while imaging the heart in the apical four-chamber view, saline microbubbles appear in the right heart as a cloud of echoes. If an individual has a PFO, microbubbles have a pathway to travel through the opening between the two atria and can rapidly appear on the left side of the heart. The appearance of saline microbubbles in the left side of the heart within three cardiac cycles of their initial appearance in the right heart is a positive test for a PFO. Those bubbles not passing through a PFO flow into the pulmonary artery and into the pulmonary microcirculation.

Upon injection of microbubbles into the blood, the gas inside the bubbles begins rapidly diffusing out of the bubbles, causing them to shrink in size. As the bubbles shrink, the surface tension increases, causing the bubble to be less stable, ultimately leading to its total diffusion into the blood and disappearance (202, 203). Those bubbles that are large enough to maintain their stability are larger than the pulmonary capillaries and become

trapped and eventually completely dissolve, preventing their appearance in the left heart. However, if a large diameter intrapulmonary arteriovenous anastomoses is open, bubbles that are large enough to stabilize have a pathway to bypass the sieve of the pulmonary microcirculation and can eventually flow through to the left side of the heart. Because of the increased time needed for bubbles to flow from the right heart, into the pulmonary circulation and finally return to the left heart, we are able to detect patent IPAVA based on the delayed appearance of saline microbubbles in the left heart. However, if a subject has a PFO, bubbles have the potential to travel through the opening between the right and left atria more quickly than the bubbles traveling through IPAVA. Thus, in subjects with a PFO, it is impossible to differentiate the appearance of bubbles traveling through the PFO and those traveling through IPAVA and thus these subjects must be excluded from participation.

The screening to determine if a subject is positive for the presence of a PFO begins with an initial bubble injection with the subject at rest. Subsequently, we instruct the subject to perform a Valsalva maneuver. This involves bearing down against a closed glottis to increase the intrathoracic pressure for a minimum of 15 sec. This maneuver temporarily prevents blood from returning to the right side of the heart and into the pulmonary circulation, while blood continues to drain from the pulmonary circulation and is pumped to the body. Upon release of the Valsalva maneuver there is a large increase in venous blood returning to the heart, increasing the pressure on the right side of the heart to greater than the pressure on the left side. Thus, the release of this maneuver transiently increases the pressure gradient directed through a potential PFO and provides the best opportunity to detect a PFO. Based on the screenings of ~200 subjects in our lab over the

past five years, this screening procedure has detected a PFO in ~39% of healthy individuals volunteering to participate as research subjects in our lab. Approximately 2/3 of subjects positive for PFO must release this Valsalva maneuver in order to detect blood flow through the PFO. Nevertheless, the detection of a PFO under any condition is an exclusion criterion for participation in research studying IPAVA. Following the PFO screening the cardiac sonographer continued with a general heart screening of all valves and great vessels to ensure there were no signs of cardiac disease or other undiagnosed cardiac abnormality.

PULMONARY ARTERY SYSTOLIC PRESSURE

The gold standard measurement for measuring pulmonary artery pressures involves floating a catheter with a pressure transducer through the right heart into the pulmonary artery and directly measuring pulmonary artery pressures. This, however, is an invasive procedure that cannot be conducted in our campus research setting. Using Doppler ultrasound we can estimate pulmonary artery systolic pressure (PASP), which has been shown to correlate well with direct catheter measurements (62, 204). PASP is the peak blood pressure developed in the pulmonary artery during each cardiac cycle. During systole, or heart contraction, the right ventricle contracts, increasing intraventricular pressure. Once this pressure exceeds the pulmonary artery pressure on the opposite side of the pulmonic valve, blood flows down a pressure gradient and enters the pulmonary artery. The tricuspid valve, which prevents blood from flowing back into the right atrium during systole, has a small leak in almost all individuals. Doppler ultrasound can be used to measure the peak velocity of blood leaking through the tricuspid valve. Using the peak tricuspid regurgitation velocity (v) and the estimate of right atrial pressure

(P_{RA}) an estimate of PASP can be calculated using the modified Bernoulli equation: $PASP = 4v^2 + P_{RA}$ (142). P_{RA} is estimated based on the collapsibility of the inferior vena cava upon a quick inspiration and is assumed to remain constant from rest through exercise. If the inferior vena cava just proximal to the entrance into the right atrium is ≤2.1cm and collapses >50% upon a quick sniff by the subject, right atrial pressure is assumed to be normal (0-5 mmHg) and assigned a value of 3 mmHg. If the sniff results in <50% collapse and the diameter of the inferior vena cava is >2.1 cm, this suggests elevated right atrial pressure (10-15 mmHg) and is assigned a value of 15 mmHg. If either of these values is indeterminate, an intermediate value of 8 mmHg is assigned. Because this technique is actually estimating the peak pressure developed by the right ventricle, any obstruction in the outflow tract of the pulmonary artery could cause this measurement of PASP to overestimate the peak pressure developed in the pulmonary artery beyond the obstruction. However, this limitation is typically not a concern in healthy individuals, and we ensure there is no obstruction during the heart screening.

In subjects with a small tricuspid regurgitation jet, the Doppler waveform of the regurgitation velocity can be difficult to measure. We developed a technique to enhance the ability to measure the jet by injecting a small volume of saline contrast microbubbles to provide additional contrast for the ultrasound beam to reflect off of in addition to the few red blood cells leaking through the valve (62). By doing this "contrast-enhancement" we increased our ability to detect the Doppler waveform developed through the tricuspid valve at rest and during exercise (unpublished observations) and used this technique for all measurements of PASP made for this dissertation.

LUNG FUNCTION

Forced Vital Capacity

The first lung function test performed is known as spirometry and is used to determine how well subjects inhale and exhale air. This test determines the forced vital capacity (FVC), which is the maximum volume of air a subject can exhale with a maximum effort. The American Thoracic Society/European Respiratory Society have created joint guidelines to standardize the maneuver, acceptability, and reproducibility of this test (111). The subject is instrumented with a nose clip and breathes through a low resistance mouthpiece and pneumotach to measure airflow. The subject inhales a rapid and full breath of air and, without a pause, "blasts out the air" fully and completely and continues exhalation for a minimum of 6 sec. Of note, the subject is prompted to "blast" out the air and verbal encouragement is continued throughout the full 6 sec of exhalation.

In addition to the FVC measurement, the volume of air expired in the first 1 sec is the forced expiratory volume in 1 sec (FEV_1). In young healthy individuals the FEV_1/FVC ratio is ~0.80. However, if there is any sort of increased airway reactivity or obstruction, such as asthma, the volume of air expired in the first second will be reduced and consequently the FEV_1/FVC ratio will be reduced.

The rate at which the air is flowing out during the middle portion of the FVC maneuver is referred to as the forced expiratory flow at 25-75% of the FVC (midexpiratory flow, $FEF_{25-75\%}$) and provides a measure of small distal airway function that is mostly independent of subject effort during the maneuver. Individuals with reactivity of their small airways or other obstruction will demonstrate small distal airway

closure earlier than predicted and thus the FEV_1 and $FEF_{25-75\%}$ will be less than predicted based on age, sex, and height.

The validity and reproducibility of the test is determined after a minimum of 3 trials in which the difference between the two largest FVC measurements is ≤0.150 L and difference between the two largest FEV_1 measurements is ≤0.150 L. For all studies carried out for this dissertation, subjects demonstrating an FVC, FEV_1, or FEV_1/FVC ratio less than 90% predicted were excluded.

Slow Vital Capacity

The slow vital capacity (SVC) maneuver is the second lung function test performed by all subjects. This test is conducted by having the subject breathe a minimum of four tidal breaths, ensuring they end each breath at a consistent lung volume, which is determined to be their functional residual capacity (FRC). This lung volume is a result of the balance between the force from the rib cage pulling outward and the elasticity of the lung tissue pulling inward. Once this lung volume is determined, the subjects conduct an inspiratory capacity (IC) maneuver to completely fill their lungs. Once at total lung capacity (TLC) subjects slowly and in a controlled fashion let all of the air out of their lungs, squeezing it out completely. When the expiration is complete and no more air can be forced out of the lung, there is still a volume of air remaining, termed residual volume (RV), which can be measured using another technique discussed in the next section. The volume measured from FRC to RV represents the expiratory reserve volume (ERV). Conducting this vital capacity in a slower maneuver reduces the rate of airway collapse compared to the FVC maneuver and typically results in a slightly larger

vital capacity measurement. The largest SVC measured throughout the testing protocol is chosen for the SVC measurement.

Whole-body Plethysmography

The FVC and SVC are unable to measure the volume of air remaining in the lung at the point when no more air can be expelled and is termed residual volume (RV). The gold standard way of measuring RV uses a technique called whole-body plethysmography. Subjects in studies conducted for this dissertation were seated in a MedGraphics Elite Series Plethysmograph, which is a sealed plexiglass box approximately the size of a phone booth, and they breathed through a mouthpiece and pneumotach. This test began similar to the SVC maneuver with the recording of a minimum of four tidal breaths ending at FRC. The subject as then instructed to begin a "panting maneuver" at a rate between 70-90 pants per min. Once panting in the correct range, a shutter closed to prevent airflow from entering or leaving the mouth. During the 2 sec while the shutter was closed, the subject continued the in-and-out panting and pressure transducers on either side of the shutter measured pressure at the mouth as well as of the box. Because the volume of the box is known, the pressure in the box was measured, and the measured mouth pressure was assumed to equal the intrathoracic pressure, the volume of the thoracic cavity could be calculated based on Boyle's law. This law states that, under isothermic conditions, a volume of a compressible gas will change in relation to the change in pressure such that the product of volume and pressure remains constant. Thus, this measurement determines the volume in the thoracic cavity at FRC. Subtracting the measured ERV from this volume nets RV, and adding RV to the SVC determined TLC.

Diffusion Capacity for Carbon Monoxide

The final test was done to determine if the diffusion of gases between the alveolar air and pulmonary blood is normal (102). To do this, the diffusion capacity for carbon monoxide (DL_{CO}) was conducted using a MedGraphics Elite Series Plethysmograph. The subject began the test by blowing the air completely out of their lungs, down to RV. Next, subjects inhaled a full and breath of a gas mixture containing 21% oxygen with 0.3% carbon monoxide, 0.5% neon, and balance nitrogen. This gas mixture was held for 8 sec and a sample of the exhaled alveolar gas sample was analyzed using a gas chromatograph containing diatomaceous earth to separate the different gas molecules. Based on the difference between the carbon monoxide in the initial gas mixture and that measured in the alveolar gas sample, the volume of gas that diffused into the blood can be calculated. The volume of CO taken up by the blood is standardized to the time of the breath hold, including a portion of time during both inspiration and expiration (80). The resulting value can also be standardized for alveolar volume (V_A, measured during the max inhalation using an estimated deadspace based on height and sex) so that individuals with smaller lung volumes, resulting in a smaller surface area for diffusion, will not result in artificially low measurements of diffusion capacity.

SUBJECT INSTRUMENTATION

Intravenous Catheter

I placed a 20G intravenous catheter (i.v.) (ProtectIV Plus, 20Gx1¼") into a peripheral arm vein for all screening procedures and bubble studies. Two 3-way stopcocks were attached in series to allow for the agitation of 3 ml sterile saline with 1 ml of air to create saline contrast microbubbles.

Radial Artery Catheter

In Chapter VI of this dissertation arterial blood samples were required. To minimize the risk associated with the placement of the radial artery catheter, an Allen's test was conducted to ensure adequate collateral blood flow to the hand. Because both the radial and ulnar arteries provide blood flow to the hand, anastomoses in the palm of the hand connect the two arteries and allow for the ulnar artery to provide the entirety of blood flow to the hand if the radial were blocked or blood was prevented from flowing into the hand. To test the adequacy of these anastomoses to allow the ulnar artery to perfuse the entire hand, both arteries were manually and temporarily occluded. Once the majority of venous blood had drained and the hand appeared blanched in color, the occlusion over the ulnar artery was removed and the return of color depicting the return of blood flow into the hand was visualized. To pass the Allen's test complete reperfusion needed to occur in less than 7 sec. This was always attempted on the subject's non-dominant hand first. If the complete return of blood flow was questionable, the dominant hand was checked and the medical doctor made the final decision on which wrist to use for placement of the arterial catheter.

The placement of a radial artery catheter (20Gx1¾", Arrow International) was placed under local anesthesia (1% lidocaine, 1% by volume nitroglycerine to prevent vasospasm) by a licensed cardiologist (Jerold Hawn) or neonatologist (Igor M. Gladstone). A 20G needle was used to gain access to the artery, and a wire threaded through the needle until the stiff portion of the wire was at the entrance to the artery. After removing the needle, the catheter was threaded over the wire into the artery and the wire removed. The catheter, extension set, and stopcock were subsequently flushed with

~4 ml of heparinized saline (1U/ml) to minimize the possibility of a clot forming in the catheter. This catheter was used for sampling arterial blood for measurement of PO_2, PCO_2, pH, SaO_2, lactate, and hematocrit, see *Arterial Blood Draw and Analysis* for details.

Esophageal Temperature Probe

Determination of body core temperature was necessary to correct blood gas measurements for the increase in body temperature that occurs during exercise. While body temperature can be measured in a variety of ways such as an ingestible thermister pill, rectal temperature probe, or tympanic temperature, these do not respond fast enough to the increase in body temperature occurring during the first few minutes of exercise. Thus, we chose to use the gold-standard measurement of an esophageal temperature probe, which measures temperature from the esophagus immediately next to the heart. I placed the probe (Mon-a-therm General Purpose probe, 7-french) in all subjects. The subject self-administered 1 ml of Lidocaine jelly to coat their nasal passage and back of their throat. I slid the probe up one nostril until the tip could be visualized in the back of their throat. Then, the subject began swallowing small sips of water as I advanced the temperature probe until it was completely in place and only the final 2-3 cm of the probe extended from their nostril, which could be secured to the top of their nose with tape. For subjects with a strong gag reflex that could not tolerate the placement, 1-2 sprays of HurriCaine spray (20% Benzocaine oral anesthetic) were used to temporarily numb the back of throat while the placement occurred. Once in place, the temperature probe remained in place for the duration of the study.

Oxygen Saturation and Heart Rate

Peripheral estimate of arterial oxygen saturation (S_pO_2) and heart rate were measured using a pulseoximeter (Nelcor, Oxymax sensor) with forehead sensor. The sensor contains two light emitting diodes (LEDs) that transmit red and infrared light, respectively, and is placed above the pupil of either eye to shine through blood-perfused tissue. These wavelengths of light are reflected differently by oxygenated and deoxygenated hemoglobin and their ratio of reflected light is used to estimate hemoglobin saturation, while the pulsatile changes in color are used to determine heart rate. The heart rate was also determined from Lead II of the electrocardiogram (ECG) used with echocardiography. A 12-lead was also placed during the infusion of drugs in Chapter IV to monitor electrical activity of the heart more precisely.

ECHOCARDIOGRAPHY MEASUREMENTS

Saline Contrast Echocardiography

For all studies in Chapters IV-VI, transthoracic saline contrast echocardiography (TTSCE) was performed for detection of open IPAVA. The sonographer obtained an apical four-chamber view of the heart, making sure the plane of view sliced through the apex of the heart and the middle of the base of the heart so as to prevent a foreshortened view. For each bubble injection, 20 cardiac cycles were recorded beginning with the appearance of bubbles in the right heart. The sonographer reviewed the entire 20 cardiac cycles and determined the greatest number and/or spatial distribution of bubbles appearing in the left ventricle in a single frame. A 0-5 score was assigned based on the following criteria: 1-3 bubbles received a score of 1; 4-12 bubbles received a score of 2; >12 bubbles appearing in a bolus received a score of 3; >12 bubbles in which the bolus

filled the left ventricle, but was heterogeneous in density received a score of 4; and if the bubbles appearing filled the left ventricle, a score of 5 was assigned. During the first study conducted in our lab, two independent sonographers scored over 100 bubble studies spanning all bubble scores and found perfect agreement on all 100 studies. During preparation of a second manuscript, 57 images were scored by the sonographer and by a licensed cardiologist who was blinded to the conditions and there was 93% agreement. The echocardiograms in which there was disagreement were from images in which either 0 or only 1-3 bubbles appeared throughout the 20 cardiac cycles. A single sonographer scored all bubble scores during the studies conducted for this dissertation.

In Chapter IV, subjects reclined in the left lateral decubitus position and a baseline bubble injection was done before the first infusion of either EPI or DA while breathing room air or 100% oxygen. TTSCE was performed 2-4 min after the start of each infusion rate to allow the heart rate to stabilize, which we used as an indicator that the plasma catecholamine concentration had reached stability.

In Chapter V, subjects were seated on a cycle ergometer in the forward leaning aerobar position for both resting and exercise study visits. For the exercise visits, subjects warmed up for 2 min at 50% of their power output attained at VO_2peak and continued for another 3 min at 85% of their max. The bubble injection was conducted 2 min into the 3 min bout at 85% of their max.

In Chapter VI, the resting bubble injection during the room air bout was conducted in the forward leaning position once the metabolic rate reached a stable respiratory exchange ratio (usually 5-10 min), whereas subjects breathed the hyperoxic gas mixture for 15 min at rest prior to the resting bubble injection during the hyperoxic

bout. During all exercise bouts, subjects exercised for 3.5 min before the bubble injection occurred, which occurred simultaneously with the arterial blood draw (see *Arterial Blood Draw and Analysis,* below).

Pulmonary Artery Systolic Pressure

The peak velocity of the tricuspid regurgitation was measured immediately prior to all bubble injections using the "contrast enhanced" bubble injection described above in the screening details. The average of three velocities was used in determining PASP based on the modified Bernoulli equation: $PASP=4v^2 + P_{RA}$.

Cardiac Output

From the 20 cardiac cycles recorded in the apical four-chamber view during the bubble injection, the sonographer determined end diastolic and end systolic left ventricular volumes from three representative cardiac cycles using the Modified Simpson's technique. This technique is the most common measurement technique for determining volumes and is recommended by the American Society of Echocardiography (88). The endocardial border of the left ventricle is traced from an image frame at end systole and end diastole and is divided into 20 stacked discs based on the height of the long axis of the ventricle. Because we used a single plane (apical four-chamber view) for determining the endocardial border, each disc is assumed to be circular, an assumption that is only a limitation when there is extensive wall-motion abnormalities, which was not demonstrated by any of our subjects. The difference between the end diastolic left ventricular volume and the end systolic left ventricular volume provides an estimate of stroke volume. This value was multiplied by the heart rate obtained from the ECG to determine cardiac output. Because the same sonographer made all measurements on all

subjects for studies conducted throughout this dissertation, any bias or error introduced by the sonographer should have occurred in all measurements and thus the *difference* between various perturbations throughout these studies should be a reliable indicator of changes in cardiac output.

EXERCISE TESTING

Metabolic Rate

All metabolic testing was measured using a MedGraphics CardioO2 metabolic system. Prior to every study a pneumotach was calibrated to 5 varying flow rates using a 3L syringe. A fast responding zirconia oxygen cell and CO_2 infrared analyzer allowed for inspiratory and expiratory concentrations of these gases to be measured and breath-by-breath metabolic analysis with end tidal O_2 and CO_2 partial pressures to be determined. All metabolic measurements reported in this dissertation represent ~15 sec averages.

VO_2peak Testing

In Chapters V and VI subjects exercised on a cycle ergometer (Lode Excalibur Sport) at various workloads, some of which were standardized to a percentage of their max. We set the wattage attained at VO_2peak to 100% and set relative workloads accordingly. After the initial echocardiography and lung function screenings, subjects (all male) reported to the lab for a graded exercise protocol. After being fit on the bike, they warmed up at a self-selected wattage for 5-10 min, during which time an individualized protocol was devised. Each protocol began at 90W and was increased each minute by 20-30W depending on the predicted fitness of the subject. Verbal encouragement was provided and in all cases the test was terminated when the subject could no longer maintain a pedal cadence >80. Retrospective analysis indicated that at the conclusion of

the test respiratory exchange ratio for all subjects was greater than 1.10 and a plateau in oxygen consumption.

Exercise Protocols

In Chapter V our goal was to quantify the amount of blood flowing through IPAVA during exercise and quantify a reduction in blood flow during the same intensity of exercise while the subjects breathed 100% oxygen. Pilot work indicated that having subjects warm up at 50% of their max before progressing to 85% of their wattage attained at VO_2peak would elicit a high bubble score, but also was a workload that could be sustained for a maximum of 3-4 min. Thus, a total of three protocols were required: (1) rest breathing room air; (2) exercise breathing room air; and (3) exercise breathing 100% oxygen. The bike was placed in the same room as the Gamma camera in order to minimize the time between exercise and the start of the scanning and subjects were studied in the forward leaning aerobar position. See *Nuclear imaging and analysis,* below for a complete description of scanning procedures, which occurred immediately after the injection of the radioactive macroaggregated albumin.

In Chapter VI our goal was to determine the role of IPAVA in pulmonary gas exchange efficiency. Because the majority of previous research done in determining pulmonary gas exchange efficiency in healthy individuals has been conducted on male subjects exercising at wattages as high as >300W, we wanted to study a similar population in order to make comparisons between studies. We chose to study subjects exercising at workloads of 100W, 200W, and 300W and a relative workload at 85% of max. We had subjects exercise at each workload for 4 min, with a PASP measurement conducted at 3 min and bubbles injected at 3:30. At the same time as the bubble injection,

a 3 ml radial artery blood sample was drawn into a heparinized syringe and immediately analyzed for PO_2, PCO_2, and pH (see *Arterial blood draw and analysis* for details). We provided subjects with an active break between each of the absolute workloads, typically pedaling at approximately 150W for about 1 min, in order to provide enough time for the blood gas sample to be analyzed in triplicate before the next sample was ready to be analyzed. At the conclusion of the 300W bout, subjects were allowed to continuing spinning their legs to cool down and remained on the bike for a 10 min break. Two min before the conclusion of the break subjects began ramping up the wattage and warmed back up for the final 3.5 min bout at 85% of their max. After measurements were made, subjects took at 45 min break off the bike where they were able to drink water ad libitum. At the conclusion of the break this same protocol of exercise was conducted with subjects breathing 40% oxygen. Subjects breathed the hyperoxic gas mixture for 15 min prior to the arterial blood draw and remained on the mouthpiece throughout the 10 min break in order to ensure a stable respiratory exchange ratio. A second protocol was also undertaken with a different group of subjects exercising for 3-4 min at each 25%, 50%, and 75% of their max wattage in a continuous protocol. Subjects completed this exercise protocol first breathing an FIO2=0.21, then breathing an FIO_2=0.60, and finally breathing an FIO_2=0.14. Each bout was separated by ~45 min.

MEASUREMENT OF BLOOD GASES

Tonometry

The quality control in place for a standard blood gas machine only allows the user to determine if the blood gas electrodes are reading within an appropriate range of acceptable values, but will not allow the user to discriminate between day-to-day

fluctuations in the exact PO_2 or PCO_2 measured. In order to correct for any inherent errors of the blood gas analyzer, I used a gas-liquid tonometer to equilibrate three 6 ml samples of human blood with three known concentrations of O_2 and CO_2. After a 45-60 min equilibration period in a 37°C water bath, a blood sample was drawn from the tonometer and immediately run through the blood gas analyzer. Samples were run in duplicate, or triplicate if the difference between the first two samples was >5%. The inverse slope of 'predicted versus measured' values created a correction factor to apply to the measured values obtained during the study. For the study in Chapter VI of this dissertation I ran the tonometry procedure using two sets of O_2/CO_2 gas mixtures to create a 'predicted versus measured' slope of values expected to span the range of arterial PO_2 and PCO_2 of exercising subjects breathing (1) room air and (2) 40% oxygen, respectively. For the protocol in which subjects exercised breathing an FIO_2=0.21, 0.60, and 0.14 only one set of O_2/CO_2 gas mixtures that spanned the range of all three FIO_2s was used to tonometry correct the blood gases.

Arterial Blood Draw and Analysis

The tip of a 3 ml syringe was filled with Heparin (heparin sodium, 1,000 U/ml) and used to obtain a sample of radial artery blood. The hub of the radial artery catheter was connected to a three-inch extension set and 3-way stopcock. For each blood sample, approximately 0.5-1 ml of blood was pulled though the distal port of the stopcock as waste. The heparinized syringe connected to the side port was used to pull the arterial blood sample over ~10-15 sec in order to be representative of multiple respiratory cycles and to enable matching blood gas data with the VO_2 data acquired with the metabolic system. This syringe was immediately inspected and voided of any air bubbles, the tip

covered with a finger and handed to another researcher for blood gas analysis. Thus, the time from blood draw to the first analysis was <30 sec. The sample was analyzed using a Siemens 248 RapidLab containing a Clarke electrode for measurement of PO_2 and a Severinghaus electrode for measurement of PCO_2. While measurements were being analyzed for blood gases, direct hemoglobin saturation (SaO_2) was determined photometrically using a Radiometer OSM-3. While the sample was being analyzed, the stopcock, extension set and arterial catheter were flushed with ~4 ml heparinized saline (1U/ml heparin) by the first investigator.

After blood gas analysis was complete, a blood sample was analyzed for lactate concentration (YSI 1500 Sport Lactate Analyzer) and a sample was collected in a microcapillary tube for determination of hematocrit using the centrifugation method.

Thus, the bubble study, arterial blood draw, and record of esophageal temperature occurred simultaneously. The temperature measurement was used with the tonometry correction during data analysis to temperature correct the arterial blood gas sample (84, 146).

At the conclusion of the study a researcher removed the arterial catheter and held manual pressure over the site for at least 10 min. An ice pack was then wrapped over the site for another 10 min before a bandage was placed over the entry site.

DELIVERY OF INSPIRED GAS MIXTURES

During all resting and exercise protocols described in this dissertation, subjects breathed through a low resistance 2-way non-rebreathing valve (Hans Rudolph, 2700) and the expiratory port vented to room air. When breathing a normoxic gas mixture, the inspiratory port was open to room air. When breathing hyperoxic gas mixtures, the

inspiratory port was connected to a non-diffusing Mylar bag containing the appropriate gas mixture. The hose connecting the bag to the non-rebreathing valve was directed through a custom built humidifier.

To create hyperoxic gas mixtures, medical grade oxygen and air were attached to a high flow gas blender that was capable of varying the gas mixture between 21% and 100% oxygen, while hypoxic gas mixtures blended medical grade air and nitrogen. Prior to all studies, a zirconia oxygen cell analyzer was calibrated to a calibration and reference gas. The gas analyzer sampled the blended gas mixtures and the blender dial was adjusted to the desired fraction of oxygen. Once set, the non-diffusing bag could be continuously filled to match the ventilatory rate of the subject to ensure an adequate reservoir of air. The gas sampling line just distal the mouth of the subject, but proximal to the 2-way non-rebreathing valve allowed breath-by-breath analysis of the fraction of inspired oxygen to ensure the correct concentration was being delivered to the subject and there were no leaks.

DRUG INFUSIONS

In Chapter IV of this dissertation I present a study in which two drugs, epinephrine (EPI) and dopamine (DA), were infused into healthy human subjects at rest. EPI was diluted in sterile saline to 4,000 $ng \bullet ml^{-1}$ and DA was diluted to 1,600 $\mu g \bullet ml^{-1}$ and loaded into syringes which were infused at constant rates using a Harvard Apparatus syringe infusion pump (Pump 22). Subjects had an i.v. placed in the opposite arm as the i.v. used for the saline contrast injections for drug infusions. EPI infusion rates were chosen that would elicit a range of increases in cardiac output, result in plasma EPI concentrations similar to that seen at maximal exercise, and that had been previously used

in human subjects (28). DA infusion rates were chosen to elicit concentrations that would bind to a range of receptors: dopaminergic receptors at low doseages, β-receptors at moderate dosages, and α-receptors at dosages greater than $10\mu g \bullet kg^{-1} \bullet min^{-1}$.

NUCLEAR MEDICINE IMAGING AND ANALYSIS

The few studies that have quantified blood flow through IPAVA during exercise imaged the distribution of Technetium-99m labeled macroaggregated albumin (^{99m}Tc-MAA) using simple, two-dimensional planar imaging (32, 197). Gamma photons emitted from ^{99m}Tc-MAA lodged at various depths must pass through tissues of varying density and will lose a variable degree of energy due to attenuation and Compton scatter before reaching the collimators in the heads of the cameras. Thus, a potential limitation of this technique is the inability to correct the radioactive counts for the nonuniform attenuation and Compton scattering of photons that is known to occur (23). One way to correct for this attenuation is to reconstruct a three-dimensional map of the location of ^{99m}Tc-MAA using single photon emission computed tomography (SPECT) and fuse this image with an attenuation-correction map derived from a low dose computed tomography (CT) scan (121). Recent advances in quantitative medical imaging have combined both SPECT and CT imaging modalities into a single device so a subject can be scanned by each camera without being moved from the bed (121). When the CT data is fused to the SPECT data, it can be used to correct for the nonuniform attenuation of gamma photons that occurs based on the distance and density of tissue the photons encounter as they pass through the body (20, 23, 138, 198) as well as the Compton scattering of photons that still reach the collimators within the desired energy window (^{99m}Tc emit at an energy of 140 keV) (109).

Thus, we developed a collaboration with Dr. Matthews Fish of the Oregon Heart & Vascular Institute at Sacred Heart Medical Center in Springfield, OR and set out to employ SPECT/CT imaging using a Philips Precedence 16P SPECT/CT camera (Philips Medical Systems, The Netherlands) to overcome problems due to attenuation and scatter and thus improve the sensitivity and objectivity in quantifying blood flow through large diameter IPAVA, known as the shunt fraction.

MAA Filtering and Technetium-99m Labeling

The gold standard for measuring blood flow through large diameter MAA would be to use large diameter solid microspheres of an exact known size. Unfortunately, these are no longer available for use in human subjects. Rather, macroaggregated albumin (MAA) are used despite the range of particle sizes contained in each batch (>90% between 10-70μm). While the mean length of MAA particles is significantly larger than the largest pulmonary capillary, there is the potential that some small particles could travel through pulmonary capillaries and circulate freely in the blood. After preliminary scans revealed potential errors in the quantified shunt fraction, I developed a filtering procedure in which the reconstituted MAA were drawn through a 20μm nylon filter (20μm x 25mm nylon net filter, Millipore) to remove as many small particles as possible. During development of this technique a sample of reconstituted MAA solution was placed on a hemacytometer and visualized under a microscope. The hemacytometer had markings every 5 μm so the number and size of MAA could be determined. Prior to filtering, the size distribution of MAA demonstrated 2 peaks, one over the 0-15 μm range and a second over ~30-35μm. After filtering, the percentage of MAA in the 0-15μm range was reduced from 17.7% to 6.5%. Thus, for all procedures moving forward this

filtering procedure was conducted prior to labeling with ^{99m}Tc. This had the added benefit that after labeling, which is described in more detail in Chapter V, the ^{99m}Tc-MAA was pulled through the filter again to remove any free ^{99m}Tc, and potentially removed even more small particles, and fresh saline added before the final dose was drawn up for injection into the subject.

All radioactivity was handled by the licensed nuclear medicine technicians, including the labeling of MAA with ^{99m}Tc which occurred after the filtering procedure and immediately prior to use in each study visit. A dose of 0.057 mCi/kg was drawn up for injection into subjects for each study visit. This dose was previously used in healthy human subjects (96) and the total dose of radiation is standardized for the body weight of each subject.

SPECT/CT Imaging

After the rest or exercise protocol (described above), subjects were quickly moved to the bed attached to the SPECT/CT camera located in the same room and rested quietly. An initial "scout scan" was conducted which was a low dose CT image used to determine the location of the subject on the bed. Next, the bed slid through the CT scanner and scanned the subject from head to toe. Because the data from the CT scan was not needed to reconstruct a high-resolution image, but rather just determine tissue densities, we used a low dose, dose-modulation CT scan using a 16 slice helical CT scanner (140kv, 50 mAs/slice maximum, 0.5-s rotation time). The dose-modulation automatically reduced the radiation transmitted through the subject as lower density tissue was encountered. The entire scan took ~47 secs.

After the CT scan, the bed was automatically repositioned to line up the two Gamma cameras anteriorly and posteriorly over the head of the subject. These cameras used a step-and-shoot sequence to capture the ^{99m}Tc photopeak of 140keV with a 10% window for 20 sec and then they rotated 5.625 degrees. By rotating 32 times, the anterior and posterior cameras captured data from 360° around the subject. Post-processing of the Gamma camera data is able to reconstruct a three-dimensional data set indicating the location and intensity of the ^{99m}Tc-MAA. Once the Gamma cameras captured views encircling the entire body, the bed shifted down to begin capturing photons emitted from the next section of the body and this was repeated for a total of 4 sections to image the entire length of the body. As a consequence, the time from ^{99m}Tc-MAA injection to the completion of the fourth SPECT section took ~50-55 min.

After the initial analysis of visits using these scanning procedures (see below for details), there was concern that the total time of the scan was long enough to allow some of the ^{99m}Tc to unbind from the MAA, resulting in free ^{99m}Tc throughout the blood. If this were the case, then any detection of radioactive counts outside the body could not be assumed to be attached to large diameter MAA. We were also concerned that the breathing movement artifact while imaging over the lung during the first two SPECT segments could have been artificially inflating the shunt fraction. To address both of these concerns, we shortened the Gamma camera imaging time from 20 sec to 10 sec per stop and had the subjects conduct a breath hold at FRC during the 10 sec image acquisition. Halving the stop-time reduced the total imaging time by 21 min to ~30-32 min total. The camera took ~3 sec to rotate to the next stop before continuing to aquire data. Thus, we were able to coach the subjects to inhale and exhale to FRC during the 3

sec transition and thus all SPECT data during the first two stops was subsequently collected at a constant lung volume with minimal breathing motion artifact. We then repeated our initial studies using this updated protocol in our first subject and all subsequent studies.

Post-processing Data Reconstruction and Analysis

In order to quantify the percentage of blood flowing through large diameter IPAVA using SPECT/CT imaging, we assume that the percentage of radiation counts detected outside of the lung versus inside of the lung represents counts emitted from ^{99m}Tc-MAA that have traveled through IPAVA and are proportional to blood flow through IPAVA. To determine this ratio, I used Philips proprietary software to analyze the SPECT/CT data. First, the SPECT data was transformed into transverse slices using AutoSPECT+, aligned with the CT data to create the attenuation correction map, and Syntegra was used to reconstruct attenuation-corrected SPECT data for all 4 acquisitions covering the body. The reconstruction method used the Astonish algorithm (2 iterations, 16 subsets, Hanning filter max 1.20), which is a three dimensional ordered subsets expectation maximization reconstruction that applies the attenuation map derived from the low-dose CT to correct each voxel for attenuation and compensates for the blurring effects of the collimator built into the reconstruction. This is intended to allow for greater resolution recovery and improve the signal-to-noise ratio.

The head-to-toe CT image was reconstructed into 10mm thick slices, an objective region of interest (ROI) determined for each slice, and the resulting three-dimensional region applied to the fused SPECT data to determine the whole body ROI. The lung ROI was determined automatically by setting a minimum threshold of 5 counts per pixel to

represent the border of the lung. Blood flow through IPAVA, known as the shunt fraction, was quantified as follows: (whole body counts–lung counts) / (whole body counts).

While the use of SPECT/CT imaging has the potential to increase the sensitivity of detecting radioactive counts by using attenuation correction, this technique has never been used to quantify shunt fractions in human subjects. Thus, we repeated the rest and exercise visits breathing room air that were scanned with SPECT/CT in order to compare the calculated shunt fractions to those determined using simple planar imaging. Based on the results of these 4 visits (rest or exercise breathing room air), we decided to continue with the exercise breathing 100% oxygen visit using the planar imaging method, as described below. Thus, in addition to the pilot work visits during which we (1) developed the filtering technique, (2) began acquiring SPECT data during a breath hold at FRC, and (3) shortened the SPECT acquisition in half, four subjects completed a total 5 visits to the Nuclear Medicine department to collect the data presented in Chapter V of this dissertation.

Planar Imaging

After either the rest or exercise protocol breathing room air, subjects were moved to the bed of the SPECT/CT camera, however there was no CT scan performed. Rather, the bed was immediately positioned to put the head of the subject between the anterior and posterior Gamma cameras. The scan began within 3 min of the ^{99m}Tc-MAA injection and the bed moved in a continuous fashion to capture photons down the length of the entire body. This scan took 17:15. Thirty min and 60 min after the MAA injection, we began subsequent Gamma camera scans to determine if the shunt fraction was changing

the longer the ^{99m}Tc-MAA was in the subject. In order to determine if ^{99m}Tc was unbinding from the MAA and circulating freely in the blood, we obtained a 1ml venous blood sample at the conclusion of each scan. This blood sample was placed in a scintillation counter, corrected for time decay, and the total free radioactivity in the body estimated using an estimate of total blood volume (114). By dividing this total blood radioactivity by the total initial radioactivity (mCi) injected, we could estimate the portion of the quantified shunt fraction due to free-^{99m}Tc. While this technique helped to correct for free-^{99m}Tc in the blood, the longer SPECT/CT scan was still quantifying large shunt fractions that appeared physiologically implausible for reasons that may have been due to the longer acquisition time as well as errors inherent to the Astonish algorithm reconstruction method being applied to the data. While I developed a way to correct for free-^{99m}Tc in the blood, the longer scanning acquisitions would allow some of the free-^{99m}Tc to be filtered from the blood and accumulate in the kidneys, bladder, salivary glands, and thyroid and these counts would be counted as part of the shunt fraction. Thus, because planar scanning proved more accurate than the SPECT/CT procedure due to its shorter acquisition time, we continued with the planar imaging for the exercise protocol with subjects breathing 100% oxygen.

CHAPTER IV

CATECHOLAMINE-INDUCED OPENING OF INTRAPULMONARY ARTERIOVENOUS ANASTOMOSES IN HEALTHY HUMANS AT REST

This chapter is in review with the *Journal of Applied Physiology* and Jonathan E. Elliott, Randall D. Goodman, and Andrew T. Lovering are co-authors. I performed the experimental work and the methods were developed equally between all authors. The writing is entirely mine. J.E. Elliott and A.T. Lovering provided editorial assistance.

INTRODUCTION

Intrapulmonary arteriovenous anastomoses (IPAVA) are closed at rest in healthy humans. These vessels can open during exercise (32, 35, 159) or at rest when breathing hypoxic gas mixtures (89, 94) and can be detected using a technique called saline contrast echocardiography. Additionally, IPAVA are not open during exercise in subjects breathing 100% oxygen (35, 97). However, the mechanism(s) that regulate blood flow through IPAVA under these conditions remain unknown.

During exercise, plasma epinephrine (EPI) and dopamine (DA) concentrations both increase (67). In subjects breathing hypoxic gas mixtures for brief periods of time the change in plasma EPI concentration is reportedly varied depending on the duration and level of hypoxia (140), with most demonstrating an increase (82, 107, 117, 141). Therefore, an increase in plasma EPI or DA concentrations during exercise or when breathing hypoxic gas mixtures may represent a common link causing IPAVA to open during both of these conditions in healthy humans. Indeed, using 15- to 30-μm radioactive albumin microspheres Nomoto, *et al.* (116) demonstrated that IPAVA open in dogs infused with EPI. Additionally, Berk and colleagues also suggested a direct effect of

EPI increasing venous admixture in anesthetized dogs based on an immediate fall in arterial PO_2 during EPI infusion (16-18), while Huckauf, *et al.* (75) suggested a similar effect in patients with left heart failure receiving DA infusion. Thus, these catecholamines could potentially be opening IPAVA; however, their role and mechanism of action in opening IPAVA in healthy humans is unknown.

When EPI binds to β_2-adrenergic receptors on pulmonary vascular smooth muscle, it activates a receptor-linked pathway to increase the intracellular concentration of cAMP leading to pulmonary vascular smooth muscle relaxation (40, 125). Alternatively, the binding of EPI to α-receptors on pulmonary vascular smooth muscle leads to vasoconstriction. Under conditions of normal pulmonary vascular tone, EPI infusion appears to favor an increased pulmonary vascular resistance, while EPI infusion during conditions of increased basal tone causes dilation and a decrease in resistance (77, 78, 123, 124, 199). Thus, the net change in pulmonary vascular resistance due to EPI infusion is due to a balance between its α- and β-adrenergic effects.

Dopamine stimulates dopaminergic receptors when administered at low doses (0.5-3 $\mu g \bullet kg^{-1} \bullet min^{-1}$), weakly stimulates β_1-adrenergic receptors at intermediate doses (3-10 $\mu g \bullet kg^{-1} \bullet min^{-1}$), and stimulates α_1-adrenergic receptors at higher infusion rates (119). Binding to dopaminergic receptors on renal vascular smooth muscle induces vasodilation (108), as do higher doses of 5 and 10 $\mu g \bullet kg^{-1} \bullet min^{-1}$ (33). In the pulmonary circulation DA has been shown to have no effect (65), increase (53), or decrease (132) vascular resistance.

Thus, the purpose of this study was to investigate if the intravenous infusion of the vasoactive substances EPI or DA opens IPAVA in healthy human subjects at rest

breathing room air and, additionally, to determine if breathing 100% oxygen prevents IPAVA from opening during a repeated EPI or DA infusion, respectively. We hypothesized that the intravenous infusion of EPI and DA would open IPAVA in healthy human subjects at rest breathing room air. We also hypothesized that if EPI or DA had a direct effect on IPAVA by binding to a receptor-mediated vasodilatory pathway, then a repeated infusion of EPI or DA would also open IPAVA in the same healthy human subjects breathing 100% oxygen at rest. We subsequently investigated the contribution of a β-receptor mediated pathway in the opening of IPAVA in subjects breathing hypoxic gas mixtures. We hypothesized that if the hypoxia-induced opening of IPAVA occurred via β-receptor mediated pathway, then IPAVA would remain closed when breathing an FIO_2=0.10 after the infusion of 10mg of the β-blocker Propranolol.

METHODS

The University of Oregon Office for Protection of Human Subjects approved this project and all subjects provided verbal and written informed consent prior to participation. All studies were performed in accordance with the Declaration of Helsinki.

Echocardigraphic Screening and Lung Function Testing

Upon initial screening, 10/21 (48%) subjects demonstrated bubbles in the left heart within 3 cardiac cycles and were excluded from further participation due to the presence of a patent foramen ovale. Two additional subjects demonstrated 1-3 bubbles in the left ventricle not due to a patent foramen ovale and were also excluded. The remaining 9 subjects (1 female) participated in the study protocol. Spirometry including forced vital capacity (FVC) and slow vital capacity (SVC), and whole body plethysmography were performed according to ATS/ERS standards to determine lung

function indices, lung volumes, and capacities (111, 188). The single-breath, breath-hold technique was used for determination of lung diffusion capacity for carbon monoxide according to ATS/ERS standards (102) using the Jones and Meade method for timing (80).

Resting Epinephrine and Dopamine Infusions

During a subsequent visit, subjects were instrumented with a 20G intravenous catheter in each arm and reclined in the left lateral decubitus position at rest before and during all catecholamine infusions. EPI was diluted in sterile saline to 4,000ng/ml and DA was diluted to 160μg/ml and delivered at a constant rate using a Harvard Apparatus syringe infusion pump (Pump 22). Bubble injections used for transthoracic saline contrast echocardiography (TTSCE) were injected through an intravenous catheter placed in the opposite arm. TTSCE was performed at rest, before and during the infusions of EPI at 20, 40, 80, 160, and 320 $ng \bullet kg^{-1} \bullet min^{-1}$ for 3-4 min each with minimal breaks between each infusion rate. At the conclusion of the highest EPI infusion rate, subjects took a 30 min break before TTSCE was again performed before and during the infusions of EPI (as above) in subjects breathing 100% oxygen. After another 30 min break, TTSCE was performed at rest, before and during the infusions of DA at 1, 2, 4, 8, and 16 $\mu g \bullet kg^{-1} \bullet min^{-1}$ for 3-4 min each with minimal breaks between each infusion rate (1 subject failed to complete the final infusion concentration of DA due to nausea). After a final 30 min break, TTSCE was performed again before and during the infusions of DA (as above) in subjects breathing 100% oxygen. The female subject did not participate in any DA infusions due to the feeling of nausea during EPI infusions breathing 100% oxygen. For each bubble injection the apical four-chamber view was recorded for 20 cardiac cycles

after the initial appearance of bubbles in the right ventricle. Using a previously published scoring system, a 0-5 score was assigned based on the greatest number and spatial distribution of bubbles appearing in the left ventricle during a single frame >3 cardiac cycles after their appearance in the right heart (35, 89, 97). A score of 1 = 1-3 bubbles; 2 = 4-12 bubbles; 3 = >12 bubbles in a bolus; 4 = >12 bubbles heterogeneously filling the left ventricle; and 5 = >12 bubbles homogenously filling the left ventricle (35, 89, 97). End systolic and end diastolic volumes were determined using the Modified Simpson's technique from the apical four-chamber view by tracing the left ventricular endocardial border during systole and diastole from a minimum of three cardiac cycles (88). Stroke volume was determined as the difference between end diastolic and end systolic volumes. Heart rate was obtained from lead II of the ECG and multiplied by stroke volume for determination of cardiac output. Pulmonary artery systolic pressure was determined by measuring the peak velocity (v) of the tricuspid regurgitation jet and applying that to the modified Bernoulli equation $4v^2 + 3$ (26, 62, 142, 204).

Hypoxia and Beta-blockade

During a subsequent visit, 5 of the initial 9 subjects returned and were instrumented with an intravenous catheter and forehead saturation monitor (Nellcor, OxyMax sensor). TTSCE was performed with subjects at rest breathing room air, and then every 10 min throughout a 30 min period breathing an FIO_2=0.10. We have previously shown that IPAVA open in subjects at rest breathing this FIO_2 (89). Subjects were then given a 45 min break breathing room air before the infusion of 10mg Propranolol at an infusion rate of 1mg/min. After performing TTSCE in these subjects

while still breathing room air, subjects again breathed an FIO_2=0.10 for 30 min with TTSCE performed at 10 min intervals.

Statistics

All statistical calculations were made using GraphPad Prism statistical software (v5.0d) and significance was set to $p<.05$. Bubble scores for all EPI infusions in subjects breathing room air and 100% oxygen were analyzed using a Friedman's test with Dunn's multiple comparison posttest. Bubble scores obtained before and during all DA infusion rates and those obtained in subjects breathing hypoxic gas mixtures were analyzed in the same manner. Mean cardiac output and PASP measured during each infusion rate were analyzed using a one-way ANOVA with Tukey posttest.

RESULTS

Subject Characterization and Lung Function

Anthropometric, pulmonary function, and diffusion capacity data were within normal limits for all subjects and are presented in Table 4.1.

Bubble Scores

Bubble scores for every subject breathing room air and 100% oxygen before and during the infusion of EPI and DA are presented in Fig. 4.1 and representative echocardiograms are presented in Fig. 4.2. In subjects breathing room air during EPI infusion of 80, 160, and 320ng•kg^{-1}•min^{-1}, bubble scores were significantly greater compared to both 0 and 20ng•kg^{-1}•min^{-1}. However, during EPI infusions in subjects breathing 100% oxygen the bubble scores never increased compared to 0ng•kg^{-1}•min^{-1}. Thus, the bubble scores during EPI infusions from 80-320ng•kg^{-1}•min^{-1} were

Table 4.1. ***Anthropometrics, pulmonary function, and DL_{CO} data.***

Height, cm	184.9 ± 6.6	
Weight, kg	81.0 ± 6.9	
Age, yrs	27.8 ± 7.6	
BMI, $kg \cdot m^{-2}$	23.7 ± 1.3	
FVC, L	5.52 ± 1.06	(95.1 ± 7.4)
FEV1, L	4.52 ± 0.74	(95.4 ± 6.5)
FEV1/FVC	0.82 ± 0.06	(99.3 ± 5.9)
FEF 25-75%, $L \cdot sec^{-1}$	4.51 ± 0.89	(95.6 ± 16.6)
SVC, L	5.57 ± 1.06	(96.7 ± 6.6)
IC, L	3.45 ± 0.90	(94.4 ± 16.0)
ERV, L	2.11 ± 0.56	(101.1 ± 25.2)
FRC, L	3.83 ± 0.78	(104.7 ± 13.9)
RV, L	1.68 ± 0.64	(98.9 ± 10.8)
TLC, L	7.34 ± 1.51	(100.0 ± 10.8)
DL_{CO}, $ml \cdot min^{-1} \cdot mmHg^{-1}$	37.4 ± 6.8	(107.8 ± 11.5)
DL_{co}/VA, $ml \cdot min^{-1} \cdot mmHg\text{-}1 \cdot L^{-1}$	5.4 ± 11.5	(111.9 ± 12.3)

Note. Values are means±SD (percent predicted±SD).

significantly lower in subjects breathing 100% oxygen compared to room air. In subjects breathing room air, IPAVA were open in 5/7 subjects at the highest infusion rate of DA, however this set of scores was not significantly greater than the set of bubble scores seen at $0 \mu g \bullet kg^{-1} \bullet min^{-1}$. When breathing 100% oxygen the bubble scores during 8 and $16 \mu g \bullet kg^{-1} \bullet min^{-1}$ were significantly lower than scores when breathing room air.

Breathing an FIO_2=0.10 led to increased bubble scores, as expected, and these were not reduced after the infusion of propranolol (Fig. 4.3).

Cardiac Output and PASP

Mean cardiac output and PASP before and during each infusion rate of EPI and DA in subjects breathing room air and 100% oxygen are presented in Fig. 4.4. There

were no differences in either cardiac output or PASP between room air and 100% oxygen conditions for any infusion rate. The infusion of EPI at 40 ng•kg^{-1}•min^{-1} through 320ng•kg^{-1}•min^{-1} resulted in significant increases in cardiac output compared to 0ng•kg^{-1}•min^{-1}. DA infusion resulted in a significant increase in cardiac output only at the highest infusion rate of 16µg•kg^{-1}•min^{-1}. Of note, cardiac output measured during the EPI infusion of 40ng•kg^{-1}•min^{-1} was the same as cardiac output measured during the DA infusion of 16µg•kg^{-1}•min^{-1} (6.17 ± 0.65 L•min^{-1} vs. 6.16 ± 0.91 L•min^{-1}, respectively) and the bubble scores were the same (Fig. 4.1).

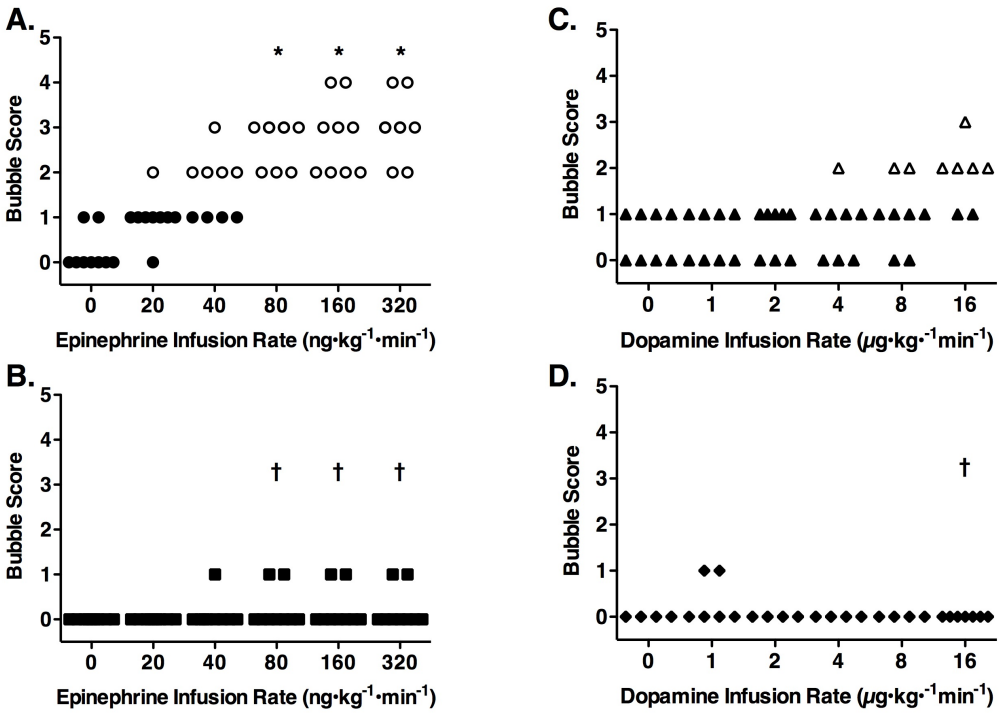

Figure 4.1. Bubble Scores. Individual bubble scores during EPI infusion in subjects breathing (A) room air (circles) or (B) 100% oxygen (squares) and during DA infusion in subjects breathing (C) room air (triangles) or (D) 100% oxygen (diamonds). Closed symbols, IPAVA are closed; open symbols, IPAVA are open. *$p<.05$ vs. 0 and 20 ng•kg^{-1}•min^{-1}. † $p<.05$ vs. room air (Friedman's test, Dunn's posttest).

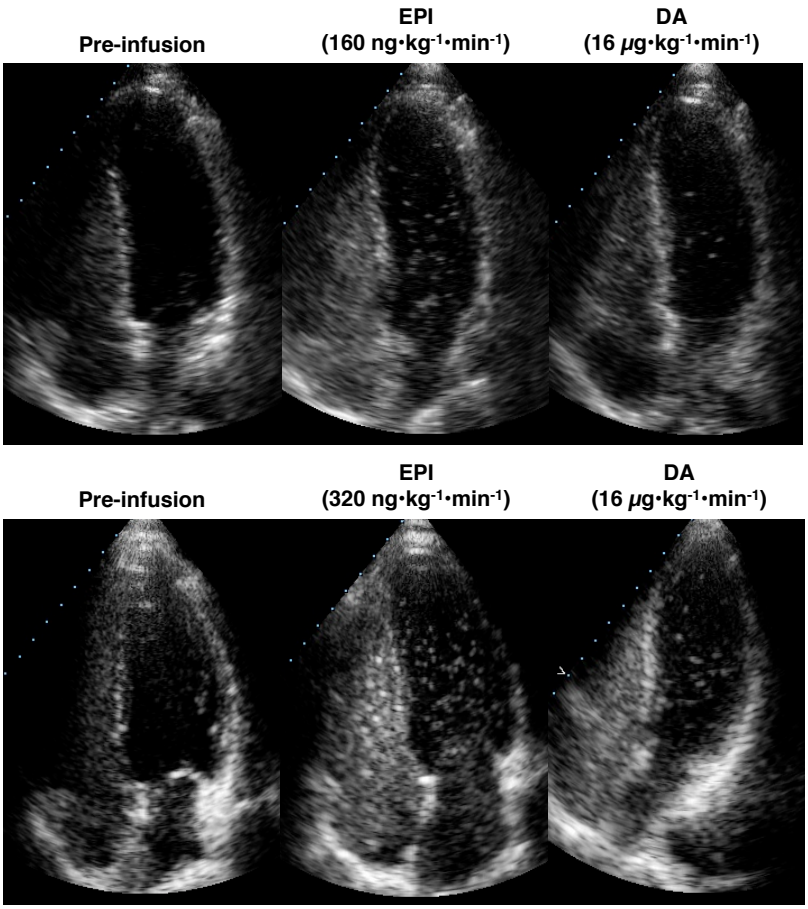

Figure 4.2. Representative Echocardiograms. *Upper row.* One subject breathing room air at rest (A) before EPI or DA infusion, score=0; (B) during EPI infusion (160 ng•kg^{-1}•min^{-1}), score=3; and (C) during DA infusion (16 μg•kg^{-1}•min^{-1}), score=2. *Bottom row.* A different subject breathing room air at rest (D) before EPI or DA infusion, score=0; (E) during EPI infusion (160 ng•kg^{-1}•min^{-1}), score=3; and (F) during DA infusion (16 μg•kg^{-1}•min^{-1}), score=2.

There was a significant increase in PASP during the infusion of EPI at 80 through 320 ng•kg^{-1}•min^{-1} while DA did not result in a significant increase in PASP for any infusion rate. Similar to cardiac output measurements, PASP measurements were the same during the infusion of EPI at 40ng•kg^{-1}•min^{-1} and during the infusion of DA at 16μg•kg^{-1}•min^{-1} (32.0 ± 6.1 mmHg vs. 31.8 ± 4.5 mmHg, respectively) and bubble scores were essentially identical.

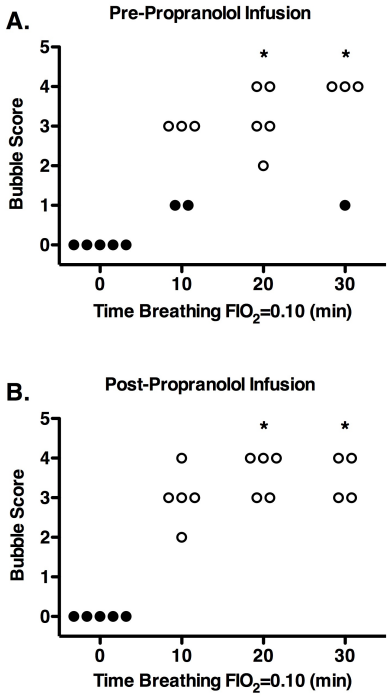

Figure 4.3. Bubble Scores Before and After Propranolol Infusion. Individual bubble scores in subjects breathing an FIO_2=0.10 for 30 min (A) Pre- and (B) Post-infusion of 10 mg Propranolol. *p<.05 vs. 0 min. *Note*: 1 subject stopped each hypoxic bout after 20 min because SpO_2 was ≤65%.

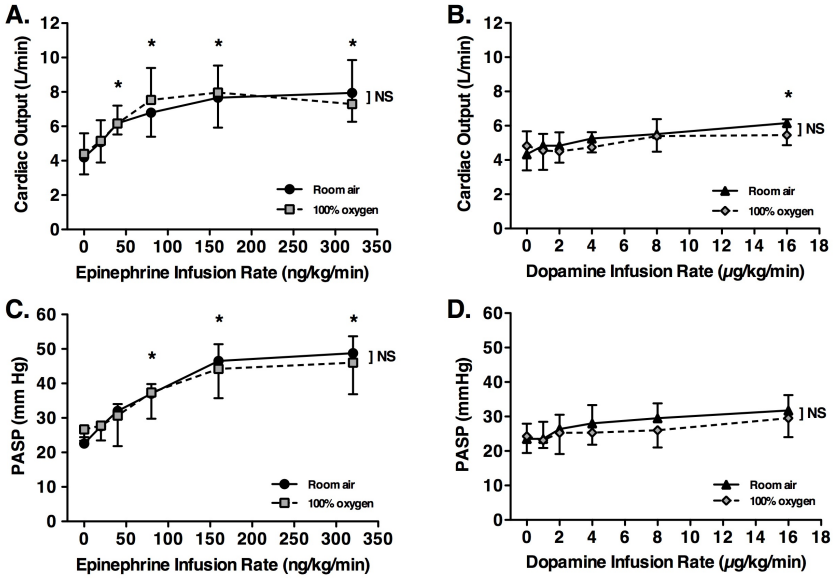

Figure 4.4. Cardiac Output and PASP. Mean cardiac output before and during each infusion concentration of (A) EPI and (B) DA in subjects breathing room air and 100% oxygen. Mean PASP before and during each infusion concentration of (C) EPI and (D) DA in subjects breathing room air and 100% oxygen. Circles and squares indicate subjects breathing room air and 100% oxygen during EPI infusions, respectively. Triangles and diamonds indicate subjects breathing room air and 100% oxygen during DA infusions, respectively. * p<.05 vs 0 $ng \bullet kg^{-1} \bullet min^{-1}$ or 0 $\mu g \bullet kg^{-1} \bullet min^{-1}$, respectively. NS, no significant difference between room air and 100% oxygen.

Figure 4.5 demonstrates PASP as a function of cardiac output for all subjects breathing room air before and during all infusion rates of EPI and DA and identified bubble scores <2 versus scores ≥2, revealing a potential cardiac output/PASP threshold that resulted in open IPAVA.

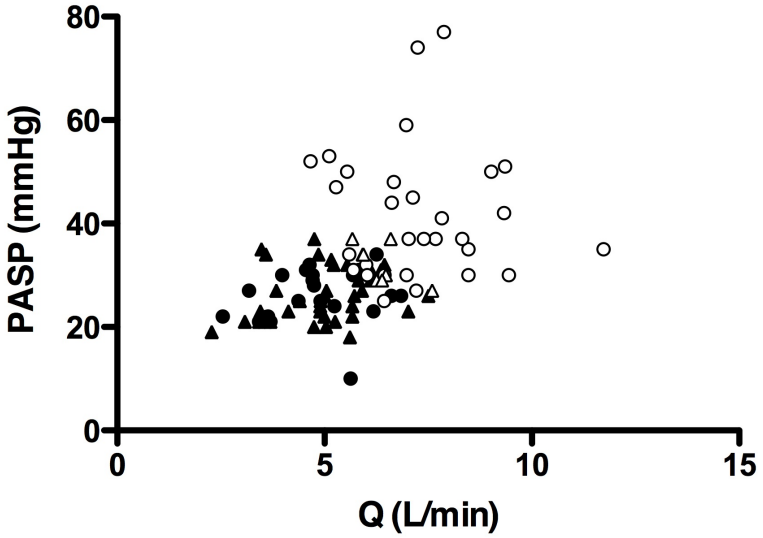

Figure 4.5. Cardiac Output vs. PASP. Cardiac output vs. PASP before and during the infusions of EPI and DA in subjects breathing room air. Closed symbols represent bubble scores of 0 or 1, open symbols represent bubble scores of 2, 3, or 4 as indicated in Fig. 4.1.

DISCUSSION

The main finding of this study was that the intravenous infusion of EPI caused IPAVA to open in healthy humans at rest breathing room air, while the infusion of DA did not result in a significant increase in bubble score for any infusion rate. Additionally, β-blockade did not prevent hypoxia-induced opening of IPAVA. Cardiac output during EPI infusions ≥40 $ng \bullet kg^{-1} \bullet min^{-1}$ was significantly greater than pre-infusion, while DA only increased cardiac output during a DA infusion of $16 \mu g \bullet kg^{-1} \bullet min^{-1}$. PASP also increased significantly during EPI infusions ≥80 $ng \bullet kg^{-1} \bullet min^{-1}$, but did not increase for

any DA infusion rate. However, both the cardiac output and PASP measured during the DA infusion of 16μg •kg^{-1}•min^{-1} were the same as those achieved during the infusion of EPI at 40 ng•kg^{-1}•min^{-1} (Fig. 4.2) and the bubble scores for these infusion rates were the same (Fig. 4.1). Conversely, when subjects breathed 100% oxygen while receiving the same infusions of EPI or DA as they did breathing room air, IPAVA were prevented from opening despite similar cardiac output and PASP measurements.

Saline Contrast Echocardiography

The limitations of the use of saline contrast echocardiography have been extensively discussed in previous manuscripts (32, 35, 89, 94, 97, 159). While neither the size of the bubbles, nor the quantification of blood flow through IPAVA can be determined using this technique, the minimum size of bubbles entering the pulmonary microcirculation has been estimated to be 60- to 90-μm in diameter in order for the bubbles to be stable enough to survive and be visualized in the left ventricle (32). We have also shown that neither the internal, nor the external partial pressure gas composition of the bubbles affect the ability of TTSCE to detect patent IPAVA (35). Furthermore, extensive anatomical evidence using solid microspheres supports the existence of large diameter pathways existing in the pulmonary circulation (115, 129, 151, 170, 172). More recently, 50-μm microspheres have been shown to pass through the pulmonary circulation of isolated human and baboon lungs ventilated and perfused under physiologic conditions (99) and 70-μm microspheres pass through the pulmonary circulation of rats breathing hypoxic gas mixtures (10). Finally, the data obtained in the current study using saline contrast echocardiography are directly supported by anatomical work using 15- to 30-μm albumin microspheres by Nomoto, *et al* (116) in which

increasing the infusion of EPI led to increases in the percentage of blood flowing through large diameter intrapulmonary arteriovenous anastomoses. Thus, evidence obtained with TTSCE supporting the dynamic regulation of IPAVA in healthy humans continues to accumulate and is identical to data obtained with microspheres in animals and isolated lungs.

Epinephrine and Dopamine Effects on Pulmonary Vasculature

EPI and DA each have the ability to mediate pulmonary vascular dilation or constriction through their respective α, β, or dopaminergic receptor mediated pathways. Thus, if β-adrenergic receptors are located on IPAVA, EPI could have theoretically directly induced vasodilation. Conversely, if α-receptors are located on IPAVA, EPI infusion could have induced vasoconstriction of these vessels, potentially limiting even greater flows through IPAVA. At the highest DA infusion rate, IPAVA opened in 5/7 subjects, however as a group the bubble scores were not significantly increased for any DA infusion rate. This suggests that the dopaminergic receptors stimulated at low doses of DA infusion probably do not induce vasodilation of IPAVA, while the higher concentrations that stimulate α-adrenergic receptors could theoretically be preventing IPAVA from fully opening. This seems unlikely however because the DA concentration used in the current study has not been shown to cause pulmonary vasoconstriction (65) and is not expected to significantly increase flow or pressure (60), which is supported by our data.

Hypoxia and Beta-Blockade

We chose to investigate the role of β-receptors in the hypoxia-induced opening of IPAVA during a subsequent visit in five subjects. If the hypoxia-induced opening of

IPAVA occurred via a β-receptor mediated pathway, then IPAVA would have remained closed during the second period of hypoxia. However, all five subjects demonstrated increased bubble scores while breathing an FIO_2=0.10 after β-receptor blockade (Fig. 4.3). This suggested to us that the mechanism opening IPAVA during EPI or DA infusion was not via a β-receptor mediated pathway, but rather could be due to the secondary effects of these catecholamine infusions on cardiopulmonary hemodynamics.

Because IPAVA are open in human subjects and rats breathing hypoxic gas mixtures at rest (10, 89) and during exercise (94), this suggests that blood flow entry into these vessels is occurring upstream of the small pulmonary resistance arteries which constrict in hypoxic environments and thus may branch from the large conducting vessels which demonstrate a lesser degree of hypoxic pulmonary vasoconstriction (103). This permissive or passive opening could allow for a reduction in total pulmonary vascular resistance in the face of increased pulmonary blood flow and help attenuate increases in pressure at the pulmonary capillary or right ventricular afterload as originally suggested by Stickland, *et al* (159). Indeed, La Gerche, *et al.* (87) has demonstrated that individuals demonstrating a greater degree of agitated saline contrast bubbles traversing the pulmonary circulation have a lower pulmonary resistance compared with those who demonstrate a low degree of left sided contrast. Future work is needed to determine the role of changes in blood flow, pressure, and hypoxic pulmonary vasoconstriction in the recruitment of IPAVA.

Cardiac and PASP Effects Due to Epinephrine and Dopamine

If the opening of IPAVA during EPI or DA infusions are not due to the active binding to receptor-linked vasomotor pathways, it may be due to the secondary effects of

increased cardiac output and/or PASP. We demonstrated an increase in cardiac output during the infusion of 40, 80, 160, and 320ng•kg^{-1}•min^{-1} of EPI and the three highest EPI infusion rates produced bubble scores that were significantly greater than scores at 0ng•$^{-1}$kg•min^{-1}. During DA infusions, cardiac output was only significantly increased from rest at the highest infusion concentration of 16μg•kg^{-1}•min^{-1} and resulted in the same cardiac output as that achieved during the infusion of EPI at 40ng•kg^{-1}•min^{-1} (Fig. 4.4a, b). Thus, when bubble scores achieved during the infusion of EPI at 40ng•kg^{-1}•min^{-1} were compared to those achieved during the infusion of DA at 16μg•kg^{-1}•min^{-1} (Fig. 4.1) the bubble scores were the same. We demonstrated an increase in PASP from baseline in subjects breathing room air when EPI was infused at 80, 160, and 320ng•$^{-1}$kg•$^{-1}$min, while DA infusions did not result in significant increases in PASP. The minimal response by IPAVA to DA infusion may be the result of the minimal increases in cardiac output or PASP compared to those increases that occurred during EPI infusions, as the slopes of the cardiac output versus PASP relationship were not significantly different between the EPI and DA infusions.

If a bubble score of 1, which represents only 1-3 bubbles appearing in the left ventricle over the twenty cardiac cycles after the opacification in the right ventricle, is considered to be insignificant, then a bubble score of 2 or greater can define when blood begins to flow through open IPAVA. In Fig. 4 PASP is plotted as a function of cardiac output for every bubble injection throughout the EPI and DA infusions in subjects breathing room air and indicates the combinations of flow and pressure that induced IPAVA to open. This demonstrates that there may be some critical combination of pressure and/or flow that opens IPAVA in healthy human subjects at rest. Additionally, if

large diameter IPAVA branch from pulmonary arteries proximal to the resistance arterioles, catecholamine-induced increases in pulmonary vascular resistance may increase the backpressure at the entrance to IPAVA, helping to direct flow through these vessels even at the relatively low cardiac outputs measured in this study.

Effect of Breathing 100% Oxygen During EPI and DA Infusions on Blood Flow Through IPAVA

In subjects breathing 100% oxygen in the current study, we demonstrated no increase in bubble scores during the infusion of either EPI or DA. This resulted in bubble scores that were significantly less than those occurring in subjects breathing room air for EPI infusions of 40 through 320 $ng \bullet kg^{-1} \bullet min^{-1}$ and for DA infusions of 8 and 16 $\mu g \bullet kg^{-1} \bullet min^{-1}$ despite no differences in cardiac output or PASP between the room air and 100% oxygen conditions. Of note, we have previously demonstrated that neither breathing 100% oxygen, nor the duration of breathing 100% oxygen affects the detection of saline contrast microbubbles in vivo (35).

In subjects breathing 100% oxygen during exercise, the increased arterial oxygen content can allow cardiac output to be slightly reduced (~10%) while maintaining a relatively constant oxygen delivery. However, the ~10% fall in cardiac output still results in higher flows than occur during low to moderate exercise when IPAVA are known to be patent (32, 94). These data suggest that the effect of hyperoxia on IPAVA is not simply due to a reduction in pulmonary artery blood flow. This is supported by data from the current study in which the increases in cardiac output and PASP were the same in subjects breathing room air or 100% oxygen. Furthermore, the reduction in bubble scores during hyperoxic exercise is probably not due to a reduction in the plasma concentration

of EPI or DA because in the current study we infused EPI and DA at the same rate in subjects breathing room air and 100% oxygen.

These data suggest that the effect of breathing 100% oxygen on preventing IPAVA from opening is not simply due to reductions in cardiac output, PASP, or reduced plasma catecholamine concentration; rather, there may be a separate mechanism that actively closes IPAVA or prevents them from opening. The active closure of IPAVA by hyperoxia is an attractive hypothesis because oxygen has been shown to induce constriction in other vascular beds such as increasing systemic vascular resistance (59), coronary vascular resistance (36), and has been implicated in hyperoxia-induced retinal vasoconstriction (27, 61, 167, 205). In the fetal circulation, the ductus arteriosus closes in response to increased oxygen tension (37) which may be mediated by oxygen sensitive K^+ channels (176). Microsphere data indicate that pulmonary blood flow is redistributed in sheep ventilated with 100% oxygen to a similar degree as occurs during hypoxic ventilation (110), which may further suggest active vasomotor activity in response to 100% oxygen. Additional microsphere data demonstrate that ventilating lungs with 100% oxygen reduces the number of large diameter microspheres collected from the pulmonary venous effluent (115). Together, these data lend further support to indicate that oxygen could be directly and actively preventing blood flow through IPAVA as we have previously suggested (89). However, the mechanism(s) regulating the hyperoxic closure of IPAVA remain elusive.

Similarities Between IPAVA and Supernumerary Arteries

At rest, IPAVA are not perfused, but we have shown that increases in cardiac output and/or PASP may recruit these vessels. This is supported by previous work in

which Stickland, *et al* (159) suggested such passive recruitment. Interestingly, the supernumerary arteries first described by Elliott and Reid (34) were also described as being closed under resting conditions, but could be recruited during increases in flow. Because supernumerary arteries branch at right angles from the conventional arteries, blood flow may preferentially follow the more direct conventional artery branching pattern unless increases in pressure and/or flow, such as during exercise or when breathing hypoxic gas mixtures, direct blood flow through them. Recaverran (133) also described the recruitment of 'preterminal arterioles' as branching from pulmonary arteries at a ninety-degree angle, being closed at rest, and recruited with increases in pulmonary artery pressure (Fig. 4.6). Shaw, *et al.* (148) further described the dynamic

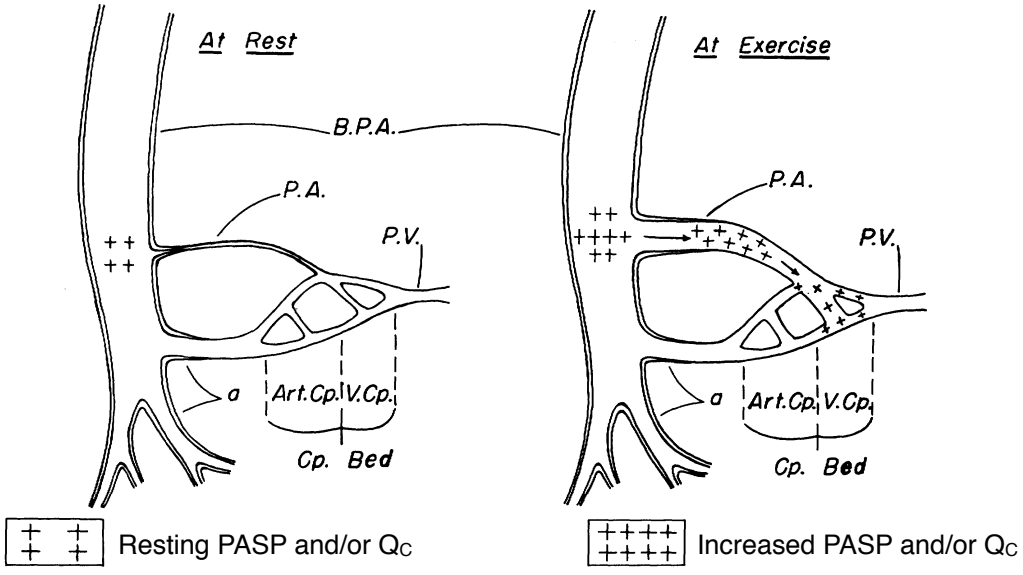

Figure 4.6. Schematic of 'Preterminal Arteriole'. Modified schematic of a 'preterminal arteriole' branching at a right angle from a pulmonary artery that is closed under resting conditions, but opens due to increased PASP and/or cardiac output and delivers a portion of the blood flow to the distal end of the pulmonary capillary bed, effectively acting as an arteriovenous anastomoses. B.P.A., medium sized branch of the pulmonary artery; a, pulmonary arteriole; P.A., preterminal arteriole; P.V., pulmonary venule; Art.Cp., arterial capillary; V.Cp., venous capillary; Cp.Bed, capillary bed. (Reproduced with permission from: Recavarren. *Circulation.* 33(2):177-180, 1966.)

opening of supernumerary arteries as occurring when the conventional artery from which they branch is physically stretched. Increases in cardiac output and/or PASP would accomplish this physical distension of conventional arteries and thus open the baffle valve at the entrance of supernumerary arteries. Additional anatomical evidence for the opening of large diameter IPAVA is provided in a study by Berk, *et al* (18) in which the opening of large "angioid structures" were visualized in lung biopsies taken during epinephrine infusion, but appeared closed in biopsies taken prior to and after the end of EPI infusion. Furthermore, they suggested that EPI caused a change in pulmonary resistance, which redistributed pulmonary blood flow and would fit with our data suggesting a role for changes in cardiac output and/or PASP.

Summary

We have demonstrated for the first time that EPI opens IPAVA in healthy humans at rest which supports previous anatomic work in dogs in which EPI infusions caused an increase in the transpulmonary passage of radioactive microspheres (116). While a direct effect of EPI or DA on IPAVA smooth muscle is a possibility, β-receptor mediated dilation of IPAVA appears unlikely. Rather, it appears more likely that the resulting catecholamine-induced increases in cardiac output and/or PASP due to EPI or DA infusions may be passively opening IPAVA, as first proposed by Stickland, *et al* (159). IPAVA are prevented from opening in subjects breathing 100% oxygen during either EPI or DA infusions, which suggests that the hyperoxic closure mechanism is independent from the opening mechanism and requires further investigation.

In Chapter V I shift to quantify blood flow through IPAVA using nuclear medicine imaging and determine if the lack of bubbles in subjects breathing 100% oxygen truly represents a reduction in blood flow through IPAVA, as we have suggested.

CHAPTER V

BREATHING 100% OXYGEN DURING EXERCISE REDUCES BLOOD FLOW THROUGH INDUCIBLE INTRAPULMONARY ARTERIOVENOUS ANASTOMOSES IN HEALTHY HUMANS

This chapter is in preparation for publication in *Journal of Applied Physiology* and Randall D. Goodman, Dixie Aaring, Thomas Voelkel, Scott Stewart, Toni Bamford, Igor M. Gladstone, Mathews I. Fish, and Andrew T. Lovering will be coauthors. I developed all the protocols, including the filtering of MAA, and performed all data analysis. The coauthors assisted with protocol development and data collection. The writing is entirely mine and co-authors provided editorial assistance.

INTRODUCTION

"It is now generally accepted that arterio-venous anastomoses exist in the lungs." – *M. Sirsi and K Bucher, 1953* (151)

Studies of the pulmonary circulation using large diameter solid microspheres have definitively demonstrated the existence of intrapulmonary arteriovenous anastomoses (IPAVA) in humans, dogs, cats, rabbits, and baboons (99, 115, 129, 131, 151, 156, 170, 172). Recently, the dynamic regulation of large diameter (>50μm) IPAVA that bypass the pulmonary capillaries has reemerged in the scientific literature because of data obtained using microspheres in exercising dogs (156) as well as data obtained using transthoracic saline contrast echocardiography (TTSCE) in exercising healthy humans (32, 35, 157).

In addition to exercise, Niden and Aviado (115) appear to be the first to suggest that ventilating lungs with hypoxic gas mixtures increased blood flow through large

diameter anastomoses, determined using glass microspheres, which has recently been confirmed using large diameter microspheres in the rat (10), and demonstrated in healthy humans breathing hypoxic gas mixtures at rest and during exercise using TTSCE (89, 94). Conversely, Niden and Aviado also demonstrated that ventilating lungs with 100% oxygen reduced the number of large diameter microspheres retrieved from the venous effluent of the pulmonary vasculature, which is also supported by TTSCE data in humans breathing 100% oxygen during exercise (35, 97).

While TTSCE offers a simple, noninvasive technique for detecting the opening and closing of IPAVA under a variety of conditions, this technique is unable to quantify the percentage of cardiac output flowing through these large diameter anastomoses and no studies have quantified if the reduction or absence of saline contrast microbubbles in the left ventricle during exercise in healthy human subjects breathing 100% oxygen is actually the result of a reduction (or prevention) of blood flow through IPAVA. However, Technetium-99m (^{99m}Tc)-labeled macroaggregated albumin (^{99m}Tc-MAA) has been used to quantify the percentage of blood flow, known as the shunt fraction, bypassing the pulmonary microcirculation (100, 160, 162). This technique has been used to quantify small increases in blood flow through IPAVA in exercising humans (96, 197), however the use of commercially available MAA includes a percentage of MAA that are small enough to have the potential to travel through pulmonary capillaries which would overestimate the transpulmonary passage through IPAVA. In the current study we improved the quantification of blood flow through MAA by developing a procedure to filter out the small MAA and thus remove this source of error from the absolute quantification of shunt fraction.

The purpose of this study was to use filtered MAA to determine if there was a reduction in blood flow through IPAVA in subjects exercising breathing 100% oxygen compared to exercise breathing room air.

METHODS

This project was approved by the University of Oregon Office for Protection of Human Subjects and the PeaceHealth Institutional Review Board. Written informed consent was obtained from subjects prior to their participation in the study.

Echocardigraphic Screening, Lung Function, and VO_2peak Testing

An initial echocardiographic screening and bubble study were performed with and without Valsalva maneuver on five subjects. A single subject demonstrated bubbles in the left heart within 3 cardiac cycles and was excluded from participation due to presence of a PFO. The remaining four male subjects performed spirometry including FVC and SVC according to ATS/ERS standards and whole body plethysmography to determine lung volumes and capacities (111, 188). The single-breath, breath-hold technique was used for determination of lung diffusion capacity for carbon monoxide (80, 102). During a separate visit, subjects performed a graded exercise test to exhaustion to determine peak oxygen uptake and max power output at VO_2peak (MedGraphics Ultima CardiO2 metabolic system, Lode Excalibur Sport cycle ergometer).

MAA Filtering and Technetium-99m Labeling

A vial containing ~4 million lyophilized macroaggregated albumin (MAA) particles was reconstituted with 8ml of sterile saline (DraxImage, >90% of particles are 10-70µm, Kirkland, Quebec). After allowing the contents to settle for 1 min, 4ml of solution were drawn off the top through a sterile 20µm nylon net filter (20µm x 25mm

nylon net filter; Millipore, MA) and 2ml of sterile saline flushed back through the filter. After allowing this solution to settle for 1 min, the filtering procedure removing 4ml of solution and replacing with 2ml of sterile saline was repeated 2 additional times resulting in a 2ml suspension of filtered MAA. Samples of reconstituted MAA taken from a sample prior to and after filtering were placed on a hemacytometer to measure and count the MAA in the reconstituted samples. The hemacytometer had grooves spaced 5µm apart and a microscope was used to photograph the MAA on the slide. Using the grooves as a reference, the number and length of MAA were determined using four samples from non-filtered and filtered reconstituted MAA. The four samples from each the non-filtered and filtered procedures were pooled (n≈1,000 particles pre filtering) to represent an average distribution of the size of MAA pre and post filtering. These data revealed 17.7% of MAA particles were <20µm prior to filtering, whereas after filtering this was reduced to 6.5% of MAA <20µm. The percentage of MAA <15µm was reduced from 12.9% before filtering, to 2.2% after filtering. After filtering, the median length MAA particle was 35µm, with a mean of 35.3µm.

After the filtering procedure was conducted, a dose of ^{99m}Tc-pertechnetate was added to this vial to radiolabel the MAA. This entire solution was pulled through the filter a fourth time and 2 ml of sterile saline flushed back through the filter to remove any free ^{99m}Tc-pertechnetate. Quality control (QC) was conducted to ensure >99.5% labeling efficiency using a Tec-Control Chromatography kit (Biodex, New York) and 0.057 mCi/kg ^{99m}Tc-MAA was drawn up for injection into each subject resulting in a standardized dose based on subject body weight and a dose that was less than a standard clinical dose to help minimize total radioactive exposure (96).

Study Conditions

Subjects reported to the Nuclear Medicine Department at the Oregon Heart & Vascular Institute in Springfield, OR on 5 occasions, each separated by a minimum of 7 days. Each subject performed the following protocols while seated in the cycle ergometer in the forward leaning, aerobar position: (1) rest breathing room air, followed by a SPECT/CT scan; (2) exercise breathing room air followed by a SPECT/CT scan; (3) rest breathing room air, followed by a planar scan; and (4) exercise breathing room air, followed by a planar scan. The SPECT protocols were conducted before the planar scan visits, but the order of rest and exercise visits were random between subjects. The final visit for all subjects was (5) exercise breathing 100% oxygen, followed by a planar scan. Subjects breathed 100% oxygen for 5-10 min prior to the MAA injection and continued breathing 100% oxygen throughout the duration of the planar scan. Exercise consisted of 2 min at 50% of the power output (warm up) obtained at VO_2peak and then continued for an additional 3 min at 85% of peak power output. A bubble study was performed 2 min into the 85% workload using 3 ml of sterile saline and 1 ml of room air during echocardiography of an apical 4-chamber view of the heart; this was immediately followed by the ^{99m}Tc-MAA injection. Immediately after the ^{99m}Tc-MAA injection, the intravenous catheter was removed and the subject moved to the bed of the SPECT/CT scanner located in the same room. During SPECT/CT scans, an initial scout CT scan and a dose-modulated CT scan resulted in ~7-9 mins total between MAA injection and start of SPECT data acquisition. During planar scans, the scanning began within 3 min following the ^{99m}Tc-MAA injection. The syringe, stopcock, extension set, and

intravenous catheter were placed in the scintillation counter to determine residual radioactivity and thus determine the net injected dose.

Imaging

All imaging was performed on a dual-headed Philips Precedence 16P SPECT/CT camera (Philips Medical Systems, The Netherlands). For the SPECT/CT protocols (Visits 1 & 2), a low dose, dose-modulated whole body CT scan was performed using a 16x slice helical CT scanner (140kV, 50mAs/slice maximum, 0.5-s rotation time) during a breath hold at total lung capacity. SPECT imaging acquisition occurred using a step-and-shoot mode over 32 stops per camera at 10 sec per stop and was repeated over a total of 4 sections of the body in order to acquire SPECT data from head to toe. During the first two sections, which completely spanned the lungs, subjects performed a 10 sec breath hold at functional residual capacity during SPECT acquisition in order to limit respiratory lung motion and were verbally coached to inhale and exhale back to FRC as the Gamma camera rotated to the next stop. SPECT datasets were acquired with a 10% symmetric energy window centered on 140 keV, which is the energy emitted by ^{99m}Tc. The total scan time including pauses during camera movements was ~28min.

During visits 3-5, whole body planar scanning (PLANAR) was conducted using anterior and posterior Gamma cameras to capture emitted photons in a continuous scan protocol that began at the head and was completed in 17 min 15 sec. To estimate the rate of ^{99m}Tc unbinding from the MAA, we repeated the PLANAR scan protocol 30 min and 60 min post ^{99m}Tc-MAA injection after the rest and exercise bouts in subjects breathing room air. The labeling efficiency of ^{99m}Tc-MAA remaining in the initial vial was again determined at the conclusion of the 30 min and 60 min planar scans.

Post-processing Data Reconstruction and Analysis

The raw SPECT data were reconstructed in Autospect+ using the Astonish reconstruction algorithm (2 iterations, 16 subsets, Hanning filter max 1.20) (Philips Healthcare), which is a three dimensional ordered subsets expectation maximization reconstruction that applies the attenuation map derived from the low-dose CT to correct each voxel for attenuation and compensates for the blurring effects of the collimator built into the reconstruction (177). This is intended to allow for greater resolution recovery and improve the signal-to-noise ratio. An objective region of interest (ROI) using a minimum threshold of 5 counts per cm^2 was drawn on each transverse slice through the lung of the attenuation-corrected SPECT reconstruction data and the sum of the counts from these ROIs determined the total lung ROI. Sagittal and coronal slices through the image were also used to determine if the lung counts varied depending on the slices used to determine the ROI. Because of high counts appearing in the kidneys and splanchnic region, the objective lung ROI needed to be manually adjusted to remove splanchnic counts from the lung ROI. The CT data was used to objectively determine the attenuation-corrected whole body ROI. When significant counts from the bladder, kidneys, or salivary glands appeared in the images, they were assumed to represent free-^{99m}Tc that had come unbound from the MAA and been filtered from the blood and attempts were made to remove these counts from the whole body ROI. Despite these efforts, the large number of counts visualized in the splanchnic region required a subjective determination of the lung ROI. This made differentiating counts believed to be due to free-^{99m}Tc from those still bound to MAA not possible.

PLANAR data was analyzed using the MultiViewer (Philips). ROIs were determined from anterior and posterior images and used to calculate geometric mean counts (GMT) by taking the square root of the product of anterior and posterior counts (23). The whole body ROI was determined by drawing a box around the entire body because the edge along the extremities of the whole-body MAA image was difficult to identify. Mean background counts (counts per cm^2) were determined from a region above the right shoulder and to the right of the head and these counts per cm^2 subtracted from all ROIs. The lung ROI was drawn at the edge of the lung border by maximizing the contrast at the edge of the lung border using the color map Step20 with Gamma = 0.6.

For all scanning procedures, the raw shunt fraction was calculated using the standard lung-to-whole body ratio as follows: [Total body counts – lung counts] / total body counts.

Correction for Free-^{99m}Tc in the Blood

A venous blood sample was drawn at the conclusion of each PLANAR scan. One ml of this blood sample was placed in a scintillation counter to determine the counts per minute, which were corrected for time decay by standardizing back to time zero when the MAA injection occurred using the equation $A_t=A_0 * e^{[-0.693(t)]/[t_{1/2}]}$, where A_t = the counts determined t minutes after MAA injection, A_0 = the corrected counts, t = number of minutes after MAA injection, and $t_{1/2}$ = the half life of ^{99m}Tc (361.2 min). After converting the counts per minute to mCi using the counting efficiency of the scintillation counter (avg. 79%), the percent free radioactivity in the blood was calculated by extrapolating the mCi in 1ml of blood to an estimated total blood volume (114) and dividing by the net injected dose. This percentage of free-^{99m}Tc was determined for each

visit and subtracted from the raw shunt fraction to determine the shunt fraction due to the passage of large MAA through IPAVA.

Statistics

Bubble scores were analyzed using a Friedman's test with Dunn's multiple comparison posttest. Difference in shunt fractions were determined using a reapeated measures ANOVA with Tukey posttest.

RESULTS

Anthropometrics, pulmonary function, diffusion capacity for carbon monoxide, and exercise capacity data are presented in Table 5.1. Labeling of MAA with ^{99m}Tc occurred immediately prior to every study and resulted in >99.5% binding efficiency before every scan and these data are presented in Table 5.2, along with the binding efficiency determined after PLANAR scans.

The use of SPECT/CT imaging provides the unique ability to co-register data acquired from SPECT imaging with CT data, without needing to move the subject from the bed to acquire both data sets, and is used to create a non-uniform attenuation-coefficient map for the correction of Gamma radiation interacting with variable density tissue before being captured by the Gamma camera. This technique has shown promise in improving the accuracy in the enhancement of diagnostic pulmonary imaging (161, 163) and we initially attempted to use this new technology to improve the quantification of blood flow through IPAVA. The first problem we encountered was that the length of time needed to acquire CT data and SPECT data covering the entire body resulted in the accumulation of activity in the kidneys, bladder, salivary glands, thyroid, and stomach of many subjects, suggesting the *in vivo* unbinding of ^{99m}Tc from MAA, as seen in

Table 5.1. ***Anthropometrics, pulmonary function, diffusion capacity for CO, and peak exercise capacity data.***

Height, cm	185.4	±	7.2			
Weight, kg	79.7	±	4.8			
Age, yrs	32.0	±	7.3			
BMI, $kg \cdot m^{-2}$	23.2	±	1.1			
FVC, L	6.16	±	0.82	(103.3	±	6.9)
FEV1, L	4.81	±	0.68	(100.0	±	9.5)
FEV1/FVC	78.00	±	2.94	(95.5	±	4.2)
$FEF_{25-75\%}$, $L \cdot sec^{-1}$	4.275	±	0.92	(92.0	±	19.0)
SVC, L	5.93	±	0.72	(101.3	±	7.3)
IC, L	3.57	±	0.90	(95.0	±	22.1)
ERV, L	2.36	±	0.41	(113.8	±	24.2)
FRC, L	3.99	±	0.80	(106.8	±	15.9)
RV, L	1.65	±	0.51	(90.0	±	22.7)
TLC, L	7.58	±	0.98	(101.5	±	6.9)
DL_{CO}, $ml \cdot min^{-1} \cdot mmHg^{-1}$	38.5	±	6.6	(107.0	±	14.8)
DL_{CO}/VA, $ml \cdot min^{-1} \cdot mmHg^{-1} \cdot L^{-1}$	5.3	±	0.6	(109.0	±	12.7)
VO_{2peak}, $L \cdot min^{-1}$	4.55	±	0.79			
VO_{2peak}, $ml \cdot kg^{-1} \cdot min^{-1}$	58	±	7.3			
Workload at VO_{2peak}, W	380	±	95			

Note. Values are means±SD (percent predicted±SD).

Table 5.2. ***Ex vivo binding efficiency of ^{99m}Tc-MAA***

			Binding efficiency			
Activity	Scan Type	FIO_2	Pre Scan 1	Post Scan 1	Post Scan 2	Post Scan 3
Rest	Planar	0.21	99.9±0.3	99.5±1.0	99.2±1.2	99.3±0.7
Exercise	Planar	0.21	99.6±0.3	99.3±0.6	98.9±0.7	98.8±0.9
Exercise	Planar	1.00	99.9±0.1	99.9±0.1		

Note. Values are means±SD.

reconstructed images (Fig. 5.1). A second problem was the possible inaccuracies involved in the Philips proprietary reconstruction algorithm (Astonish) in quantifying total radioactive counts. This algorithm was designed to create clearer pictures during myocardial stress perfusion studies (9, 55, 177) and may have artificially adjusted the quantification of radioactive counts during reconstruction of our data despite providing the clearest pictures for determining the lung ROI. A third problem was the difficulty to objectively determining the lung ROI despite minimizing breathing artifact by having subjects conduct a breath hold at functional residual capacity during SPECT data acquisition. The attenuation-corrected image created from the SPECT/CT data was reconstructed from the 32 views surrounding the body into a three-dimensional image and the lung ROI could be determined from coronal, transverse, or saggital slices, each of which resulted in different total counts.

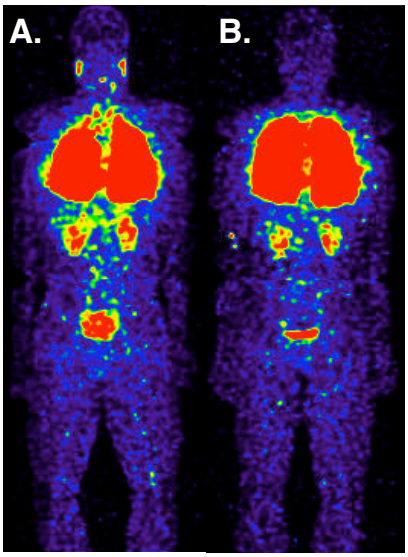

Figure 5.1. SPECT/CT Reconstructions. Representative SPECT/CT reconstructions of a single subject after ^{99m}Tc-MAA injection (A) at rest and (B) during 85%max exercise. Note the significant uptake of free-^{99m}Tc in the salivary glands of (A) as well as the kidneys and bladder in both images. The purple and blue color indicates freely-circulating ^{99m}Tc in the blood.

Ito, *et al.* quantified a mean shunt fraction at rest in healthy subjects of 6.6% using planar imaging and the lung-to-whole body ratio as we did, although without filtering the MAA or correcting for free ^{99m}Tc, and suggested a 10% shunt be used for the cutoff value for normal versus abnormal shunt fraction. Phantom and *in vivo* studies also suggest that the error using SPECT reconstruction for absolute quantifications may range from 2-10% (138). In our SPECT images, which required ~17 min longer acquisition time than the PLANAR scans, the unbinding and uptake of free ^{99m}Tc by the liver, kidneys, bladder, stomach, and salivary glands in addition to the free ^{99m}Tc circulating in the blood prevented us from accurately quantifying blood flow through IPAVA, even when attenuation-correction was incorporated into the reconstruction algorithm.

Because of these problems that emerged in our attempt to use SPECT/CT imaging to quantify blood flow through large diameter IPAVA, we chose to use PLANAR imaging to quantify blood flow through inducible IPAVA in healthy humans and improved upon previous research by (1) using filtered MAA and (2) correcting for free-^{99m}Tc circulating in the blood to determine the shunt fraction in subjects at rest and during exercise breathing room air and during exercise breathing 100% oxygen.

Bubble scores determined prior to the three PLANAR scans, presented in Figure 5.2, increased from rest to 85%max exercise breathing room air, and were reduced during exercise breathing 100% oxygen. The mean shunt fractions calculated from PLANAR data after removing contributions due to free-^{99m}Tc increased from -0.11% ± 0.45% at rest to 0.83% ± 0.58% at 85%max exercise breathing room air, and was reduced to -0.24% ± 0.99% during exercise breathing 100% oxygen (p=.0843) and are shown in Figure 5.3. The data are plotted to show the raw shunt fraction without correcting for

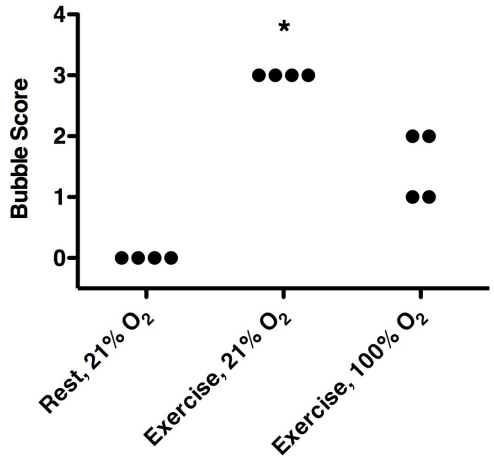

Figure 5.2. Bubble Scores. Bubble scores for each individual at rest and during 85%max exercise breathing room air and during 85%max exercise breathing 100% oxygen. *p<.05 vs Rest, 21% O_2 (Friedman's test, Dunn's posttest).

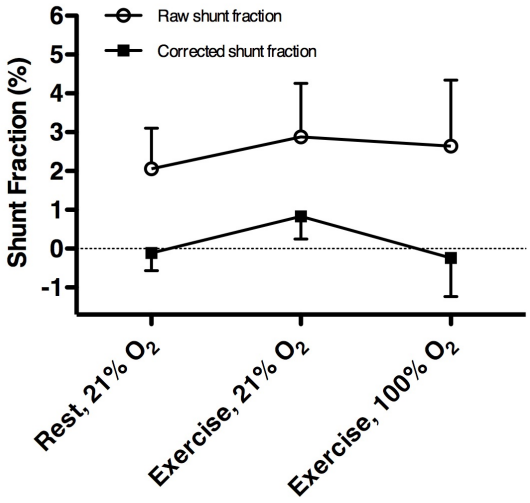

Figure 5.3. Shunt Fractions. Mean shunt fraction determined from planar imaging in subjects breathing room air at rest and during 85% max exercise, and while breathing 100% oxygen during 85% max exercise. Open circles represent shunt fractions without removing estimate of free ^{99m}Tc (Raw shunt fraction), closed squares represent shunt fractions after removal of free ^{99m}Tc (Corrected shunt fraction), p=.08 (repeated measures ANOVA).

free-^{99m}Tc and the corrected shunt fraction that removed our calculation of free-^{99m}Tc based on the blood sample taken immediately at the conclusion of each scan. The calculated contribution from free-^{99m}Tc during the planar scans are shown for each individual in Figure 5.4 and demonstrates variability between subjects, between FIO_2, and an increasing percentage of unbinding at 30 and 60 min that exceeds the free-^{99m}Tc detected using the QC kits (Table 5.2). However, even when the free-^{99m}Tc is removed from the raw shunt fractions, increasing the length of time for the completion of the scan

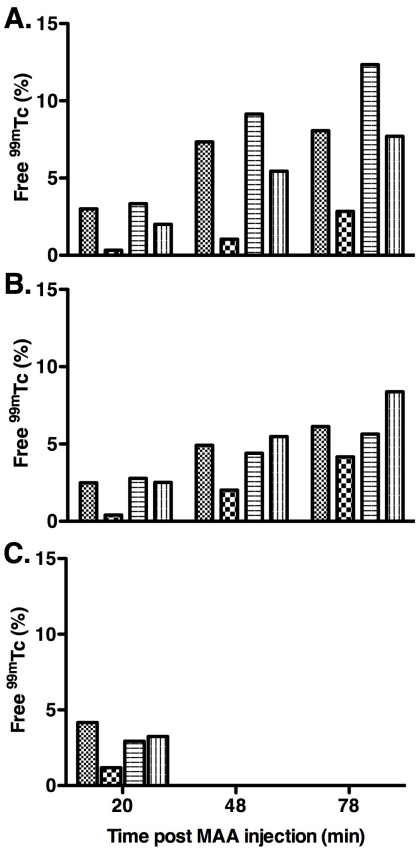

Figure 5.4. Free-^{99m}Tc. *In vivo* calculated percentage of free-^{99m}Tc from blood samples taken 20, 48, and 78 min after ^{99m}Tc-MAA injection in subjects (A) at rest breathing 21% oxygen, (B) during exercise breathing 21% oxygen, and (C) during exercise breathing 100% oxygen. Each bar represents an individual subject.

increases the counts outside of the lung, resulting in an overestimation of the shunt fraction (Fig. 5.5).

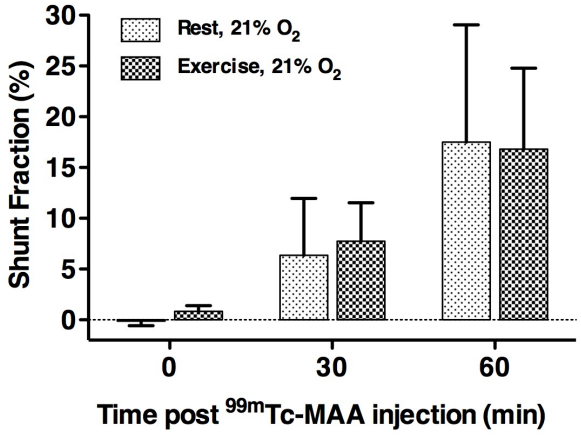

Figure 5.5. Timing Effect on Shunt Fraction. Mean shunt fractions determined from PLANAR imaging beginning immediately, 30, and 60 min after ^{99m}Tc-MAA injection at rest or during 85%max exercise.

DISCUSSION

The main finding from this study was that we quantified an increase in the shunt fraction using PLANAR imaging from -0.11% ± 0.45% at rest to 0.83% ± 0.58% at 85%max exercise breathing room air, which was reduced to -0.24% ± 0.99% during exercise breathing 100% oxygen (p=.0843) using filtered MAA and correcting for free-^{99m}Tc in the blood (Fig. 5.3). These quantified shunt fractions follow the increase in bubble scores from rest to exercise breathing room air, which were reduced during exercise breathing 100% oxygen (Fig. 5.2).

Filtering of MAA

The first methodological advancement in this study was the development of a filtering procedure of reconstituted MAA from a standard clinical kit through a 20μm filter that reduced the percentage of MAA <20μm in the sample from 17.7% to 6.5% and the percentage of MAA <15μm from 12.9% to 2.2%. However, the actual percentage of MAA <20μm was probably even less because the radiolabeled MAA were filtered one additional time to remove any free-^{99m}Tc remaining after the labeling procedure. This resulted in >99.5% labeling efficiency for all scans.

Quantification of Free-^{99m}Tc

The second major methodological advancement from this study was due to the finding that there was significant unbinding of ^{99m}TC from the MAA *in vivo* throughout the first ~78 mins after the injection of ^{99m}Tc-MAA, while the *ex vivo* unbinding of ^{99m}Tc from MAA determined from the QC kit did not occur to the same degree (Table 5.2, Fig. 5.4). The percentage of free-^{99m}Tc varied between subjects and varied based on the FIO_2. While the cause of the intersubject variability in unbinding of ^{99m}Tc is not entirely clear,

accounting for this and the intrasubject variability that occurs due to changes in the FIO_2 is absolutely necessary in order to accurately quantify blood flow through large diameter IPAVA.

The time-dependent unbinding of ^{99m}Tc from MAA presents a problem for accurately calculating the right-to-left shunt fraction, which assumes that all counts detected outside of the lung represent the passage of MAA through large diameter IPAVA. Our attempts to use SPECT/CT imaging to quantify blood flow through IPAVA revealed problems associated with the time necessary to acquire SPECT/CT data spanning the entire length of the body. Because our calculation of free-^{99m}Tc can only determine the radioactivity circulating in the blood, it is insensitive to free-^{99m}Tc once it is removed from the blood by the salivary and thyroid glands, and through the kidneys to be excreted in urine. Longer scans, such as our attempts to use SPECT/CT imaging, as well as our 30 and 60 min PLANAR scans, demonstrated radioactive counts outside of the lung due to free-^{99m}Tc that had been removed from the blood and could not be corrected using our calculation of free-^{99m}Tc in the blood and these counts became part of the quantified shunt fraction. Thus, any delays between MAA injection and the start of the PLANAR scan will increase the probability of measuring free-^{99m}Tc outside of the lung that is not due to blood flow through large diameter IPAVA. Thus, by minimizing the total time from MAA injection to the conclusion of our first PLANAR scan we feel confident that we have minimized sources of error due to free-^{99m}Tc in quantifying the absolute shunt fraction through large diameter IPAVA.

Consistencies Between TTSCE and MAA Data

Transthoracic saline contrast echocardiography has been used to detect blood flow through IPAVA in healthy humans during exercise breathing room air (32, 158, 159). These data are supported by data obtained using solid MAA that quantified an increase in shunt fraction in exercising humans (96, 197), which was confirmed in the present study even when small particles from the MAA kit were removed and the unbinding of ^{99m}Tc from MAA was accounted for. TTSCE has also detected the transpulmonary passage of microbubbles at rest and during exercise in subjects breathing hypoxic gas mixtures (89, 94), which is supported by data obtained using large diameter solid microspheres in rats ventilated with hypoxic gas mixtures (10). Finally, TTSCE has demonstrated a reduction or prevention of saline contrast microbubbles from passing through large diameter IPAVA in exercising subjects breathing 100% oxygen (35, 97). However, some have raised the concern that changing the partial pressure environment of the microbubbles by altering the FIO_2 may alter bubble dynamics and their lifespan (66). We have shown that neither the FIO_2, nor the bubble gas composition affect the stability of *in vivo* microbubbles (35). The current study is now the first to demonstrate a reduction in the shunt fraction using solid MAA in exercising subjects breathing 100% oxygen, supporting the results obtained using TTSCE that 100% oxygen reduces blood flow through large diameter IPAVA.

Summary

This study improved the accuracy and sensitivity of nuclear medicine imaging for quantifying blood flow through anatomical right-to-left intrapulmonary arteriovenous

anastomoses by first filtering a reconstituted kit of MAA and second accounting for the *in vivo* unbinding of ^{99m}Tc from MAA occurring during the scanning procedure.

We have shown that in order for nuclear medicine imaging to accurately quantify blood flow through IPAVA, the scan must be completed as quickly as possible after the injection of ^{99m}Tc-MAA so that the unbinding of ^{99m}Tc from MAA can be quantified while it is still circulating in the blood. Once the free-^{99m}Tc begins to be taken up by various organs, these counts will be quantified as part of the shunt fraction, but do not represent the passage of large diameter MAA through IPAVA. Using this technique we quantified an increase in the shunt fraction during exercise in subjects breathing room air when saline contrast microbubbles also passed through the pulmonary circulation; however, the shunt fraction was not increased in subjects exercising at the same absolute intensity breathing 100% oxygen when the bubble scores were reduced.

Future work using this new technique that removes small MAA particles from a standard kit and accounts for free-^{99m}Tc in the blood due to unbinding from MAA that occurs *in vivo* needs to be conducted to quantify the shunt fractions that occur in subjects demonstrating bubble scores of 4 and 5 when bubbles completely fill the left ventricle.

This chapter has demonstrated that there is an increase in blood flow through large diameter IPAVA in healthy humans during exercise, which does not occur during exercise breathing 100% oxygen. However, the role of increasing blood flow through these vessels in affecting pulmonary gas exchange efficiency still remains a controversial topic that has not been resolved. Chapter VI of this dissertation directly investigates the role for IPAVA in affecting pulmonary gas exchange efficiency.

CHAPTER VI

THE CONTRIBUTION OF INDUCIBLE INTRAPULMONARY ARTERIOVENOUS ANASTOMOSES TO PULMONARY GAS EXCHANGE EFFICIENCY DURING EXERCISE IN HEALTHY HUMANS

This chapter is in preparation for submission to the *Journal of Applied Physiology* and will be coauthored with Jonathan E. Elliott, Kara M. Beasley, Randall D. Goodman, Igor M. Gladstone, Jerold M. Hawn, and Andrew T. Lovering. Drs. I.M. Gladstone and J.M. Hawn placed the radial artery catheters in all subjects. All coauthors assisted in data collection. A.T. Lovering helped develop the protocols and provided editorial assistance.

INTRODUCTION

"Physiologically, pulmonary arteriovenous shunting is commonly defined as the passage of blood through the lungs without taking part in gas exchange; an incomplete exchange of gas is usually not considered." – Genovesi, et.al. (1976)

The reduction in pulmonary gas exchange efficiency, as defined and quantified by the alveolar-to-arterial oxygen difference ($AaDO_2$) that occurs with increased exercise intensity, can be caused by diffusion limitation, ventilation-perfusion ($\dot{V}/\dot{Q}$) heterogeneity, and/or all sources of shunt (30). Recent work by our group and others has demonstrated the transpulmonary passage of saline contrast bubbles through intrapulmonary arteriovenous anastomoses (IPAVA) during exercise, which the authors have proposed may represent an intrapulmonary shunt (35, 94, 96, 97, 159). However, as pointed out by Hopkins, Olfert & Wagner (66, 71), it has yet to be directly demonstrated that the transpulmonary passage of saline contrast bubbles represents a true 'shunt' that negatively impacts pulmonary gas exchange efficiency. Instead, they suggest that

intrapulmonary shunt does not occur in healthy humans based on data obtained using the multiple inert gas elimination technique (MIGET) (58, 136, 144, 173, 182).

Furthermore, Wagner and colleagues (178) have suggested that their data using the 100% oxygen technique also demonstrates that there is no significant contribution of shunt to pulmonary gas exchange inefficiency. The use of 100% O_2 is important to note because in subjects breathing 100% O_2, the contributions of diffusion limitation and $\dot{V}/\dot{Q}$ heterogeneity are prevented leaving only shunt, *assuming* that there is no effect of breathing 100% O_2 on the patency of IPAVA which have the potential to act as a shunt. Interestingly, we have demonstrated that breathing 100% O_2 during exercise does in fact prevent the transpulmonary passage of saline contrast bubbles (35, 97). Thus, if the transpulmonary passage of saline contrast bubbles is occurring through IPAVA which act as a true shunt, then it would not be detected in subjects breathing 100% O_2. Accordingly, it would be necessary to eliminate diffusion limitation and $\dot{V}/\dot{Q}$ heterogeneity without affecting the patency of inducible intrapulmonary arteriovenous anastomoses in order to make definitive statements regarding their contribution as a shunt to pulmonary gas exchange efficiency during exercise.

The purpose of this study was to determine the contribution of blood flow through IPAVA in determining pulmonary gas exchange efficiency during exercise in healthy humans. We hypothesized that breathing 40% O_2 during exercise would allow for blood to flow through IPAVA, but eliminate diffusion limitation and $\dot{V}/\dot{Q}$ heterogeneity as potential contributors to the $AaDO_2$ during exercise, leaving the only possible contributing factor as shunt. Thus, any measured $AaDO_2$ in a subject breathing 40% O_2

who demonstrate open IPAVA would be caused solely by the contribution of postpulmonary and intrapulmonary shunt.

METHODS

The University of Oregon Office of Protection for Human Subjects approved this study, and all subjects provided written informed consent before beginning study procedures. All studies were performed according to the declaration of Helsinki.

Echocardigraphic Screening, Lung Function, and VO_2peak Testing

An initial echocardiographic screening and bubble study were performed with and without Valsalva maneuver. Six subjects demonstrated bubbles in the left heart within 3 cardiac cycles and were excluded from participation due to presence of a PFO. The remaining 16 subjects (3 female) completed spirometry including FVC and SVC maneuvers according to ATS/ERS standards (111) and underwent whole body plethysmography to determine lung volumes and capacities (188). The single-breath, breath-hold technique was used for determination of lung diffusion capacity for carbon monoxide (80, 102). During a separate visit, subjects performed a graded exercise test to exhaustion on a cycle ergometer (Lode Excalibur Sport) to determine peak oxygen uptake and power output at VO_2peak (MedGraphics CardioO2, St. Paul, MN).

Subject Instrumentation

A radial artery catheter (Arrow International, USA) was placed under local anesthesia (1% lidocaine, 2% by volume nitroglycerine (5 mg/ml) to minimize vasospasm). During *Protocol 1* core temperature was determined using an ingested temperature pill (CorTemp Ingestible Sensor, HQInc, Palmetto, FL), while an esophageal temperature probe (Mon-a-them General Purpose, 9 Fr) was placed for monitoring core

body temperature during *Protocol 2*. These temperature measurements were used to temperature-correct blood gases. A 22G intravenous catheter was placed in the antecubital fossa for injection of saline contrast microbubbles.

Exercise Protocols

We conducted two different protocols to investigate the patency of IPAVA in exercising subjects breathing various fractions of inspired oxygen (FIO_2s) and to ascertain the role open IPAVA play in determining pulmonary gas exchange efficiency.

*Protocol 1:*The first protocol determined the patency of IPAVA at various *relative* workloads (25%, 50%, and 75% of max) in 5 *male and* 3 *female* subjects breathing an FIO_2=0.21, 0.60, and 0.14. Subjects exercised continuously for 4 min at each relative intensity workload while breathing each FIO_2 and a 45 min break separated each FIO_2 bout.

Protocol 2: A second protocol investigated 8 *male* subjects exercising at three *absolute* (100W, 200W, and 300W) and one *relative* (85% of max) workload breathing an FIO_2=0.21 and 0.40. Subjects exercised continuously for 4-5 min each at 100W, 200W, and 300W breathing room air. They then took a 10 min break before exercising for 4-5 min at 85% of their peak wattage obtained during the VO_2peak test. After a 45 min break the same exercise protocol was repeated breathing 40% oxygen. Subjects breathed 40% oxygen for 15 min at rest before resting measurements were obtained and throughout the 10 min break prior to the 85% max exercise bout.

Pulmonary Gas Exchange Efficiency

Pulmonary gas exchange efficiency was quantified as the difference between the alveolar O_2 partial pressure (PAO_2) and the arterial O_2 partial pressure (PaO_2). The PAO_2

was estimated using the ideal gas equation using the arterial partial pressure of CO_2 ($PaCO_2$) obtained from the radial artery blood draw, RER measured during the arterial blood draw, and corrected for body temperature,

$PAO_2 = [(P_B - e^{(0.05894809*Tc+1.688589)}) * FIO_2] – PaCO_2*[FIO_2 + (1 - FIO_2)/RER]$ (3). At rest and 3 (*Protocol 1*) or 3.5 min (*Protocol 2*) into each exercise bout a 3-5ml sample of radial artery blood was drawn anaerobically over 10-20 seconds for direct measurements of arterial oxygen saturation (OSM-3, Radiometer) and arterial PO_2, PCO_2 and pH with a blood-gas analyzer (Siemens 248). Prior to each study, 3 samples of blood were aerated with known concentrations of O_2 and CO_2 that spanned the range of expected PaO_2 values for the normoxic and hypoxic exercise bouts. In *Protocol 2* a second set of gases was tonometered to span the PaO_2 exected to result during the hyperoxic exercise bouts. These data sets were used to tonometry correct the blood samples collected during the study for any bias introduced by the blood gas analyzer.

Saline Contrast Echocardiography for Detection of IPAVA

At rest and 3 min *(Protocol 1)* or 3.5 min *(Protocol 2)* into each exercise bout (acquired simultaneously during arterial blood draw) saline contrast echocardiography was performed as previously described (35, 89, 97). Briefly, 3ml of sterile saline was agitated with 1 ml of air and forcefully injected into a peripheral arm vein. Twenty cardiac cycles were recorded after initial appearance of bubbles in the right heart and a 0-5 score assigned based on the greatest number and spatial distribution of bubbles in the left heart in a single frame (35, 89, 97).

Pulmonary Artery Systolic Pressure

Pulmonary artery systolic pressure (PASP) was calculated using the peak velocity of the tricuspid regurgitation and an estimate of right atrial pressure based on guidelines from the American Society for Echocardiography (142, 204). Because this measurement can be difficult, especially during exercise, we injected a small bolus of saline contrast microbubbles to help the sonographer visualize the envelope of the tricuspid regurgitation velocity and average of three velocities was used to calculate PASP. The same sonographer, with >25 years experience and 5 years research experience with our group, made all ultrasound measurements.

Statistics

Significance was set to $p<.05$ for all tests. Bubble scores were compared using a Friedman's Test with Dunns multiple comparison post test. Difference in the $AaDO_2$ between rest and exercise intensities in subjects breathing room air was determined using a one-way ANOVA with Tukey posttest, and was rerun for the $AaDO_2$ measured at rest and during exercise in subjects breathing 40% oxygen.

RESULTS

Anthropometric, lung function, volumes, and capacities, and exercise capacity are presented in Table 6.1. Metabolic, blood gas, and hemodynamic data at rest and during exercise for *Protocol 1* are presented in Table 6.2 and for *Protocol 2* in Table 6.3. There were no differences in resting or exercise metabolic data between the different FIO_2 concentrations (Table 6.2). Bubble scores for each subject prior to and during each exercise bout in *Protocol 1* breathing an FIO_2=0.21, 0.60, and 0.14 are presented in Fig. 6.1, while bubble scores from *Protocol 2* are presented in Fig. 6.2.

Table 6.1. ***Anthropometrics, pulmonary function, diffusion capacity for CO, and peak exercise capacity data.***

	Protocol 1	*Protocol 2*
Age, yrs	26.6 ± 6.3	24.0 ± 3.2
Height, cm	173.5 ± 8.6	181.4 ± 8.4
Weight, kg	67.2 ± 10.2	81.2 ± 7.3
VO2max, $ml \cdot kg^{-1} \cdot min^{-1}$	53.8 ± 4.8	53.9 ± 6.9
VO2max, $L \cdot min^{-1}$	3.62 ± 0.48	4.4 ± 0.7
Workload at VO_2max, W	316.9 ± 47.3	381.3 ± 67.5
FVC, L	4.94 ± 1.01 (101 ± 15.3)	5.9 ± 0.6 (98.1 ± 8.2)
FEV1, L	3.99 ± 0.86 (98.1 ± 0.86)	4.9 ± 0.4 (98.8 ± 8.3)
FEV1/FVC, %	80.63 ± 6.28 (97.1 ± 8.1)	82.6 ± 4.3 (99.3 ± 4.7)
FEF 25-75%, $L \cdot sec^{-1}$	3.81 ± 1.35 (91.1 ± 28.9)	5.0 ± 0.7 (100.4 ± 15.9)
SVC, L	5.1 ± 0.9 (109 ± 16.7)	6.1 ± 0.3 (102.4 ± 4.9)
IC, L	2.6 ± 0.6 (87.0 ± 17.2)	3.9 ± 0.6 (103.5 ± 15.9)
ERV, L	2.5 ± 0.5 (148.4 ± 29.7)	2.2 ± 0.5 (100.6 ± 24.2)
FRC, L	3.77 ± 075 (124.4 ± 22.0)	3.6 ± 0.6 (97.9 ± 14.5)
RV, L	1.36 ± 0.3 (94.9 ±17.7)	1.3 ± 0.6 (77.7 ± 34.5)
TLC, L	6.32 ± 1.1 (15.8 ± 15.8)	7.5 ± 0.8 (100.6 ± 9.8)
DL_{CO}, $ml \cdot min^{-1} \cdot mmHg^{-1}$	33.61 ± 6.66 (111.8 ± 12.4)	41.3 ± 4.7 (115.6 ± 12.7)
DL_{CO}/VA, $ml \cdot min^{-1} \cdot mmHg^{-1} \cdot L^{-1}$	5.49 ± 0.84 (116.1 ± 21.9)	5.6 ± 0.4 (114.4 ± 9.3)

Note. Data are mean±SD (percent predicted±SD).

Table 6.2. ***Metabolic, blood gas, and hemodynamic data at rest and during exercise*** **[*Protocol 1*].**

	FIO_2	Pre-Exercise	25%	50%	75%
VO_2	0.21	0.31±0.07	1.31±0.27	2.03±0.34	2.86±0.42
	0.60	0.31±0.06	1.39±0.23	2.13±0.29	3.08±0.41
	0.14	0.28±0.04	1.31±0.22	2.09±0.30	2.85±0.50
VCO_2	0.21	0.31±0.14	1.08±0.23	1.92±0.29	3.19±0.51
	0.40	0.26±0.08	0.95±0.18	1.78±0.25	2.99±0.53
	0.14	0.39±0.38	1.09±0.37	2.21±0.33	3.44±0.48
RER	0.21	0.88±0.07	0.83±0.06	0.95±0.07	1.11±0.07
	0.40	0.83±0.18	0.68±0.04	0.84±0.06	0.97±0.11
	0.14	0.90±0.08	0.90±0.08	1.06±0.07	1.24±0.06
VE	0.21	14.4±6.3	31.4±6.8	48.1±7.0	78.8±14.1
	0.40	14.1±4.8	29.9±5.6	47.0±5.6	72.5±14.0
	0.14	13.4±2.5	41.4±7.3	69.6±12.0	114.0±22.6
PaO_2	0.21	99.4±5.3	94.5±4.7	98.7±5.4	105.4±6.7
	0.40	354.4±17.1	344.6±14.1	342.5±17.7	343.4±20.5
	0.14	54.1±6.4	44.0±4.4	41.6±4.3	43.1±4.0
$PaCO_2$	0.21	37.1±7.5	39.8±3.8	42.3±3.8	40.5±4.8
	0.40	37.5±7.8	41.0±4.9	43.6±3.4	44.6±3.9
	0.14	35.7±6.4	35.0±4.5	34.2±3.7	32.6±5.4
pH	0.21	7.435±0.063	7.403±0.042	7.376±0.019	7.336±0.023
	0.40	7.433±0.071	7.397±0.037	7.368±0.018	7.328±0.026
	0.14	7.453±0.053	7.454±0.025	7.422±0.027	7.354±0.031
T_{core}	0.21	37.0±0.5	37.1±0.6	37.1±0.4	37.3±0.5
	0.40	37.1±0.5	37.1±0.5	37.1±0.5	37.3±0.6
	0.14	37.1±0.4	37.1±0.4	37.2±0.4	37.4±0.4
PASP	0.21	28.7±4.1	30.3±2.9	31.0±5.4	31.5±4.9
	0.40	28.7±4.8	29.2±4.2	30.5±1.8	30.7±5.0
	0.14	30.1±3.3	28.8±2.7	29.9±3.6	31.1±3.6

Note. Values are means±SD.

Table 6.3. ***Metabolic, blood gas, and hemodynamic data at rest and during exercise [Protocol 2].***

	FIO_2	Pre-Exercise	100W	200W	300W	85% max
VO_2	0.21	0.46±0.06	1.72±0.16	3.03±0.27	4.07±0.28	4.59±0.77
	0.40	0.48±0.09	1.89±0.18	3.19±0.26	4.29±0.36	4.64±0.83
VCO_2	0.21	0.40±0.05	1.65±0.33	3.09±0.39	4.75±0.52	4.65±1.66
	0.40	0.38±0.08	1.57±0.20	3.17±0.49	4.71±0.66	4.43±1.64
RER	0.21	0.87±0.08	0.91±0.07	1.02±0.08	1.17±0.12	1.12±0.06
	0.40	0.78±0.10	0.83±0.08	0.99±0.11	1.10±0.16	1.06±0.13
VE	0.21	13.4±3.0	41.7±7.2	76.4±13.6	127.5±26.4	155.6±20.4
	0.40	13.9±2.0	41.9±6.2	79.5±16.9	125.4±25.9	137.4±25.8
PaO_2	0.21	98.5±7.6	92.3±4.4	89.6±6.0	89.6±9.8	95.6±11.4
	0.40	219.1±8.6	215.3±9.5	219.2±8.0	224.3±9.1	227.4±9.3
$PaCO_2$	0.21	37.1±4.0	40.8±1.7	40.8±2.6	37.7±4.0	33.9±5.0
	0.40	37.1±3.3	40.7±2.1	41.1±3.9	38.5±4.8	36.5±4.4
pH	0.21	7.432±0.019	7.400±0.014	7.371±0.027	7.327±0.040	7.291±0.069
	0.40	7.418±0.024	7.393±0.019	7.365±0.024	7.331±0.036	7.300±0.052
T_{esoph}	0.21	36.6±0.1	36.6±0.2	37.1±0.4	37.6±0.3	37.9±0.3
	0.40	36.6±0.2	36.8±0.1	37.3±0.3	37.7±0.2	37.9±0.2
PASP	0.21	27.5±5.0	38.3±7.6	43.4±14.1	56.2±12.2	70.0±16.7
	0.40	27.0±3.2	38.1±9.1	48.5±9.3	59.3±20.3	52.8±16.5

Note. Values are means±SD.

In *Protocol 1* increasing the FIO_2 to 0.60 caused a reduction in bubble scores at during exercise in some subjects, while reducing the FIO_2 to 0.14 increased the bubble scores compared to those achieved breathing an FIO_2=0.21. Conversely, *Protocol 2* demonstrated no difference in bubble scores at any given exercise intensity between an

FIO_2=0.21 and 0.40 (Fig. 6.2b). Pulmonary gas exchange efficiency, as quantified by the $AaDO_2$, during exercise in *Protocol 1* and *Protocol 2* are presented in Fig. 6.3. In both protocols, increasing exercise intensity led to an increased $AaDO_2$ breathing an FIO_2=0.21. Lowering the oxygen tension resulted in a greater $AaDO_2$ at all workloads compared to the $AaDO_2$ at rest, while exercise breathing an FIO_2=0.60 did not result in an increase in the $AaDO_2$. In *Protocol 2* breathing an FIO_2 of 0.21 again increased the $AaDO_2$ while it did not increase in subjects breathing an FIO_2=0.40 despite nearly identical bubble scores.

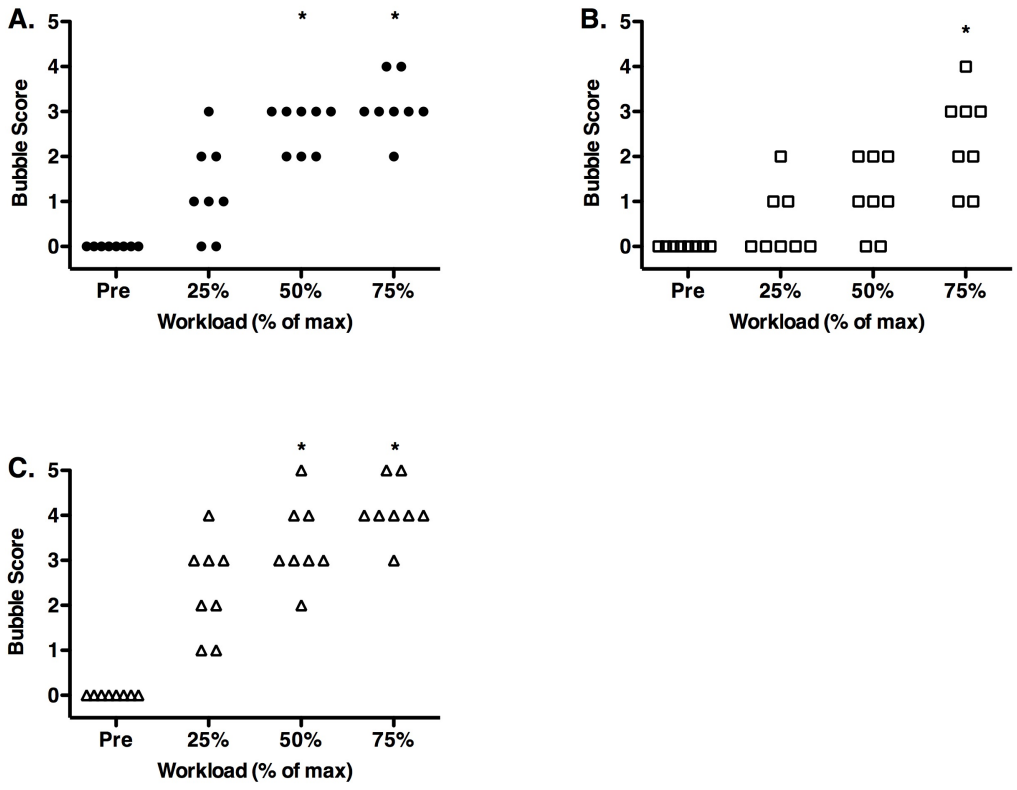

Figure 6.1. Protocol 1 Bubble Scores. Bubble scores from individual subjects before and during exercise breathing (A) 21% oxygen, (B) 60% oxygen, and (C) 14% oxygen. * p<.05 vs Pre (Friedman's test, Dunn's posttest).

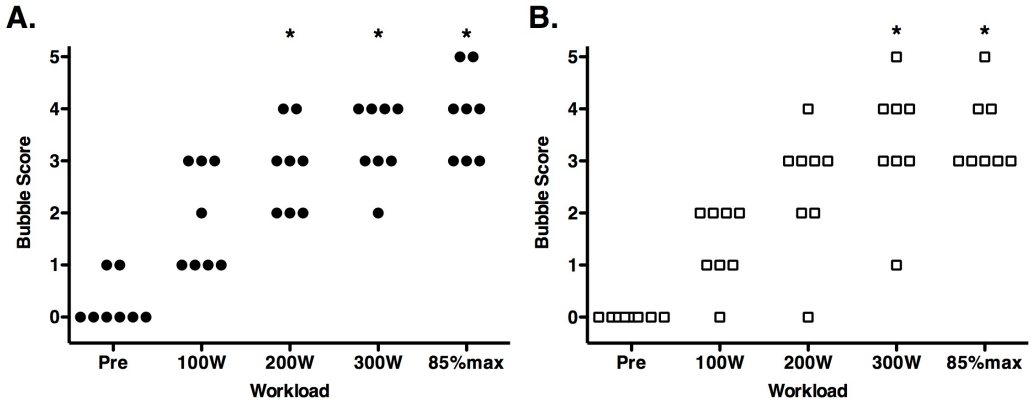

Figure 6.2. Protocol 2 Bubble Scores. Bubble scores from individual subjects before and during exercise breathing (A) 21% oxygen, (B) 40% oxygen. * p<.05 vs Pre (Friedman's test, Dunn's posttest).

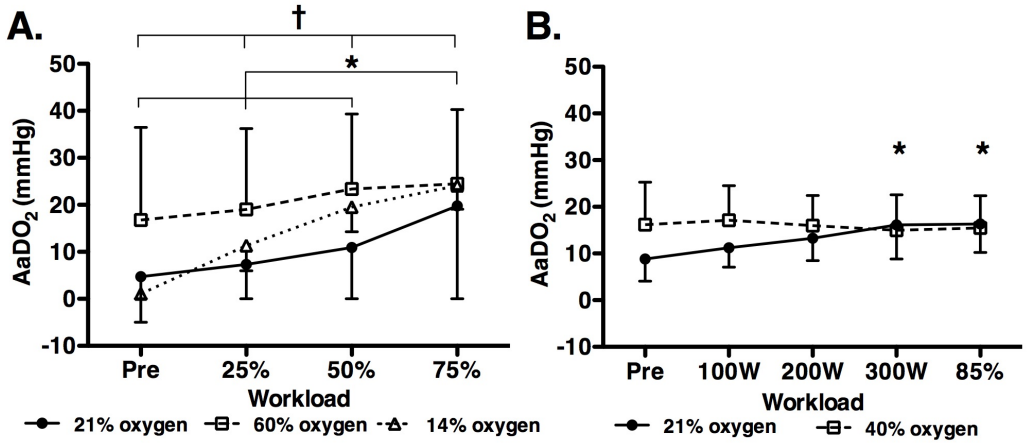

Figure 6.3. $AaDO_2$. Mean $AaDO_2$ in subjects at rest and during exercise breathing (A) 21% oxygen (solid circles), 60% oxygen (open squares), and 14% oxygen (open triangles) [*Protocol 1*] and (B) 21% oxygen (solid circles) and 40% oxygen (open squares) [*Protocol 2*]. All statistical test compared $AaDO_2$ between rest and all exercise workloads within a given percent oxygen (one-way ANOVA, Tukey posttest). (A) * p<.05 (21%), † p<.05 (14%). (B) * p<.05 vs. Pre 21%.There were no significant differences for any exercise workload when breathing 60% or 40% oxygen.

DISCUSSION

We demonstrated that in subjects breathing room air, bubble scores increased with increasing exercise intensity and that breathing an FIO_2=0.14 tended to augment the bubble scores. Additionally, while increasing the FIO_2 to 0.40 did not reduce the bubble

scores, bubble scores tended to be reduced when the FIO_2 was increased to 0.60, but not eliminated as occurs when the FIO_2 is increased to 1.0 (35, 97). This suggests that blood flow through IPAVA is the same in subjects breathing an FIO_2 of 0.21 and 0.40, but may be reduced or increased when the FIO_2 is increased or decreased beyond these levels, respectively (Fig. 6.1 and 6.2).

As expected, pulmonary gas exchange efficiency as quantified by the $AaDO_2$ worsened in subjects breathing an FIO_2=0.21 or 0.14 as exercise intensity increased in *Protocol 1*. In *Protocol 2* the $AaDO_2$ also widened with increasing exercise intensity in subjects breathing an FIO2=0.21; however, when breathing an FIO_2=0.40, the $AaDO_2$ did not increase with increases in exercise intensity (Fig. 6.3). This suggests that the factor(s) causing pulmonary gas exchange to worsen with increasing exercise intensity when breathing an FIO_2=0.21, are prevented from occurring when the FIO_2 is increased to 0.40. The potential interpretations of these data are discussed below.

First, data obtained using the MIGET and the 100% oxygen technique suggest that the widening of the $AaDO_2$ during exercise in subjects breathing 21% oxygen are due to $\dot{V}/\dot{Q}$ mismatch and diffusion limitation, while intrapulmonary shunt has no significant contribution. Therefore, these data obtained using MIGET would imply that blood flow through IPAVA is not acting like a shunt and contributing to the $AaDO_2$. As such, one interpretation of the data presented in this study is that the widening of the $AaDO_2$, which occurs in all subjects during exercise breathing room air, is not due to the increase in blood flowing through IPAVA, which also occurs in all subjects, acting like a shunt, but rather due to $\dot{V}/\dot{Q}$ and diffusion limitation. Thus, the $AaDO_2$ remained constant throughout increasing exercise intensity because $\dot{V}/\dot{Q}$ heterogeneity and diffusion

limitation were eliminated as contributing factors to pulmonary gas exchange inefficiency in exercising subjects breathing 40% oxygen. This would suggest that the $AaDO_2$ measured in exercising subjects breathing 40% oxygen was due entirely to post pulmonary shunt, such as the Thebesian drainage.

Interestingly, errors associated with measuring arterial blood gases with high PO_2 values result in an increased $AaDO_2$, which would be interpreted as a pulmonary gas exchange inefficiency. In subjects exercising breathing 40% oxygen in the current study, we did not measure an increase in the $AaDO_2$ with increasing exercise intensity, despite the relatively high PO_2 values. We interpret these data to reflect only contributions from the Thebesian drainage and that the high PO_2 gradient led to nearly perfect gas exchange within the lung. Using an estimate of cardiac output and our measures of PaO_2 and $\dot{V}O_2$, we calculated a venous admixture in subjects breathing an FIO_2=0.40 at 85%max exercise of ~0.35% of the cardiac output to account for this $AaDO_2$ which remained constant throughout increasing exercise intensity. Using these measures from the 85%max exercise bout in subjects breathing room air, we calculated a total venous admixture of 1.21%. If we assume the contribution from the Thebesian drainage is constant regardless of the FIO_2, these calculations would indicate a gas exchange inefficiency within the pulmonary circulation that could be accounted for by a venous admixture of 0.86%. This is nearly identical to the ~0.9% shunt fraction measured during 85%max exercise using ^{99m}Tc-MAA in Chapter V due to blood flow through IPAVA.

Could Blood Flowing Through IPAVA Act Like a Shunt?

We have demonstrated that with increasing exercise intensity in subjects breathing an FIO_2=0.21 bubble scores increase, suggesting increased blood flow through

IPAVA, and these scores are amplified in subjects breathing hypoxic gas mixtures and dampened when the FIO_2 is raised to 0.60. Previously, it was estimated that the minimum size bubble required to survive long enough to reach the left ventricle would be 60-90μm in diameter (32). This estimate is supported by the fact that 50μm microspheres can pass through the pulmonary circulation of human and baboon lungs (99), there is an increase in the number of 25μm microspheres passing through the pulmonary circulation of exercising dogs (156), and microspheres up to 70μm in diameter can pass through the pulmonary circulation of rats ventilated with hypoxic gas mixtures (10). Together, these data suggest that IPAVA have a diameter that is significantly larger than the largest diameter ever measured of a pulmonary capillary of 13μm (45). Additionally, in Chapter V I showed an increase in the shunt fraction during exercise based on the passage of MAA with a mean length of 35μm. As such, the diffusion distance to the core of blood flowing through IPAVA is significantly greater than any distance occurring at the alveolar capillary interface where the majority of pulmonary gas exchange is believed to occur, and this distance could limit the ability for the core of blood flowing through IPAVA to fully participate in pulmonary gas exchange.

Genovesi and colleagues studied a patient with familial hemoragic tenangiactasia, a disorder characterized by grossly distended capillaries throughout the lung parenchyma, and reported venous admixture calculations using a gas exchange method (100% oxygen technique) and an anatomical based method (^{99m}Tc-MAA) of 13% and 45%, respectively (43). The large difference in venous admixture determined by these two methods represents the major problem with using a gas exchange method versus an anatomical method when determining the percentage of blood that could be acting like a shunt. The

net effect of quantifying blood flow through pathologically distended capillaries or IPAVA would be the same. When blood flows through a normal pulmonary capillary, the diameter is just wide enough for red blood cells to travel through in a single file manner and the diffusion distance from alveoli to the center of a capillary would be ~3-5 μm. However, an IPAVA with a diameter >50μm would create a much larger diffusion distance in which the outer ring may become oxygenated, however a core of blood may travel through IPAVA without participating in gas exchange. This 'rim' of oxygenated blood is exactly what Conhaim and Staub demonstrated in excised cat pulmonary arterioles ventilated with various oxygen concentrations, definitely demonstrating the occurrence of pre capillary gas exchange (25). This core of blood would meet the definition of a 'shunt'. However, the reversal of gas exchange inefficiency during exercise in subjects breathing 40% oxygen could be argued to be the definition of very low $\dot{V}/\dot{Q}$. Of course, the semantics one chooses to define 'shunt' may be at the crux of the disagreement over the role of 'shunt' in pulmonary gas exchange efficiency. In an editorial by Robin, *et al.* (139) the term 'shunt' was described as having many meanings by pulmonary physiologists. It may be that the 'shunt' attempting to be measured by MIGET, in which $\dot{V}/\dot{Q}=0$ is different than a shunt caused by a vascular communication between the pulmonary arterial and venous circulation which some may wish to classify as creating a diffusion limitation or as having a very low $\dot{V}/\dot{Q}$.

Beyond arguments over semantics, inconsistencies in data obtained with MIGET, as well as concerns related to the statistical issues and assumptions chosen for use with MIGET (91, 92), raise the possibility that assigning the components of pulmonary gas exchange inefficiency to $\dot{V}/\dot{Q}$ heterogeneity and diffusion limitation may represent a

limitation with the MIGET technique to detect blood flow through IPAVA that could be acting like a shunt. Thus, an alternative explanation for the data presented above could be that increasing blood flow through IPAVA in exercising subjects breathing 21% oxygen causes a significant widening of the $AaDO_2$ because of blood flowing through the center of a large diameter IPAVA, which fails to completely participate in pulmonary gas exchange, and enters the pulmonary veins as venous admixture. Yet, in subjects breathing 40% oxygen, the increased driving pressure gradient of oxygen is sufficiently large to fully oxygenate even the core blood flowing through large diameter IPAVA, such that all of the blood flowing through IPAVA fully participates in pulmonary gas exchange and does not enter the pulmonary veins as venous admixture. Below I describe how MIGET may be incorrectly assigning the contributing factors to pulmonary gas exchange inefficiency to $\dot{V}/\dot{Q}$ mismatch and diffusion limitation, opening the possibility that blood flow through IPAVA could be negatively affecting pulmonary gas exchange efficiency.

Inconsistencies in data obtained using MIGET

The classical theory of the factors contributing to pulmonary gas exchange inefficiency, quantified as the $AaDO_2$, include (1) incomplete diffusion between alveolar gas and pulmonary capillary blood; (2) the direct contribution of mixed venous blood which fails has not participated in pulmonary gas exchange, termed shunt; and (3) the imperfect matching between pulmonary ventilation and pulmonary capillary blood flow, termed $\dot{V}/\dot{Q}$ mismatch (137). Data from the MIGET have crafted the accepted understanding that in healthy humans, $\dot{V}/\dot{Q}$ contributes to the entirety of the $AaDO_2$ at rest through submaximal exercise, and at higher levels of exercise intensity a diffusion contribution occurs, while shunt does not occur. Recently, the term shunt has been used

to describe the opening of large diameter IPAVA in healthy humans (32, 35, 89, 94, 97, 158, 159) and, understandably, the semantics of this description as a shunt has been met with resistance (70, 71). However, inconsistencies in data obtained with MIGET call into question if increasing $\dot{V}/\dot{Q}$ heterogeneity and diffusion limitation are the most appropriate classifications for the worsening of pulmonary gas exchange efficiency that occurs with increasing exercise intensity.

MIGET determines contributions from $\dot{V}/\dot{Q}$ mismatch and shunt to pulmonary gas exchange inefficiency by quantifying the distribution of retention and excretion of six inert gases of varying solubilities (180, 183-185). Theoretically, these gases should be retained and excreted in a predictable pattern that only depends on the $\dot{V}/\dot{Q}$ heterogeneity of the lung, including regions of shunt. An iterative mathematical modeling technique determines the best fit of a continuous distribution curve for pulmonary blood flow and alveolar ventilation spanning 48 possible $\dot{V}/\dot{Q}$ ratios and extrapolates down to shunt ($\dot{V}/\dot{Q}$ =0) and up to deadspace ($\dot{V}/\dot{Q}=\infty$). By applying the contributions of this quantified $\dot{V}/\dot{Q}$ distribution to measured cardiac output, mixed venous PO_2, and ventilation data, a predicted $AaDO_2$ is calculated. If the measured $AaDO_2$ exceeds that predicted by $\dot{V}/\dot{Q}$ and shunt, the assumption is put forth that the remainder of the $AaDO_2$ is caused by a combination of postpulmonary (bronchial and Thebesian) shunt and diffusion limitation because the MIGET cannot detect these contributions which will, without a doubt, cause the $AaDO_2$ to widen.

At sea level, the total $AaDO_2$ attributed to the combined effects of postpulmonary shunt and diffusion limitation increase with increasing exercise intensity in select studies (58, 136, 173). To separate postpulmonary shunt contributions from $\dot{V}/\dot{Q}$ mismatch and

diffusion limitation contributions, the 100% oxygen technique have been used to eliminate $\dot{V}/\dot{Q}$ mismatch and intrapulmonary shunt, thus leaving only postpulmonary shunt. Unfortunately, this is technically difficult due to the high measurement errors associated with measuring high PO_2 values and has led to a range of measured values with an experimental error spanning the range of the $AaDO_2$ occurring at both rest and heavy exercise (58). Despite these difficulties, the assumption is put forth that any gas exchange inefficiency occurring at workloads >250W that is not explained by $\dot{V}/\dot{Q}$ mismatch can only be due to a diffusion limitation (58).

Using this technique, in 1985 Gale, *et al.* (41) determined the slope of a regression line relating the dispersion of blood flow perfusion to VO_2 at various levels of exercise in nine subjects; if the slope of this line was significantly different from zero, that would indicate increased $\dot{V}/\dot{Q}$ mismatch with increases in exercise intensity. Because of the wide variability between subjects, there was only a *trend* of worsening $\dot{V}/\dot{Q}$ mismatch as exercise intensity increased that was not statistically significant. In fact, when the $AaDO_2$ data from these same subjects were displayed in a companion article, it became clear that the *predicted* $AaDO_2$ from the $\dot{V}/\dot{Q}$ distribution determined by the MIGET regressions exceeded the *measured* $AaDO_2$ in the majority of measurements for a $\dot{V}O_2$<3 L/min (173). Nevertheless, because these studies revealed a *trend* towards increasing $\dot{V}/\dot{Q}$ mismatch with increasing exercise intensity, Hammond, *et al.* employed MIGET in subjects exercising at sea level again and found a significant increase in the slope relating blood flow dispersion to $\dot{V}O_2$ (58). However, when investigating each workload, the *measured* $AaDO_2$ at all levels of exercise was significantly greater than rest, but the $AaDO_2$ *predicted* by $\dot{V}/\dot{Q}$ mismatch was only significantly increased at

higher levels of exercise ($\dot{V}O_2$>2.5 L/min), indicating a separation between the *measured* $AaDO_2$ and that *predicted* by V/Q mismatch. In yet another study, sea-level exercise data obtained by Wagner, *et al.* show that the contribution from $\dot{V}/\dot{Q}$ mismatch to the total $AaDO_2$ remained unchanged throughout all exercise intensities (182), but only when combined with data from a previous study (41) a modest, yet significant increase in $\dot{V}/\dot{Q}$ mismatch with increasing exercise intensity appeared. However, these data demonstrate no difference between the *measured* $AaDO_2$ and that *predicted* by $\dot{V}/\dot{Q}$ mismatch for workloads up to 35 ml/kg/min ($AaDO_2$ of ~10 Torr), thus leaving no room for contributions from the *known* anatomical postpulmonary shunt resulting from the Thebesian and bronchial drainage. Ultimately, even when the combination of data from multiple studies are extrapolated out to a $\dot{V}O_2$ of 4L/min $\dot{V}/\dot{Q}$ mismatch only predicts ~1/3 of the measured $AaDO_2$, a value that could be entirely accounted for by a 1.3% shunt (assuming body temperature increases to 38 degrees, mixed venous O_2 of 19 mmHg, see references (58, 182)). Of note, using ^{99m}Tc-MAA to quantify blood flow through open IPAVA during exercise, Lovering, *et al.* demonstrated a change of 1.2% in exercising subjects compared to the resting shunt fraction (96) and in Chapter V of this dissertation we demonstrated an increase in the shunt fraction from -0.11% at rest to 0.83% at 85%max exercise and increase to ~0.9% of the cardiac output. Finally, Rice *et al.* demonstrated no change in V/Q mismatch from rest through heavy exercise despite a significant increase in the *measured* $AaDO_2$ (136), while Sylvester *et al.* also determined that exercise did not alter the $\dot{V}/\dot{Q}$ distribution in exercising dogs (165). Consequently, a significant diffusion limitation was again inferred, however not directly measured. Again, this conclusion was reached indirectly due to the portion of the $AaDO_2$ not predicted by

the MIGET even though the likelihood of a diffusion limitation, even at maximal exercise, seems improbable. Further support for this improbability comes from Hsia, *et al.* who demonstrated that exercising foxhounds maintained diffusion equilibrium at maximal exercise despite pnemonectomy of 42% of the lung (72-74).

In summary, while $\dot{V}/\dot{Q}$ mismatch has been suggested to increase with exercise intensity at sea level, this often does not reach statistical significance, especially at lower workloads, while some subjects demonstrate no increase in $\dot{V}/\dot{Q}$ mismatch during exercise despite demonstrating an increase in the $AaDO_2$ (122, 136, 144, 182). Consequently, the explanation for the widening of a significant portion of the $AaDO_2$ falls on the assumption of a diffusion limitation despite neither a direct measurement of such impairment, nor any other direct support that such diffusion limitation to oxygen at the alveolar-capillary interface could theoretically or even likely occur (154, 181). Intrapulmonary and postpulmonary shunt have been relegated to negligible or non-contributing factors.

Non Capillary Gas Exchange

It is not entirely clear why the MIGET technique demonstrates such variable results regarding $\dot{V}/\dot{Q}$ mismatch or what could be causing the assumed diffusion limitation. An alternative explanation could be the large body of evidence suggesting the existence of large diameter IPAVA could be diverting blood flow away from the pulmonary gas exchange unit and acting as a shunt. One assumption employed by the MIGET is that the distribution of possible $\dot{V}/\dot{Q}$ units is constrained to a range of 50 specified values and that the distribution between these values has only one unique solution; however, some have argued that this mathematical assumption is inaccurate

because using an infinite number of possible $\dot{V}/\dot{Q}$ distributions can result in more than one distribution (169). Of course, it may be that the 'diffusion limitation' deduced from data obtained with MIGET is actually reflecting the contributions of blood flow through IPAVA. If this is the case, the root of the controversy over the role of IPAVA in pulmonary gas exchange efficiency may come down to a semantics issue over whether the contributions of blood flow represent a 'shunt', a 'diffusion limitation', or some combination of these factors.

Another potentially more problematic assumption inherent to the MIGET technique, is that the excretion of inert gases between pulmonary blood and pulmonary air only occurs at the alveolar-capillary interface (63). There is a substantial body of evidence demonstrating pulmonary precapillary or non-capillary gas exchange. Increasing the alveolar PO_2 via a single breath of 100% oxygen or voluntary hyperventilation results in the rapid detection of oxygen in pulmonary arterioles, indicating the diffusion of gas through bronchiole and arteriole walls well before the alveolar-capillary interface (79, 152). Additionally, Conhaim and Staub demonstrated gas exchange occurring in pulmonary arteries ≥500μm in diameter in anesthetized cats ventilated with 100% oxygen (25), while Genovesi and colleagues reported oxygen saturation data obtained from the pulmonary artery and then the wedged catheter in a resting male breathing room air with a history of familial hemorrhagic telangiectasia that measured 69.0% and 96.0%, respectively (43). Clearly, increasing the mixed venous saturation to 96% before the alveolar-capillary interface would be considered pre-capillary gas exchange. Thus, while the maximum rate of diffusion likely occurs at the alveolar-capillary interface, it is clear that gases can diffuse through arterioles well

proximal to the traditional site of pulmonary gas exchange. While this does not suggest that the complete exchange of oxygen is occurring in pulmonary arteries with a large diameter when the driving gradient is relatively low such as when breathing room air, the high driving gradient from 100% oxygen or the highly insoluble SF_6 will create a very large diffusion gradient for these gases. Thus, SF_6 may be excreted prior to reaching IPAVA rendering it useless for the detection of vessels downstream that may act as shunts for oxygen. Furthermore, the exchange of high-molecular weight gases, such as those used in MIGET, has been shown to occur as high up the airway tree as the trachea and conducting airways (164). The degree of such airway gas exchange is dependent on both diffusion and perfusion and thus, increases in bronchial blood flow led to increases in the perfusion of conducting airways and subsequent gas exchange within these airways. The positive correlation between blood flow and inert gas excretion highlight a potentially problematic assumption in the overall analysis of the excretion and retention pattern of the MIGET gases, which assumes it is only reflecting changes to the specific pattern of $\dot{V}/\dot{Q}$ heterogeneity present. MIGET does not account for bronchial blood flow exchanging gases with the airways that would influence the overall excretion and retention profile of inert gases (44, 153). This possibility of conducting airway gas exchange highlights the problem of attempting to quantify pulmonary gas exchange efficiency using a gas exchange-dependent technique, which must rely on assumptions about the locations of inert gas exchange, and may be incorrect. While it is not entirely clear *how* these potential flaws would affect the resulting $\dot{V}/\dot{Q}$ distribution predicted by MIGET, it is clear that these assumptions represent a real concern and has led to controversy (91) over a technique that has never been validated by an independent

method (169) in its ability to detect and categorize factors affecting pulmonary gas exchange of O_2 and CO_2.

100% Oxygen Technique

Another assumption used to support the lack of intrapulmonary shunt detection by the MIGET was by Vogiatzis, *et al* who attempted to quantify intrapulmonary shunt in subjects exercising while breathing 100% oxygen and apply that shunt fraction to normoxic exercise. The assumption was that breathing 100% oxygen was not causing any alteration to the pulmonary vasculature that could affect the quantification of shunt (143, 178). However, hyperoxia dynamically closes IPAVA (97) and causes a redistribution in pulmonary blood flow, as measured with microspheres (110). In this situation, any potential contribution from IPAVA to the $AaDO_2$ would not be detected because these large diameter vessels would not have blood flowing through them and thus the 100% oxygen technique could only detect post-pulmonary and intracardiac shunt contributions.

To summarize, MIGET has been used to quantify the contributions from $\dot{V}/\dot{Q}$ mismatch and shunt to pulmonary gas exchange inefficiency and assumes that any gas exchange inefficiency not explained by these two factors can only be due to diffusion limitation. Anatomical data demonstrate that large diameter IPAVA exist in the pulmonary circulation that could theoretically act like a shunt, but the MIGET and the 100% oxygen technique do not detect shunt as a contributing factor during exercise. Thus, the role of IPAVA acting as shunts remains a controversial, not yet proven hypothesis.

We recognize that our argument that IPAVA have the potential to act as shunts directly challenges the prevailing understanding of factors contributing to pulmonary gas

exchange inefficiency. However, the inconsistencies presented above, from which the prevailing understandings rest, should highlight the possibility that another explanation for a contributing factor to pulmonary gas exchange inefficiency should and can be considered.

Classifying Pulmonary Gas Exchange Inefficiency into Three Discrete Categories

Part of the debate about the contributing factors to pulmonary gas exchange inefficiency may lie in the semantics used to describe the three discrete factors of $\dot{V}/\dot{Q}$ mismatch, diffusion limitation, and shunt. Wagner (181) has completely and eloquently described the role of diffusion in pulmonary gas exchange and in healthy subjects, the transit time of red blood cells through *pulmonary capillaries* presents more than adequate time for the complete diffusion of oxygen. The notion that is not considered, however, is if this exchange of oxygen is occurring in a vessel with a significantly larger diameter than a pulmonary capillary, such as an IPAVA, in which the diffusion distance is significantly larger. Thus, should blood flow through IPAVA be termed 'shunt' when the *reason* for the incomplete exchange of oxygen is due to a *diffusion limitation*? If so, then the classical categories contributing to pulmonary gas exchange inefficiency ($\dot{V}/\dot{Q}$ mismatch, diffusion limitation, and shunt) may represent categories that are too discrete for the true complexity of the pulmonary circulation.

If blood flow through large diameter IPAVA fails to fully participate in pulmonary gas exchange during exercise in subjects breathing an FIO_2=0.21 due to the large diffusion distance from the rim to the core blood, then lowering the driving gradient due to alveolar hypoxia would be expected to result in even greater venous admixture when a greater percentage of blood flow through IPAVA would not participate in

pulmonary gas exchange. In *Protocol 1* we measured the $AaDO_2$ in eight subjects (3 female) exercise at 25%, 50%, and 75% of their max while breathing an FIO_2=0.21, and then repeated that breathing an FIO_2=0.14. While the $AaDO_2$ increased with increasing exercise intensity in both conditions, it was surprising that the $AaDO_2$ widened to an even greater degree in subjects breathing an FIO_2=0.14. Our calculations indicated the total venous admixture within the pulmonary circulation required to account for the AaDO2 at 85%max exercise was ~17.5%. Because some of this could be due to a diffusion limitation, future research needs to be conducted to quantify the blood flow through IPAVA in subjects breathing hypoxic gas mixtures using solid MAA. Using that anatomical data with the calculated venous admixture required to account for the total $AaDO_2$ will provide the best estimates of each factor contributing to pulmonary gas exchange inefficiency.

Summary

Our anatomical evidence for the opening of IPAVA with increasing exercise intensity occurs at workloads when the $AaDO_2$ widens, suggesting that these vessels play a role in pulmonary gas exchange efficiency. Our data demonstrating no change in the $AaDO_2$ in subjects exercising breathing an FIO_2=0.40 suggests that changing the driving pressure gradient of oxygen influences the efficiency of pulmonary gas exchange via pre capillary gas exchange of the PvO_2 which could include blood flowing through IPAVA. Finally, this would also suggest that during alveolar hypoxia, when the driving gradient of oxygen is reduced, the contribution by blood flowing through IPAVA on pulmonary gas exchange inefficiency would be even greater. Predictably, the venous admixture required to account for the $AaDO_2$ during hypoxic exercise is significantly greater than

that required to account for the $AaDO_2$ during normoxic exercise, while that during exercise with an FIO_2=0.40 is less and *only* represents contributions from post pulmonary shunt.

Jameson has suggested that the tradition view of where pulmonary gas exchange occurs within the lung should be reconsidered because the act of diffusion is not isolated to the alveolar-capillary interface, but rather begins to occur through pulmonary arteries before blood reaches the capillaries (79). We would agree and suggest that the original compartmentalization of three categories affecting pulmonary gas exchange (diffusion, shunt, and $\dot{V}/\dot{Q}$) have led to inappropriate oversimplifications regarding their potential interactions. Accordingly, because large diameter IPAVA respond to changing FIO_2, they may not meet the strictest definition of a 'shunt', but rather may represent the source of pulmonary gas exchange inefficiency being derived by MIGET as $\dot{V}/\dot{Q}$ mismatch, despite improved $\dot{V}$ and $\dot{Q}$ homogeneity, or may represent the diffusion limitation inferred by MIGET. Furthermore, the belief of a diffusion limitation occurring at the alveolar-capillary interface seems highly improbable due to the small diffusion distance and sufficient red blood cell transit time. However, the core of blood flowing through a large diameter IPAVA may present a diffusion distance large enough to prevent the complete (if any) equilibration of blood flowing through these vessels, especially during exercise when red blood cell transit time is reduced or when the FIO_2 is decreased compared to sea level. As such, gas exchange may occur at the core of these vessels to varying degrees, ranging from some to none, depending on the PAO_2, PvO_2, and red blood cell transit time. Hence, while we believe blood flow though the core of IPAVA that does not participate in pulmonary gas exchange represents a source of mixed venous blood, it is

left to the reader to decide if blood flow through IPAVA should be categorized as a shunt, $\dot{V}/\dot{Q}$ heterogeneity, diffusion limitation, or some other description which may not be limited to these finite and potentially oversimplified classifications. Regardless of semantics, the contribution of blood flow through these vessels to pulmonary gas exchange inefficiency during normoxic exercise should be considered a real possibility, with increasing contributions when the FIO_2 is reduced, and decreasing contribution when the FIO_2 is increased.

CHAPTER VII

CONCLUSIONS

The dogmatic understandings of pulmonary physiology have taken wrong turns on more than one occasion throughout the course of history. From Galen's theory on interventricular pores to Haldane's hypothesis that the lung secreted oxygen, there have been decades and even centuries that have propagated these inaccuracies associated with the pulmonary vasculature and how oxygen ultimately enters our arterial blood. However, for the majority of these inaccuracies, history has ultimately fallen on the correct side of the story. We are now in the midst of another potentially historical inaccuracy in which many have chosen not to accept the existence of inducible large diameter intrapulmonary arteriovenous anastomoses (IPAVA) and their potential roles in both gas exchange and as an anatomical filter. This dissertation focused on furthering our anatomical and physiological understanding of the pulmonary vasculature and the regulation and significance of intrapulmonary arteriovenous anastomoses in healthy humans.

MAIN FINDINGS

IPAVA have consistently been shown to open in healthy human subjects exercising breathing room air, or at rest and during exercise breathing hypoxic gas mixtures. In Chapter IV I tested the hypothesis that the infusion of epinephrine or dopamine would open IPAVA in healthy human subjects at rest. The data demonstrated that while infusions of these catecholamines did open IPAVA, the mechanism appeared to be due to a secondary affect of these drugs causing an increase in pressure and/or blood flow through the pulmonary circulation acting as the stimulus to open IPAVA.

Conversely, the closure of these vessels by breathing 100% oxygen appears to be due to a different mechanism than that which opens IPAVA because in subjects breathing 100% oxygen, pressures and flows were equally elevated during epinephrine and dopamine infusions, yet IPAVA remained closed. The mechanism of hyperoxic-closure of IPAVA represents a significant area for future research.

Of course, some have argued that the 'closure' of IPAVA in subjects breathing 100% oxygen simply represents an alteration in the partial pressure environment surrounding saline contrast microbubbles, which is preventing their survival and thus their appearance in the left ventricle (66). Despite the fact that we have definitively shown this not to be the case by changing both the internal and external partial pressure environment of saline contrast microbubbles which did not affect our ability to detect them (35), anatomical proof using solid particles presents indisputable evidence. I developed a filtering technique to reduce the number of small MAA particles that could travel through pulmonary capillaries and developed a way to quantify and remove the variable contribution from free-^{99m}Tc to the quantification of the shunt fraction. Using this newly developed technique, I demonstrated anatomically for the first time that during exercise in subjects breathing 100% oxygen there is a reduction in blood flow through IPAVA compared to exercise when breathing 21% oxygen. Because of this study, data using solid microspheres or MAA now exist to support all data obtained using TTSCE regardless of exercise or the FIO_2.

Finally, in Chapter VI I addressed a concern that has been the focus of debate surrounding IPAVA: are they 'shunts'? While the answer to this question is not easily determined, I believe reworking our model for *where* pulmonary gas exchange occurs

and critically reviewing long held assumptions about the roles of various contributing factors reveals one answer: yes, blood flow through IPAVA can act like a shunt. Anatomical data consistently support the existence of inducible large diameter IPAVA in healthy humans and an increased driving partial pressure gradient of oxygen to the core of that blood will affect the complete diffusion of oxygen to that core. As such, I showed that increasing the FIO_2, and hence the partial pressure driving gradient, prevented pulmonary gas exchange from worsening with increases in exercise intensity. Conversely, when exercising at sea level or when the FIO_2 is reduced, the diffusion gradient to the core of blood is not always sufficient to complete equilibration between the alveolar PO_2 and the PO_2 in the core of blood. Thus, a portion of the blood returns to the pulmonary venous circulation to enter the systemic circulation without completely participating in gas exchange. This represents a shunt.

COMPARISONS BETWEEN EXERCISE-INDUCED AND HYPOXIA-INDUCED OPENING OF IPAVA

A combination of both cardiac output and PASP is an attractive mechanism to explain the recruitment of IPAVA because these physiologic variables both increase to varying degrees during exercise, when breathing hypoxic gas mixtures, or during EPI infusion as demonstrated in Chapter IV, and all of these conditions result in open IPAVA. During exercise, cardiac output and left atrial pressure increase to help recruit and distend pulmonary capillaries (135) which helps to prevent excessive increases in driving pressure at the pulmonary alveolar-capillary interface. Alternatively, when breathing hypoxic gas mixtures at rest, left atrial pressure does not increase and cardiac output increases to a lesser degree and not above the flows demonstrated at the highest EPI

infusions in Chapter IV (31, 134, 182, 194), yet bubble scores of 4 and 5 are typically observed (89). When breathing hypoxic gas mixtures, hypoxic pulmonary vasoconstriction occurs in small pulmonary resistance arteries (103) and if this is occurring downstream from IPAVA, may provide an additional stimulus to preferentially direct blood flow through IPAVA. If IPAVA are located in more apical regions of the lung, as suggested by anatomical data (172), and exercise as well as hypoxic pulmonary vasoconstriction both cause blood flow to be redistributed to more apical regions of the lung (69), the perfusion of IPAVA may be in part related to downstream vasoactive mechanisms related to hypoxia that aid in directing blood flow through IPAVA.

An interesting difference between exercise and breathing hypoxic gas mixtures at rest or during EPI infusion is that during exercise left atrial pressure increases at the onset of exercise to recruit and distend the pulmonary vasculature (135); however, this does not occur when breathing hypoxic gas mixtures (52) or during EPI infusion (199). During EPI infusion IPAVA may open during very small increases in cardiac output and/or PASP when a significant portion of the conventional pulmonary vasculature may not be recruited. However, during exercise, it may take a larger increase in cardiac output before flow through IPAVA occurs because a larger portion of the 'normal' pulmonary microvasculature may be recruited and thus limit the diversion of blood flow through IPAVA until a higher cardiac output is achieved. The modest increases in cardiac output achieved due to EPI infusion in Chapter IV, versus greater increases in cardiac output achieved during exercise, may have prevented complete perfusion of IPAVA and explain the lack of bubble scores of 4 and 5. However, we do not have any data to directly support this hypothesis.

IMPLICATIONS & FUTURE DIRECTIONS

Research is already underway looking into how increasing the oxygen concentration may be modulating IPAVA and what role, if any, pulmonary vascular smooth muscle may play in their patency. We know from studies of the systemic vasculature that arteriole dysfunction is associated with the aging process (145) and pulmonary artery pressure increases with increasing age (85, 86). Preliminary data from our lab indicate that the aging process may negatively affect IPAVA as well. If blood flow through IPAVA is reduced with increasing age, what consequences, if any, are associated with this decline?

It has been suggested that because of the large diameter of IPAVA, these vessels may play a role in controlling pulmonary vascular resistance to minimize large increases in pulmonary artery pressure during dynamic increases in pulmonary blood flow. If true, these vessels represent a possible target for treatments associated with pathologies, such as pulmonary artery hypertension or complications stemming from chronic obstructive pulmonary disease.

Their contribution to pulmonary gas exchange inefficiency during exercise does not typically result in arterial hypoxemia in the majority of healthy humans who are able to mount a ventilatory response that allows for the maintenance of PaO_2 in the face of a widening $AaDO_2$. However, as the FIO_2 decreases during ascent to high altitude or in patients with pathological disorders, the regulation of blood flow through IPAVA may represent a critical target for maintaining normal blood gases in the face of hypoxemia. Conversely, until we understand how oxygen affects IPAVA patency, as well as how oxygen affects the normal pulmonary vasculature, a full understanding of the

consequences associated with the use of supplemental oxygen in critical care settings will be incomplete, at best.

Because we have shown that IPAVA are dynamically regulated large diameter pathways, future research should be conducted to determine what role patent IPAVA play in breaching the pulmonary microcirculation sieve. If emboli are traversing the pulmonary circulation through IPAVA and gaining entry to the systemic circulation, IPAVA may play a previously underappreciated role in migraines, transient ischemic attacks, and/or stroke.

Significant advancements in our understanding of the regulation and significance of IPAVA have been made over the past decade as research has been conducted specifically addressing questions about these vessels. However, now that we are beginning to gain a better understanding of the dynamic regulation of these vessels, research using an animal model and/or isolating IPAVA *ex vivo* will be necessary to fully characterize the pathways involved in the regulation of these vessels. Data from Tobin and Zariquiey (172) suggest these vessels may be predominantly located in the apices of the lungs. We have data currently in preparation for publication that would support this anatomical location of IPAVA because bubble scores can be reduced or eliminated in subjects moving from supine to upright posture. Interestingly, exercise and hypoxia, which both recruit IPAVA, lead to a redistribution of pulmonary blood flow towards the apices of the lung (69). These data, combined with the similarities between IPAVA and supernumerary arteries provide ample evidence to at least begin the search for IPAVA by searching for supernumerary arteries located in the apices of the lung and determining if an arteriovenous connection can by found.

Ironically, Galen's theory about interventricular 'pores' had no anatomical support, yet was widely held as truth for centuries; conversely, anatomical evidence for the existence and potential importance of IPAVA as part of the normal pulmonary vasculature continues to accumulate, yet has been disregarded, ignored, and diminished in importance because it doesn't fit the accepted 'model' of the lung. Despite much resistance to displace long-held theories and accept these new data, the time has come to acknowledge the oversimplification in categorizing the lung into a three-compartment model and appreciate the complexities of the pulmonary circulation. I hope the scientific data presented in this dissertation helps direct history to land on the correct side of the story.

REFERENCES CITED

1. **Aaronson PI, Robertson TP, Knock GA, Becker S, Lewis TH, Snetkov V, and Ward JPT**. Hypoxic pulmonary vasoconstriction: mechanisms and controversies. *J Physiol (Lond)* 570: 53-58, 2006.

2. **Aaronson PI, Robertson TP, and Ward JPT**. Endothelium-derived mediators and hypoxic pulmonary vasoconstriction. *Resp Physiol & Neurobiol* 132: 107-120, 2002.

3. **Anthonisen NR, and Fleetham J**. Ventilation: total, alveolar, and dead space. In: *Handbook of Physiology The Respiratory System Gas Exchange*. Bethesda, MD: Am Physiol Soc, 1987, sect. 3, vol. IV, chapt. 7, p. 115.

4. **Arai TJ, Henderson AC, Dubowitz DJ, Levin DL, Friedman PJ, Buxton RB, Prisk GK, and Hopkins SR**. Hypoxic pulmonary vasoconstriction does not contribute to pulmonary blood flow heterogeneity in normoxia in normal supine humans. *J Appl Physiol* 106: 1057-1064, 2009.

5. **Archer SL, London B, Hampl V, Wu X, Nsair A, Puttagunta L, Hashimoto K, Waite RE, and Michelakis ED**. Impairment of hypoxic pulmonary vasoconstriction in mice lacking the voltage-gated potassium channel Kv1.5. *FASEB J* 15: 1801-1803, 2001.

6. **Archer SL, Wu X-C, Thébaud B, Nsair A, Bonnet S, Tyrrell B, McMurtry MS, Hashimoto K, Harry G, and Michelakis ED**. Preferential expression and function of voltage-gated, O2-sensitive K+ channels in resistance pulmonary arteries explains regional heterogeneity in hypoxic pulmonary vasoconstriction: ionic diversity in smooth muscle cells. *Circ Res* 95: 308-318, 2004.

7. **Asmussen E, and Nielsen M**. Alveolo-arterial gas exchange at rest and during work at different 02 tensions. *Acta Physiol Scand* 50: 153-166, 1960.

8. **Aviasdo D, Daly M, Lee C, and Schmidt C**. The contribution of the bronchial circulation to the venous admixture in pulmonary venous blood. *J Physiol (Lond)* 155: 602-622, 1961.

9. **Bateman TM, Heller GV, Mcghie AI, Courter SA, Golub RA, Case JA, and James Cullom S**. Multicenter investigation comparing a highly efficient half-time stress-only attenuation correction approach against standard rest-stress Tc-99m SPECT imaging. *J Nucl Cardiol* 16: 726-735, 2009.

10. **Bates ML, Fulmer BR, Farrell ET, Drezdon A, Pegelow DF, Conhaim RL, and Eldridge MW**. Hypoxia recruits intrapulmonary arteriovenous pathways in intact rats but not isolated rat lungs. *J Appl Physiol* 2012.

11. **Beck KC, and Rehder K**. Differences in regional vascular conductances in isolated dog lungs. *J Appl Physiol* 61: 530-538, 1986.

12. **Benumof JL, Pirlo AF, Johanson I, and Trousdale FR**. Interaction of PVO2 with PAO2 on hypoxic pulmonary vasoconstriction. *J Appl Physiol Respirat Environ Exercise Physiol* 51: 871-874, 1981.

13. **Berger RM, Geiger R, Hess J, Bogers AJ, and Mooi WJ**. Altered arterial expression patterns of inducible and endothelial nitric oxide synthase in pulmonary plexogenic arteriopathy caused by congenital heart disease. *Am J Respir Crit Care Med* 163: 1493-1499, 2001.

14. **Bergofsky E, Bass B, Ferretti R, and Fishman A**. Pulmonary vasoconstriction in response to precapillary hypoxemia. *J Clin Invest* 42: 1201-1215, 1963.

15. **Bergofsky E, Haas F, and Porcelli R**. Determination of the sensitive vascular sites from which hypoxia and hypercapnia elicit rises in pulmonary arterial pressure. *Fed Proc* 27: 1420-1425, 1968.

16. **Berk J, Hagen J, Koo R, Nomoto S, and Rupright M**. Pulmonary arteriovenous shunting due to epinephrine. *Horm Metab Res* 5: 65, 1973.

17. **Berk JL, Hagen JF, and Koo R**. Effect of alpha and beta adrenergic blockade on epinephrine induced pulmonary insufficiency. *Ann Surg* 183: 369-376, 1976.

18. **Berk JL, Hagen JF, Koo R, Beyer W, Dochat GR, Rupright M, and Nomoto S**. Pulmonary insufficiency caused by epinephrine. *Ann Surg* 178: 423-435, 1973.

19. **Bourbon J, Boucherat O, Chailley-Heu B, and Delacourt C**. Control Mechanisms of Lung Alveolar Development and Their Disorders in Bronchopulmonary Dysplasia. *Pediatric Research* 57: 38R-46R, 2005.

20. **Brown S, Bailey DL, Willowson K, and Baldock C**. Investigation of the relationship between linear attenuation coefficients and CT Hounsfield units using radionuclides for SPECT. *Appl Radiat Isot* 66: 1206-1212, 2008.

21. **Bunton D, MacDonald A, Brown T, Tracey A, McGrath JC, and Shaw AM**. 5-hydroxytryptamine- and U46619-mediated vasoconstriction in bovine pulmonary conventional and supernumerary arteries: effect of endogenous nitric oxide. *Clin Sci* 98: 81-89, 2000.

22. **Burrowes KS, Hunter PJ, and Tawhai MH**. Anatomically based finite element models of the human pulmonary arterial and venous trees including supernumerary vessels. *J Appl Physiol* 99: 731-738, 2005.

23. **Cherry S, Sorenson J, and Phelps M**. *Physics in Nuclear Medicine*. Philadelphia: Saunders, 2003.

24. **Clara M**. *Die Arterio-Venosen Anastomosen*. Leipzig: J.A. Barth, 1939.

25. **Conhaim RL, and Staub NC**. Reflection spectrophotometric measurement of O2 uptake in pulmonary arterioles of cats. *J Appl Physiol: Respirat Environ Exercise Physiol* 48: 848-856, 1980.

26. **Currie PJ, Seward JB, Chan KL, Fyfe DA, Hagler DJ, Mair DD, Reeder GS, Nishimura RA, and Tajik AJ**. Continuous wave Doppler determination of right ventricular pressure: a simultaneous Doppler-catheterization study in 127 patients. *J Am Coll Cardiol* 6: 750-756, 1985.

27. **Dallinger S, Dorner GT, Wenzel R, Graselli U, Findl O, Eichler HG, Wolzt M, and Schmetterer L**. Endothelin-1 contributes to hyperoxia-induced vasoconstriction in the human retina. *Invest Ophthalmol Vis Sci* 41: 864-869, 2000.

28. **Darbar D, Smith M, Mörike K, and Roden DM**. Epinephrine-induced changes in serum potassium and cardiac repolarization and effects of pretreatment with propranolol and diltiazem. *Am J Cardiol* 77: 1351-1355, 1996.

29. **Dempsey JA, Hanson PG, and Henderson KS**. Exercise-induced arterial hypoxaemia in healthy human subjects at sea level. *J Physiol (Lond)* 355: 161-175, 1984.

30. **Dempsey JA, and Wagner PD**. Exercise-induced arterial hypoxemia. *J Appl Physiol* 87: 1997-2006, 1999.

31. **Dorrington KL, Clar C, Young JD, Jonas M, Tansley JG, and Robbins PA**. Time course of the human pulmonary vascular response to 8 hours of isocapnic hypoxia. *Am J Physiol* 273: H1126-1134, 1997.

32. **Eldridge MW, Dempsey JA, Haverkamp HC, Lovering AT, and Hokanson JS**. Exercise-induced intrapulmonary arteriovenous shunting in healthy humans. *J Appl Physiol* 97: 797-805, 2004.

33. **Elkayam U, Ng TMH, Hatamizadeh P, Janmohamed M, and Mehra A**. Renal Vasodilatory Action of Dopamine in Patients With Heart Failure: Magnitude of Effect and Site of Action. *Circulation* 117: 200-205, 2008.

34. **Elliott FM, and Reid L**. Some new facts about the pulmonary artery and its branching pattern. *Clin Radiol* 16: 193-198, 1965.

35. **Elliott JE, Choi Y, Laurie SS, Yang X, Gladstone IM, and Lovering AT**. Effect of initial gas bubble composition on detection of inducible intrapulmonary arteriovenous shunt during exercise in normoxia, hypoxia, or hyperoxia. *J Appl Physiol* 110: 35-45, 2011.

36. **Farquhar H, Fracp MW, Mbbs MW, Fracp KP, Mbchb AR, Fracp MS, and Dsc RB**. Systematic review of studies of the effect of hyperoxia on coronary blood flow. *Am Heart J* 158: 371-377, 2009.

37. **Fay FS**. Guinea pig ductus arteriosus. I. Cellular and metabolic basis for oxygen sensitivity. *Am J Physiol* 221: 470-479, 1971.

38. **Fishman A**. Respiratory gases in the regulation of the pulmonary circulation. *Physiol Rev* 41: 214-280, 1961.

39. **Franco-Obregon A, and Lopez-Barneo J**. Differential oxygen sensitivity of calcium channels in rabbit smooth muscle cells of conduit and resistance pulmonary arteries. *J Physiol* 491: 511-518, 1996.

40. **Fullerton DA, Agrafojo J, and McIntyre RC**. Pulmonary vascular smooth muscle relaxation by cAMP-mediated pathways. *J Surg Res* 61: 444-448, 1996.

41. **Gale GE, Torre-Bueno JR, Moon RE, Saltzman HA, and Wagner PD**. Ventilation-perfusion inequality in normal humans during exercise at sea level and simulated altitude. *J Appl Physiol* 58: 978-988, 1985.

42. **Geiger R, Berger RM, Hess J, Bogers AJ, Sharma HS, and Mooi WJ**. Enhanced expression of vascular endothelial growth factor in pulmonary plexogenic arteriopathy due to congenital heart disease. *J Pathol* 191: 202-207, 2000.

43. **Genovesi MG, Tierney DF, Taplin GV, and Eisenberg H**. An intravenous radionuclide method to evaluate hypoxemia caused by abnormal alveolar vessels. Limitation of conventional techniques. *Am Rev Respir Dis* 114: 59-65, 1976.

44. **George SC, Souders JE, Babb AL, and Hlastala MP**. Modeling steady-state inert gas exchange in the canine trachea. *J Appl Physiol* 79: 929-940, 1995.

45. **Glazier JB, Hughes JM, Maloney JE, and WEST JB**. Measurements of capillary dimensions and blood volume in rapidly frozen lungs. *J Appl Physiol* 26: 65-76, 1969.

46. **Glenny R**. Counterpoint: Gravity is not the major factor determining the distribution of blood flow in the healthy human lung. *J Appl Physiol* 104: 1533-1535; discussion 1535-1536, 2008.

47. **Glenny R, Bernard S, Neradilek B, and Polissar N**. Quantifying the genetic influence on mammalian vascular tree structure. *Proc Natl Acad Sci USA* 104: 6858-6863, 2007.

48. **Glenny RW, Bernard S, Robertson HT, and Hlastala MP**. Gravity is an important but secondary determinant of regional pulmonary blood flow in upright primates. *J Appl Physiol* 86: 623-632, 1999.

49. **Glenny RW, Lamm WJ, Albert RK, and Robertson HT**. Gravity is a minor determinant of pulmonary blood flow distribution. *J Appl Physiol* 71: 620-629, 1991.

50. **Glenny RW, Lamm WJ, Bernard SL, An D, Chornuk M, Pool SL, Wagner WW, Hlastala MP, and Robertson HT**. Selected contribution: redistribution of pulmonary perfusion during weightlessness and increased gravity. *J Appl Physiol* 89: 1239-1248, 2000.

51. **Glenny RW, and Robertson HT**. Fractal properties of pulmonary blood flow: characterization of spatial heterogeneity. *J Appl Physiol* 69: 532-545, 1990.

52. **Goldring RM, Turino GM, Cohen G, Jameson AG, Bass BG, and Fishman AP**. The catecholamines in the pulmonary arterial pressor response to acute hypoxia. *J Clin Invest* 41: 1211-1221, 1962.

53. **Graham R, Skoog C, Macedo W, Carter J, Oppenheimer L, Rabson J, and Goldberg HS**. Dopamine, dobutamine, and phentolamine effects on pulmonary vascular mechanics. *J Appl Physiol* 54: 1277-1283, 1983.

54. **Groves BM, Reeves JT, Sutton JR, Wagner PD, Cymerman A, Malconian MK, Rock PB, Young PM, and Houston CS**. Operation Everest II: elevated high-altitude pulmonary resistance unresponsive to oxygen. *J Appl Physiol* 63: 521-530, 1987.

55. **Gutte H, Mortensen J, Jensen CV, Johnbeck CB, von der Recke P, Petersen CL, Kjaergaard J, Kristoffersen US, and Kjaer A**. Detection of pulmonary embolism with combined ventilation-perfusion SPECT and low-dose CT: head-to-head comparison with multidetector CT angiography. *J Nucl Med* 50: 1987-1992, 2009.

56. **Hagen PT, Scholz DG, and Edwards WD**. Incidence and size of patent foramen ovale during the first 10 decades of life: an autopsy study of 965 normal hearts. *Mayo Clin Proc* 59: 17-20, 1984.

57. **Hakim TS, Lisbona R, and Dean GW**. Gravity-independent inequality in pulmonary blood flow in humans. *J Appl Physiol* 63: 1114-1121, 1987.

58. **Hammond MD, Gale GE, Kapitan KS, Ries A, and Wagner PD**. Pulmonary gas exchange in humans during exercise at sea level. *J Appl Physiol* 60: 1590-1598, 1986.

59. **Haque WA, Boehmer J, Clemson BS, Leuenberger UA, Silber DH, and Sinoway LI**. Hemodynamic effects of supplemental oxygen administration in congestive heart failure. *J Am Coll Cardiol* 27: 353-357, 1996.

60. **Harrison DC, Pirages S, Robison SC, and Wintroub BU**. The pulmonary and systemic circulatory response to dopamine infusion. *Br J Pharmacol* 37: 618-626, 1969.

61. **Higgins RD, Hendricks-Munoz KD, Caines VV, Gerrets RP, and Rifkin DB**. Hyperoxia stimulates endothelin-1 secretion from endothelial cells; modulation by captopril and nifedipine. *Curr Eye Res* 17: 487-493, 1998.

62. **Himelman RB, Stulbarg M, Kircher B, Lee E, Kee L, Dean NC, Golden J, Wolfe CL, and Schiller NB**. Noninvasive evaluation of pulmonary artery pressure during exercise by saline-enhanced Doppler echocardiography in chronic pulmonary disease. *Circulation* 79: 863-871, 1989.

63. **Hlastala MP**. Multiple inert gas elimination technique. *J Appl Physiol: Respirat Environ Exercise Physiol* 56: 1-7, 1984.

64. **Hlastala MP, Lamm WJE, Karp A, Polissar NL, Starr IR, and Glenny RW**. Spatial distribution of hypoxic pulmonary vasoconstriction in the supine pig. *J Appl Physiol* 96: 1589-1599, 2004.

65. **Holloway EL, Polumbo RA, and Harrison DC**. Acute circulatory effects of dopamine in patients with pulmonary hypertension. *British Heart Journal* 37: 482-485, 1975.

66. **Hopkins S, Olfert I, and Wagner P**. Rebuttal from Hopkins, Olfert, and Wagner. *J Appl Physiol* 107: 997-998, 2009.

67. **Hopkins SR, Bogaard HJ, Niizeki K, Yamaya Y, Ziegler MG, and Wagner PD**. Beta-adrenergic or parasympathetic inhibition, heart rate and cardiac output during normoxic and acute hypoxic exercise in humans. *J Physiol* 550: 605-616, 2003.

68. **Hopkins SR, Henderson AC, Levin DL, Yamada K, Arai T, Buxton RB, and Prisk GK**. Vertical gradients in regional lung density and perfusion in the supine human lung: the Slinky effect. *J Appl Physiol* 103: 240-248, 2007.

69. **Hopkins SR, Kleinsasser A, Bernard S, Loeckinger A, Falor E, Neradilek B, Polissar NL, and Hlastala MP**. Hypoxia has a greater effect than exercise on the redistribution of pulmonary blood flow in swine. *J Appl Physiol* 103: 2112-2119, 2007.

70. **Hopkins SR, Olfert IM, and Wagner PD**. Last Word on Point:Counterpoint: Exercise-induced intrapulmonary shunting is imaginary vs. real. *J Appl Physiol* 107: 1002, 2009.

71. **Hopkins SR, Olfert IM, and Wagner PD**. Point: Exercise-induced intrapulmonary shunting is imaginary. *J Appl Physiol* 107: 993-994, 2009.

72. **Hsia CC, Fryder-Doffey F, Stalder-Nayarro V, Johnson RL, Reynolds RC, and Weibel E**. Structural changes underlying compensatory increase of diffusing capacity after left pneumonectomy in adult dogs. *J Clin Invest* 92: 758-764, 1993.

73. **Hsia CC, Herazo LF, Ramanathan M, and Johnson RL**. Cardiopulmonary adaptations to pneumonectomy in dogs. IV. Membrane diffusing capacity and capillary blood volume. *J Appl Physiol* 77: 998-1005, 1994.

74. **Hsia CC, Herazo LF, Ramanathan M, Johnson RL, and Wagner PD**. Cardiopulmonary adaptations to pneumonectomy in dogs. II. VA/Q relationships and microvascular recruitment. *J Appl Physiol* 74: 1299-1309, 1993.

75. **Huckauf H, Ramdohr B, and Schröder R**. Dopamine induced hypoxemia in patients with left heart failure. *Int J Clin Pharmacol Biopharm* 14: 217-224, 1976.

76. **Hughes M, and West JB**. Point: Gravity is the major factor determining the distribution of blood flow in the human lung. *J Appl Physiol* 104: 1531-1533, 2008.

77. **Hyman AL, and Kadowitz PJ**. Enhancement of alpha- and beta-adrenoceptor responses by elevations in vascular tone in pulmonary circulation. *Am J Physiol* 250: H1109-1116, 1986.

78. **Hyman AL, Nandiwada P, Knight DS, and Kadowitz PJ**. Pulmonary vasodilator responses to catecholamines and sympathetic nerve stimulation in the cat. Evidence that vascular beta-2 adrenoreceptors are innervated. *Circ Res* 48: 407-415, 1981.

79. **Jameson A**. Gaseous diffusion from alveoli into pulmonary arteries. *J Appl Physiol* 19: 448-456, 1964.

80. **Jones RS, and Meade F**. A theoretical and experimental analysis of anomalies in the estimation of pulmonary diffusing capacity by the single breath method. *Q J Exp Physiol Cogn Med Sci* 46: 131-143, 1961.

81. **Kaneko K, Milic-Emili J, Dolovich MB, Dawson A, and Bates DV**. Regional distribution of ventilation and perfusion as a function of body position. *J Appl Physiol* 21: 767-777, 1966.

82. **Kelly KR, Williamson DL, Fealy CE, Kriz DA, Krishnan RK, Huang H, Ahn J, Loomis JL, and Kirwan JP**. Acute altitude-induced hypoxia suppresses plasma glucose and leptin in healthy humans. *Metabolism* 59: 200-205, 2010.

83. **Kelman GR**. Digital computer subroutine for the conversion of oxygen tension into saturation. *J Appl Physiol* 21: 1375-1376, 1966.

84. **Kelman GR, and Nunn JF**. Nomograms for correction of blood Po2, Pco2, pH, and base excess for time and temperature. *J Appl Physiol* 21: 1484-1490, 1966.

85. **Kovacs G, Berghold A, Scheidl S, and Olschewski H**. Pulmonary arterial pressure during rest and exercise in healthy subjects: a systematic review. *European Respiratory Journal* 34: 888-894, 2009.

86. **Kovacs G, Olschewski A, Berghold A, and Olschewski H**. Pulmonary vascular resistances during exercise in normal subjects: a systematic review. *European Respiratory Journal* 39: 319-328, 2012.

87. **La Gerche A, MacIsaac AI, Burns AT, Mooney DJ, Inder WJ, Voigt J-U, Heidbüchel H, and Prior DL**. Pulmonary transit of agitated contrast is associated with enhanced pulmonary vascular reserve and right ventricular function during exercise. *J Appl Physiol* 109: 1307-1317, 2010.

88. **Lang RM, Bierig M, Devereux RB, Flachskampf FA, Foster E, Pellikka PA, Picard MH, Roman MJ, Seward J, Shanewise JS, Solomon SD, Spencer KT, Sutton MSJ, Stewart WJ, Group CQW, Committee ASoEsGaS, and Echocardiography EAo**. Recommendations for chamber quantification: a report from the American Society of Echocardiography's Guidelines and Standards Committee and the Chamber Quantification Writing Group, developed in conjunction with the European Association of Echocardiography, a branch of the European Society of Cardiology. *J Am Soc Echocardiogr* 18: 1440-1463, 2005.

89. **Laurie SS, Yang X, Elliott JE, Beasley KM, and Lovering AT**. Hypoxia-induced intrapulmonary arteriovenous shunting at rest in healthy humans. *J Appl Physiol* 109: 1072-1079, 2010.

90. **Lendrum B, Kondo B, and Katz LN**. The role of thebesian drainage in the dynamics of coronary flow. *Am J Physiol* 143: 243-246, 1945.

91. **Lim LL**. A statistical model of the VA/Q distribution. *J Appl Physiol* 69: 281-292, 1990.

92. **Lim LL, and Whitehead J**. Estimating the ventilation-perfusion distribution: an ill-posed integral equation problem. *Biometrics* 48: 175-187, 1992.

93. **Lopez-Majano V, Rhodes BA, and WAGNER HN**. Arteriovenous shunting in extremities. *J Appl Physiol* 27: 782-786, 1969.

94. **Lovering A, Romer L, Haverkamp H, Pegelow D, Hokanson J, and Eldridge M**. Intrapulmonary shunting and pulmonary gas exchange during normoxic and hypoxic exercise in healthy humans. *J Appl Physiol* 104: 1418-1425, 2008.

95. **Lovering AT, Eldridge MW, and Stickland MK**. Counterpoint: Exercise-induced intrapulmonary shunting is real. *J Appl Physiol* 107: 994-997, 2009.

96. **Lovering AT, Haverkamp HC, Romer LM, Hokanson JS, and Eldridge MW**. Transpulmonary passage of 99mTc macroaggregated albumin in healthy humans at rest and during maximal exercise. *J Appl Physiol* 106: 1986-1992, 2009.

97. **Lovering AT, Stickland MK, Amann M, Murphy JC, O'brien MJ, Hokanson JS, and Eldridge MW**. Hyperoxia prevents exercise-induced intrapulmonary arteriovenous shunt in healthy humans. *J Physiol (Lond)* 586: 4559-4565, 2008.

98. **Lovering AT, Stickland MK, Amann MK, O'Brien MJ, Hokanson JS, and Eldridge MW**. Effect of a patent foramen ovale on pulmonary gas exchange efficiency at rest and during exercise. *J Appl Physiol* 2011.

99. **Lovering AT, Stickland MK, Kelso AJ, and Eldridge MW**. Direct demonstration of 25- and 50-micron arteriovenous pathways in healthy human and baboon lungs. *Am J Physiol Heart Circ Physiol* 292: H1777-1781, 2007.

100. **Lu G, Shih WJ, Chou C, and Xu JY**. Tc-99m MAA total-body imaging to detect intrapulmonary right-to-left shunts and to evaluate the therapeutic effect in pulmonary arteriovenous shunts. *Clin Nucl Med* 21: 197-202, 1996.

101. **Lumb A**. *Nunn's Applied Respiratory Physiology*. Elsevier, 2005.

102. **Macintyre N, Crapo RO, Viegi G, Johnson DC, van der Grinten CPM, Brusasco V, Burgos F, Casaburi R, Coates A, Enright P, Gustafsson P, Hankinson J, Jensen R, McKay R, Miller MR, Navajas D, Pedersen OF, Pellegrino R, and Wanger J**. Standardisation of the single-breath determination of carbon monoxide uptake in the lung. *Eur Respir J* 26: 720-735, 2005.

103. **Madden JA, Dawson CA, and Harder DR**. Hypoxia-induced activation in small isolated pulmonary arteries from the cat. *J Appl Physiol* 59: 113-118, 1985.

104. **Madden JA, Vadula MS, and Kurup VP**. Effects of hypoxia and other vasoactive agents on pulmonary and cerebral artery smooth muscle cells. *Am J Physiol* 263: L384-393, 1992.

105. **Marshall BE, and Marshall C**. Continuity of response to hypoxic pulmonary vasoconstriction. *J Appl Physiol* 49: 189-196, 1980.

106. **Marshall C, and Marshall B**. Site and sensitivity for stimulation of hypoxic pulmonary vasoconstriction. *J Appl Physiol* 55: 711-716, 1983.

107. **Mazzeo RS, Bender PR, Brooks GA, Butterfield GE, Groves BM, Sutton JR, Wolfel EE, and Reeves JT**. Arterial catecholamine responses during exercise with acute and chronic high-altitude exposure. *Am J Physiol* 261: E419-424, 1991.

108. **McNay JL, McDonald RH, and Goldberg LI**. Direct renal vasodilation produced by dopamine in the dog. *Circ Res* 16: 510-517, 1965.

109. **Meikle SR, Hutton BF, and Bailey DL**. A transmission-dependent method for scatter correction in SPECT. *Journal of Nuclear Medicine* 35: 360-367, 1994.

110. **Melsom MN, Flatebø T, and Nicolaysen G**. Hypoxia and hyperoxia both transiently affect distribution of pulmonary perfusion but not ventilation in awake sheep. *Acta Physiol Scand* 166: 151-158, 1999.

111. **Miller MR, Hankinson J, Brusasco V, Burgos F, Casaburi R, Coates A, Crapo R, Enright P, van der Grinten CPM, Gustafsson P, Jensen R, Johnson DC, MacIntyre N, McKay R, Navajas D, Pedersen OF, Pellegrino R, Viegi G, Wanger J, and Force AE**. Standardisation of spirometry. *Eur Respir J* 26: 319-338, 2005.

112. **Motley HL, Cournand A, Werko L, Himmelstein A, and Dresdale D**. The influence of short periods of induced acute anoxia upon pulmonary artery pressures in man. *Am J Physiol* 150: 315-320, 1947.

113. **Mure M, Domino KB, Robertson T, Hlastala MP, and Glenny RW**. Pulmonary blood flow does not redistribute in dogs with reposition from supine to left lateral position. *Anesthesiology* 89: 483-492, 1998.

114. **Nadler SB, Hidalgo JH, and Bloch T**. Prediction of blood volume in normal human adults. *Surgery* 51: 224-232, 1962.

115. **Niden A, and Aviado D**. Effects of pulmonary embolism on the pulmonary circulation with special reference to arteriovenous shunts in the lung. *Circ Res* 4: 67-73, 1956.

116. **Nomoto S, Berk JL, Hagen JF, and Koo R**. Pulmonary anatomic arteriovenous shunting caused by epinephrine. *Arch Surg* 108: 201-204, 1974.

117. **Oltmanns KM, Gehring H, Rudolf S, Schultes B, Hackenberg C, Schweiger U, Born J, Fehm HL, and Peters A**. Acute hypoxia decreases plasma VEGF concentration in healthy humans. *Am J Physiol Endocrinol Metab* 290: E434-439, 2006.

118. **Orchard CH, Sanchez de Leon R, and Sykes MK**. The relationship between hypoxic pulmonary vasoconstriction and arterial oxygen tension in the intact dog. *J Physiol (Lond)* 338: 61-74, 1983.

119. **Overgaard CB, and Dzavík V**. Inotropes and vasopressors: review of physiology and clinical use in cardiovascular disease. *Circulation* 118: 1047-1056, 2008.

120. **Petersson J, Rohdin M, Sánchez-Crespo A, Nyrén S, Jacobsson H, Larsson SA, Lindahl SGE, Linnarsson D, Glenny RW, and Mure M**. Paradoxical redistribution of pulmonary blood flow in prone and supine humans exposed to hypergravity. *J Appl Physiol* 100: 240-248, 2006.

121. **Petersson J, Sánchez-Crespo A, Larsson SA, and Mure M**. Physiological imaging of the lung: single-photon-emission computed tomography (SPECT). *J Appl Physiol* 102: 468-476, 2007.

122. **Podolsky A, Eldridge MW, Richardson RS, Knight DR, Johnson EC, Hopkins SR, Johnson DH, Michimata H, Grassi B, Feiner J, Kurdak SS, Bickler PE, Severinghaus JW, and Wagner PD**. Exercise-induced VA/Q inequality in subjects with prior high-altitude pulmonary edema. *J Appl Physiol* 81: 922-932, 1996.

123. **Porcelli RJ, and Bergofsky EH**. Adrenergic receptors in pulmonary vasoconstrictor responses to gaseous and humoral agents. *J Appl Physiol* 34: 483-488, 1973.

124. **Porcelli RJ, Viau AT, Naftchi NE, and Bergofsky EH**. beta-Receptor influence on lung vasoconstrictor responses to hypoxia and humoral agents. *J Appl Physiol* 43: 612-616, 1977.

125. **Pourageaud F, Leblais V, Bellance N, Marthan R, and Muller B**. Role of beta2-adrenoceptors (beta-AR), but not beta1-, beta3-AR and endothelial nitric oxide, in beta-AR-mediated relaxation of rat intrapulmonary artery. *Naunyn Schmiedebergs Arch Pharmacol* 372: 14-23, 2005.

126. **Prichard MM, and Daniel PM**. Arterio-venous anastomoses in the tongue of the dog. *J Anat* 87: 66-74, 1953.

127. **Prichard MM, and Daniel PM**. Arteriovenous anastomoses in the human external ear. *J Anat* 90: 309-317, 1956.

128. **Prichard MM, and Daniel PM**. Arteriovenous anastomoses in the tongue of the sheep and the goat. *Am J Anat* 95: 203-225, 1954.

129. **Prinzmetal M, Ornitz EM, Simkin B, and Bergman HC**. Arterio-venous anastomoses in liver, spleen, and lungs. *Am J Physiol* 152: 48-52, 1948.

130. **Prinzmetal M, Simkin B, Bergman HC, and Kruger HE**. Studies on the coronary circulation; the collateral circulation of the normal human heart by coronary perfusion with radioactive erythrocytes and glass spheres. *Am Heart J* 33: 420-442, 1947.

131. **Rahn H, Stroud RC, and Tobin CE**. Visualization of arterio-venous shunts by cinefluorography in the lungs of normal dogs. *Proc Soc Exp Biol Med* 80: 239-241, 1952.

132. **Rapin M, Lemaire F, Regnier B, and Teisseire B**. Increase of intrapulmonary shunting induced by dopamine. *Proc R Soc Med* 70 Suppl 2: 71-75, 1977.

133. **Recavarren S**. The Preterminal Arterioles in the Pulmonary Circulation of High-Altitude Natives. *Circulation* 33: 177-180, 1966.

134. **Reeves JT, Groves BM, Sutton JR, Wagner PD, Cymerman A, Malconian MK, Rock PB, Young PM, and Houston CS**. Operation Everest II: preservation of cardiac function at extreme altitude. *J Appl Physiol* 63: 531-539, 1987.

135. **Reeves JT, Moon RE, Grover RF, and Groves BM**. Increased wedge pressure facilitates decreased lung vascular resistance during upright exercise. *Chest* 93: 97S-99S, 1988.

136. **Rice AJ, Thornton AT, Gore CJ, Scroop GC, Greville HW, Wagner H, Wagner PD, and Hopkins SR**. Pulmonary gas exchange during exercise in highly trained cyclists with arterial hypoxemia. *J Appl Physiol* 87: 1802-1812, 1999.

137. **Riley R, and Cournand A**. Ideal alveolar air and the analysis of ventilation-perfusion relationships in the lungs. *J Appl Physiol* 1: 825-847, 1949.

138. **Ritt P, Vija H, Hornegger J, and Kuwert T**. Absolute quantification in SPECT. *Eur J Nucl Med Mol Imaging* 1-9, 2011.

139. **Robin ED, Laman PD, Goris ML, and Theodore J**. A shunt is (not) a shunt is (not) a shunt. *Am Rev Respir Dis* 115: 553-557, 1977.

140. **Rostrup M**. Catecholamines, hypoxia and high altitude. *Acta Physiol Scand* 162: 389-399, 1998.

141. **Rowell LB, Johnson DG, Chase PB, Comess KA, and Seals DR**. Hypoxemia raises muscle sympathetic activity but not norepinephrine in resting humans. *J Appl Physiol* 66: 1736-1743, 1989.

142. **Rudski LG, Lai WW, Afilalo J, Hua L, Handschumacher MD, Chandrasekaran K, Solomon SD, Louie EK, and Schiller NB**. Guidelines for the echocardiographic assessment of the right heart in adults: a report from the American Society of Echocardiography endorsed by the European Association of Echocardiography, a registered branch of the European Society of Cardiology, and the Canadian Society of Echocardiography. *J Am Soc Echocardiogr* 23: 685-713; quiz 786-688, 2010.

143. **Said S, and Banerjee C**. Venous admixture to the pulmonary circulation in human subjects breathing 100 per cent oxygen. *J Clin Invest* 42: 507-515, 1963.

144. **Schaffartzik W, Poole DC, Derion T, Tsukimoto K, Hogan MC, Arcos JP, Bebout DE, and Wagner PD**. VA/Q distribution during heavy exercise and recovery in humans: implications for pulmonary edema. *J Appl Physiol* 72: 1657-1667, 1992.

145. **Seals DR, Jablonski KL, and Donato AJ**. Aging and vascular endothelial function in humans. *Clin Sci* 120: 357-375, 2011.

146. **Severinghaus JW**. Blood gas calculator. *J Appl Physiol* 21: 1108-1116, 1966.

147. **Shaw AM, Bunton DC, Brown T, Irvine J, and MacDonald A**. Regulation of sensitivity to 5-hydroxytryptamine in pulmonary supernumerary but not conventional arteries by a 5-HT(1D)-like receptor. *Eur J Pharmacol* 408: 69-82, 2000.

148. **Shaw AM, Bunton DC, Fisher A, McGrath JC, Montgomery I, Daly C, and MacDonald A**. V-shaped cushion at the origin of bovine pulmonary supernumerary arteries: structure and putative function. *J Appl Physiol* 87: 2348-2356, 1999.

149. **Siggaard-Andersen O, and Huch R**. The oxygen status of fetal blood. *Acta Anaesthesiol Scand Suppl* 107: 129-135, 1995.

150. **Siostrzonek P, Lang W, Zangeneh M, Gössinger H, Stümpflen A, Rosenmayr G, Heinz G, Schwarz M, Zeiler K, and Mösslacher H**. Significance of left-sided heart disease for the detection of patent foramen ovale by transesophageal contrast echocardiography. *J Am Coll Cardiol* 19: 1192-1196, 1992.

151. **Sirsi M, and Bucher K**. Studies on arteriovenous anastomoses in the lungs. *Experientia* 9: 217-218, 1953.

152. **Sobol B, BOTTEX G, EMIRGIL C, and GISSEN H**. Gaseous diffusion from alveoli to pulmonary vessels of considerable size. *Circ Res* 13: 71-79, 1963.

153. **Souders JE, George SC, Polissar NL, Swenson ER, and Hlastala MP**. Tracheal gas exchange: perfusion-related differences in inert gas elimination. *J Appl Physiol* 79: 918-928, 1995.

154. **Staub NC**. Alveolar-arterial oxygen tension gradient due to diffusion. *J Appl Physiol* 18: 673-680, 1963.

155. **Stenmark KR, and Abman SH**. Lung vascular development: Implications for the pathogenesis of bronchopulmonary dysplasia. *Annu Rev Physiol* 67: 623-661, 2005.

156. **Stickland, Lovering, and Eldridge**. Exercise-induced arteriovenous intra-pulmonary shunting in canines. *Am J Respir Crit Care Med* 2007.

157. **Stickland MK, and Lovering AT**. Exercise-induced intrapulmonary arteriovenous shunting and pulmonary gas exchange. *Exerc Sport Sci Rev* 34: 99-106, 2006.

158. **Stickland MK, Welsh RC, Haykowsky MJ, Petersen SR, Anderson WD, Taylor DA, Bouffard M, and Jones RL**. Effect of acute increases in pulmonary vascular pressures on exercise pulmonary gas exchange. *J Appl Physiol* 100: 1910-1917, 2006.

159. **Stickland MK, Welsh RC, Haykowsky MJ, Petersen SR, Anderson WD, Taylor DA, Bouffard M, and Jones RL**. Intra-pulmonary shunt and pulmonary gas exchange during exercise in humans. *J Physiol (Lond)* 561: 321-329, 2004.

160. **Sty JR, Thomas J, and Gallen W**. Congenital pulmonary arteriovenous aneurysm. *Clin Nucl Med* 6: 86-88, 1981.

161. **Suga K, Kawakami Y, Iwanaga H, Tokuda O, and Matsunaga N**. Automated breath-hold perfusion SPECT/CT fusion images of the lungs. *AJR Am J Roentgenol* 189: 455-463, 2007.

162. **Suga K, Kuramitsu T, Yoshimizu T, Nakanishi T, Yamada N, and Utsmi H**. Scintigraphic analysis of hemodynamics in a patient with a single large pulmonary arteriovenous fistula. *Clin Nucl Med* 17: 110-113, 1992.

163. **Suga K, Okada M, Kunihiro M, Iwanaga H, and Matsunaga N**. Clinical significance of CT density-based, non-uniform photon attenuation correction of deep-inspiratory breath-hold perfusion SPECT. *Ann Nucl Med* 1-10, 2011.

164. **Swenson ER, Robertson HT, Polissar NL, Middaugh ME, and Hlastala MP**. Conducting airway gas exchange: diffusion-related differences in inert gas elimination. *J Appl Physiol* 72: 1581-1588, 1992.

165. **Sylvester JT, Cymerman A, Gurtner G, Hottenstein O, Cote M, and Wolfe D**. Components of alveolar-arterial O2 gradient during rest and exercise at sea level and high altitude. *J Appl Physiol* 50: 1129-1139, 1981.

166. **Sylvester JT, Shimoda LA, Aaronson PI, and Ward JPT**. Hypoxic pulmonary vasoconstriction. *Physiol Rev* 92: 367-520, 2012.

167. **Takagi C, King GL, Takagi H, Lin YW, Clermont AC, and Bursell SE**. Endothelin-1 action via endothelin receptors is a primary mechanism modulating retinal circulatory response to hyperoxia. *Invest Ophthalmol Vis Sci* 37: 2099-2109, 1996.

168. **Talbot NP, Balanos GM, Dorrington KL, and Robbins PA**. Two temporal components within the human pulmonary vascular response to approximately 2 h of isocapnic hypoxia. *J Appl Physiol* 98: 1125-1139, 2005.

169. **Teplick R, Snider MT, and Gilbert JP**. A comparison of continuous and discrete foreign gas VA/Q distributions. *J Appl Physiol* 49: 684-692, 1980.

170. **Tobin CE**. Arteriovenous shunts in the peropheral pulmonary circulation in the human lung. *Thorax* 21: 197-204, 1966.

171. **Tobin CE**. The bronchial arteries and their connections with other vessels in the human lung. *Surg Gynecol Obstet* 95: 741-750, 1952.

172. **Tobin CE, and Zariquiey M**. Arteriovenous shunts in the human lung. *Proc Soc Exp Biol Med* 75: 827-829, 1950.

173. **Torre-Bueno JR, Wagner PD, Saltzman HA, Gale GE, and Moon RE**. Diffusion limitation in normal humans during exercise at sea level and simulated altitude. *J Appl Physiol* 58: 989-995, 1985.

174. **Tracey A, Bunton D, Irvine J, MacDonald A, and Shaw AM**. Relaxation to bradykinin in bovine pulmonary supernumerary arteries can be mediated by both a nitric oxide-dependent and -independent mechanism. *Br J Pharmacol* 137: 538-544, 2002.

175. **Tracey A, MacDonald A, and Shaw AM**. Involvement of gap junctions in bradykinin-induced relaxation of bovine pulmonary supernumerary arteries before and after inhibition of nitric oxide/guanylate cyclase. *Clin Sci* 103: 553-557, 2002.

176. **Tristani-Firouzi M, Reeve HL, Tolarova S, Weir EK, and Archer SL**. Oxygen-induced constriction of rabbit ductus arteriosus occurs via inhibition of a 4-aminopyridine-, voltage-sensitive potassium channel. *J Clin Invest* 98: 1959-1965, 1996.

177. **Venero CV, Heller GV, Bateman TM, Mcghie AI, Ahlberg AW, Katten D, Courter SA, Golub RJ, Case JA, and Cullom SJ**. A multicenter evaluation of a new post-processing method with depth-dependent collimator resolution applied to full-time and half-time acquisitions without and with simultaneously acquired attenuation correction. *J Nucl Cardiol* 16: 714-725, 2009.

178. **Vogiatzis I, Zakynthinos S, Boushel R, Athanasopoulos D, Guenette JA, Wagner H, Roussos C, and Wagner PD**. The contribution of intrapulmonary shunts to the alveolar-to-arterial oxygen difference during exercise is very small. *J Physiol (Lond)* 586: 2381-2391, 2008.

179. **von Euler U, and Liljestrand G**. Observations on the pulmonary arterial blood pressure in the cat. *Acta Physiol Scand* 12: 301-320, 1946.

180. **Wagner P**. The multiple inert gas elimination technique (MIGET). *Intensive Care Med* 2008.

181. **Wagner PD**. Diffusion and chemical reaction in pulmonary gas exchange. *Physiol Rev* 57: 257-312, 1977.

182. **Wagner PD, Gale GE, Moon RE, Torre-Bueno JR, Stolp BW, and Saltzman HA**. Pulmonary gas exchange in humans exercising at sea level and simulated altitude. *J Appl Physiol* 61: 260-270, 1986.

183. **Wagner PD, Laravuso RB, Uhl RR, and West JB**. Continuous distributions of ventilation-perfusion ratios in normal subjects breathing air and 100% O2. *J Clin Invest* 54: 54-68, 1974.

184. **Wagner PD, Naumann PF, and Laravuso RB**. Simultaneous measurement of eight foreign gases in blood by gas chromatography. *J Appl Physiol* 36: 600-605, 1974.

185. **Wagner PD, Saltzman HA, and West JB**. Measurement of continuous distributions of ventilation-perfusion ratios: theory. *J Appl Physiol* 36: 588-599, 1974.

186. **Wagner PD, Sutton JR, Reeves JT, Cymerman A, Groves BM, and Malconian MK**. Operation Everest II: pulmonary gas exchange during a simulated ascent of Mt. Everest. *J Appl Physiol* 63: 2348-2359, 1987.

187. **Wang J, Shimoda LA, Weigand L, Wang W, Sun D, and Sylvester JT**. Acute hypoxia increases intracellular [Ca2+] in pulmonary arterial smooth muscle by enhancing capacitative Ca2+ entry. *Am J Physiol Lung Cell Mol Physiol* 288: L1059-1069, 2005.

188. **Wanger J, Clausen JL, Coates A, Pedersen OF, Brusasco V, Burgos F, Casaburi R, Crapo R, Enright P, van der Grinten CPM, Gustafsson P, Hankinson J, Jensen R, Johnson D, Macintyre N, McKay R, Miller MR, Navajas D, Pellegrino R, and Viegi G**. Standardisation of the measurement of lung volumes. *Eur Respir J* 26: 511-522, 2005.

189. **Ward JPT**. Point: Hypoxic pulmonary vasoconstriction is mediated by increased production of reactive oxygen species. *J Appl Physiol* 101: 993-995; discussion 999, 2006.

190. **Weir EK, and Archer S**. The mechanism of acute hypoxic pulmonary vasoconstriction: the tale of two channels. *FASEB J* 9: 183-189, 1995.

191. **Weir EK, and Archer SL**. Counterpoint: Hypoxic pulmonary vasoconstriction is not mediated by increased production of reactive oxygen species. *J Appl Physiol* 101: 995-998; discussion 998, 2006.

192. **West JB**. The history of respiratoy physiology. In: *Nunn's Applied Respiratory Physiology*, edited by Lumb A. Italy: Elsevier, 2005, p. 209-225.

193. **West JB**. Ibn al-Nafis, the pulmonary circulation, and the Islamic Golden Age. *J Appl Physiol* 105: 1877-1880, 2008.

194. **West JB**. Respiratory and circulatory control at high altitudes. *J Exp Biol* 100: 147-157, 1982.

195. **West JB, and Dollery CT**. Distribution of blood flow and ventilation-perfusion ratio in the lung, measured with radioactive carbon dioxide. *J Appl Physiol* 15: 405-410, 1960.

196. **West JB, Dollery CT, and Naimark A**. Distribution of blood flow in isolated lung; relation to vascular and alveolar pressures. *J Appl Physiol* 19: 713-724, 1964.

197. **Whyte MK, Peters AM, Hughes JM, Henderson BL, Bellingan GJ, Jackson JE, and Chilvers ER**. Quantification of right to left shunt at rest and during exercise in patients with pulmonary arteriovenous malformations. *Thorax* 47: 790-796, 1992.

198. **Willowson K, Bailey DL, and Baldock C**. Quantitative SPECT reconstruction using CT-derived corrections. *Phys Med Biol* 53: 3099-3112, 2008.

199. **Witham A, and Fleming J**. The effect of epinephrine on the pulmonary circulation in man. *J Clin Invest* 30: 707-717, 1951.

200. **Woods TD, and Patel A**. A critical review of patent foramen ovale detection using saline contrast echocardiography: when bubbles lie. *J Am Soc Echocardiogr* 19: 215-222, 2006.

201. **Yaginuma G, Mohri H, and Takahashi T**. Distribution of arterial lesions and collateral pathways in the pulmonary hypertension of congenital heart disease: a computer aided reconstruction study. *Thorax* 45: 586-590, 1990.

202. **Yang WJ, Echigo R, Wotton DR, and Hwang JB**. Experimental studies of the dissolution of gas bubbles in whole blood and plasma. I. Stationary bubbles. *J Biomech* 4: 275-281, 1971.

203. **Yang WJ, Echigo R, Wotton DR, and Hwang JB**. Experimental studies of the dissolution of gas bubbles in whole blood and plasma. II. Moving bubbles or liquids. *J Biomech* 4: 283-288, 1971.

204. **Yock PG, and Popp RL**. Noninvasive estimation of right ventricular systolic pressure by Doppler ultrasound in patients with tricuspid regurgitation. *Circulation* 70: 657-662, 1984.

205. **Zhu Y, Park TS, and Gidday JM**. Mechanisms of hyperoxia-induced reductions in retinal blood flow in newborn pig. *Exp Eye Res* 67: 357-369, 1998.